INVESTIGATION OF EM EMISSIONS BY THE ELECTRODYNAMIC TETHER, INCLUSIVE OF AN OBSERVATIONAL PROGRAM

(E.M.E.T)

Contract NAS8-36809

Final Report

Principal Investigator

Dr. Robert D. Estes

October 1998

Prepared for
National Aeronautics and Space Administration
Marshall Space Flight Center, Alabama 35812

Smithsonian Institution
Astrophysical Observatory
Cambridge, Massachusetts 02138

The Smithsonian Astrophysical Observatory
is a member of the
Harvard-Smithsonian Center for Astrophysics

Table of Contents

INTRODUCTION

Our TSS-1/R investigation, which we shall refer to as EMET in this report, was an integral part of the effort by the TSS-1/R Investigators' Working Group (IWG) to come to an understanding of the complex interaction between the tethered satellite system and the ionosphere.[1] All of the space-borne experiments were designed to collect data relevant to the local interaction. Only the ground-based experiments, EMET and its Italian counterpart Observations on the Earth's Surface of Electromagnetic Emissions (OESEE), held out any hope of characterizing the long range effects of the interaction. This was to be done by detecting electromagnetic waves generated by the system in the ionosphere, assuming the signal reached the Earth's surface with sufficient amplitude. As the type of plasma waves excited to carry charge away from the charge-exchange regions of the system at each end of the tether is one of the theoretical points about which there is greatest disagreement, a definitive identification of tether-generated waves could mark significant progress in the so-called current closure problem of electrodynamic tethers.[2,3]

Dr. Mario Grossi of the Smithsonian Astrophysical Observatory (SAO) initiated the investigation, and his experience in the field of ULF-ELF waves and their detection was invaluable throughout its course. Rice University had the responsibility of setting up the EMET ULF-VLF ground stations under a subcontract from SAO. Principal Investigator (PI) for the Rice effort was Prof. William E. Gordon, who was primary observer at the Arecibo Observatory during TSS-1R. Dr. Steve Noble handled major day-to-day operations, training, and planning for the ground-based measurements. Dr. James McCoy of NASA JSC, a member of the Mona/Arecibo team, was pilot for the numerous flights ferrying personnel and equipment between Puerto Rico and Mona Island. Final responsibility for the measurements rested with SAO, and the activities of field personnel and SAO investigators were closely co-ordinated during the mission. Dr. Enrico Lorenzini of SAO served as the eyes, ears, and brain of EMET in the Science Operations Area and PI table during the mission, whenever the PI was absent during the round-the-clock mission operations.

The Rice University final report to SAO, which is included as an Appendix, contains details of the remote sites, means of communication, sensors, etc., as well as the affiliations of personnel involved in the data-gathering effort. Mona team members also included Mike Hinds, Matt Freeman, and Peter Czipott. The first two named were veterans of the TSS-1 Mona expedition as well. The Bribie Island (Australia) team consisted of Steve Noble, Rudy Frahm, and host observer Prof. David Whitehead of the University of Queensland.

The EMET investigation spanned well over a decade in planning and training and included two US Space Shuttle missions, both of which failed to reach full tether extension and terminated hours before the "overflights" of our stations were to have occurred. In this report we will confine ourselves to the TSS-1R (reflight) mission, since the first mission terminated well before tether lengths and currents of any use for our ground-based observations were obtained, especially given the distance of the ground tracks from our sites.

It is important to realize that our investigation had been designed around these overflights of our ground stations in Puerto Rico and Australia. These were the periods during which the Shuttle would make its closest approach to our stations and during which time the tether current would be preprogrammed to our specifications, based on our estimates of what would be most likely to excite detectable waves.

Despite our bad luck, which is always a possibility in "one-shot" active space experiments, the EMET team made important contributions to the TSS-1/R missions through the activity of our PI and Co-Investigators in the IWG. This activity consisted of many IWG meetings in the US and Italy devising and revising the second-by-second, multiday timeline of experiments to be conducted during the two TSS-1 missions, and in the minute-to-minute decisions that had to made by the IWG as a whole during the course of the mission, including major last-minute revisions to the experimental timeline. This activity was in addition to all the preparations that the EMET team made for data acquisition, including the transporting of equipment, supplies, and team members themselves to remote sites. Regretably, the contribution of the EMET team to the TSS-1/R missions will remain invisible to the broader space science community, as there was no overall TSS-1/R summary paper with an inclusive author list.

Use of the Arecibo 430MHz radar to probe the ionosphere for electron density and temperature variations associated with electrodynamic tether operations during the primary pass over Areciba/Mona had been secured after much effort. The problem was that the radar was being refurbished, which left it pointed in one (vertical) direction and inaccessible during the day when workmen were engaged. Rice PI Bill Gordon and Arecibo observer Mike Sulzer were instrumental in securing the radar. EMET had also lined up the participation of the Jicamarca Observatory in Peru. Unfortunately, these radar observations were never carried out due to the premature termination of the experiments. Collaborations had been obtained with several other groups around the world, including observers in Japan, Russia, Australia, Antarctica, and the Carribean. A New Zealand group led by Richard Barr and a South African group led by Arthur Hughes mounted remote measurement campaigns in the Fiji Islands and the mountains of Natal, respectively. TSS-1R came to its premature end before the closest approaches to these remote sites.

Fortunately, the observation teams at both ground sites began taking data at the beginning of satellite deployment, as planned, though the period of DC (battery-powered, rather than generator-powered) operations had not begun. Given that our "prime time" experiments never took place, our expectation of finding tether-current-generated signals in our data was not high. We had, however, collected data during the only experiment achieving Ampere-level current flow in a long, orbiting tether in the ionosphere, so a data analysis effort was justified.

The EMET team has looked for possible tether-related signals in the data acquired during the TSS-1R mission. While the data may not warrant publication, we have noted an "event" in the post-tether-break ULF data that is of sufficient interest to report in this document. Those analyzing data from ground measurements of future electrodynamic tether experiments, at least, might want to be aware of the one glimmer of significance we have extracted from our data, and of the indirect route by which we came to see it. Unfortunately, OESEE, the other group that recorded data during the TSS-1R mission, has been unable to shed any light on the situation, since they received no funding for data analysis from the Italian Space Agency.

72

BFPS voltages

0215 GMT	BF6	12.82 / 12.79	(12.82 / 12.79)
	BF4	13.01 / 13.02	(12.65 / 12.67)

03:00 GMT ~~[illegible]~~ Metrum ~1 sec behind IRIG

03:01:30 Metrum Block # 100876

03:26 GMT GPS ~~ex~~ agrees w/ IRIG

~03:35 Power glitch - Metrum ok but HP 3561 cycled.
turned off HP 3561 & plotter. will check
oil level at tape change in 11 mins. Gas ok.

~03:45 Matt called SOC, ~5 min GlobeSat

Very Bad News.

Tether broke after deploying 19.6 of the
20 km.

A page from the Mona Island team's log book: "Very Bad News."

Figure 1.

DATA DETAILS

Section 3 of the Appendix is devoted to the ULF-VLF Measurement Systems used by EMET observers on Mona Island and Bribie Island. Please see that section for a detailed description. There were six sensors at each location: three orientations (NS, EW, and vertical; see Figure 2) each for sensor sets designed to cover different bandwidths (ULF-ELF and VLF). The dynamic range limitation of our recorder (12 bits or 70 dB) required us to split the ULF-ELF data into three channels. Twelve channels of data were thus recorded at each site. Figure 3 shows the hookups for the filtering done before recording. Data recording began shortly before satellite flyaway and continued for a couple of hours after the break.

Shortly after the mission, all TSS-1R data tapes and a Magnum RSR512 recorder (one that was used to collect data during the mission) to read them were shipped to SAO. These tapes included both background and deployed data from both the Bribie and Mona stations. Background data were gathered on days prior to the scheduled overflights at the same local time as the scheduled overflights. In retrospect, it would have been good to have recorded data from other times of day, since our post-flight "prime" data turned out to have been gathered at a local time quite different from what had been anticipated, due to the premature end of the mission when the tether broke.

In order to have more precise control of the data analysis—that is, without the limitations of the electronic signal analyzer, which we also used—it was necessary to transfer the data from the tapes to a medium and format readable by our computer. We had installed a National Instruments IEEE GPIB card in our PowerMac 7100/80AV computer for this purpose. This enabled us to make the data transfer by cable, after we had written the software to unpack the data. An Iomega Jaz drive with 1-gigabyte removable cartridges was used for the storing the data. Data transfer was a slow process: around 30 hours was required to transfer one hour's worth of data. A 1-gigabyte disk stores around 23 minutes of data.

The transfer to disk was done for all of the Mona data of interest (including some background data) and some of the Bribie data. After a problem encountered with the recorder early in the transfer process, we returned it to the manufacturer for repair. With a heightened awareness of the possibility of data

49

Trode B

T	V	A
12:20	12.68	— no charge
"	12.72	3

Sensor Layout

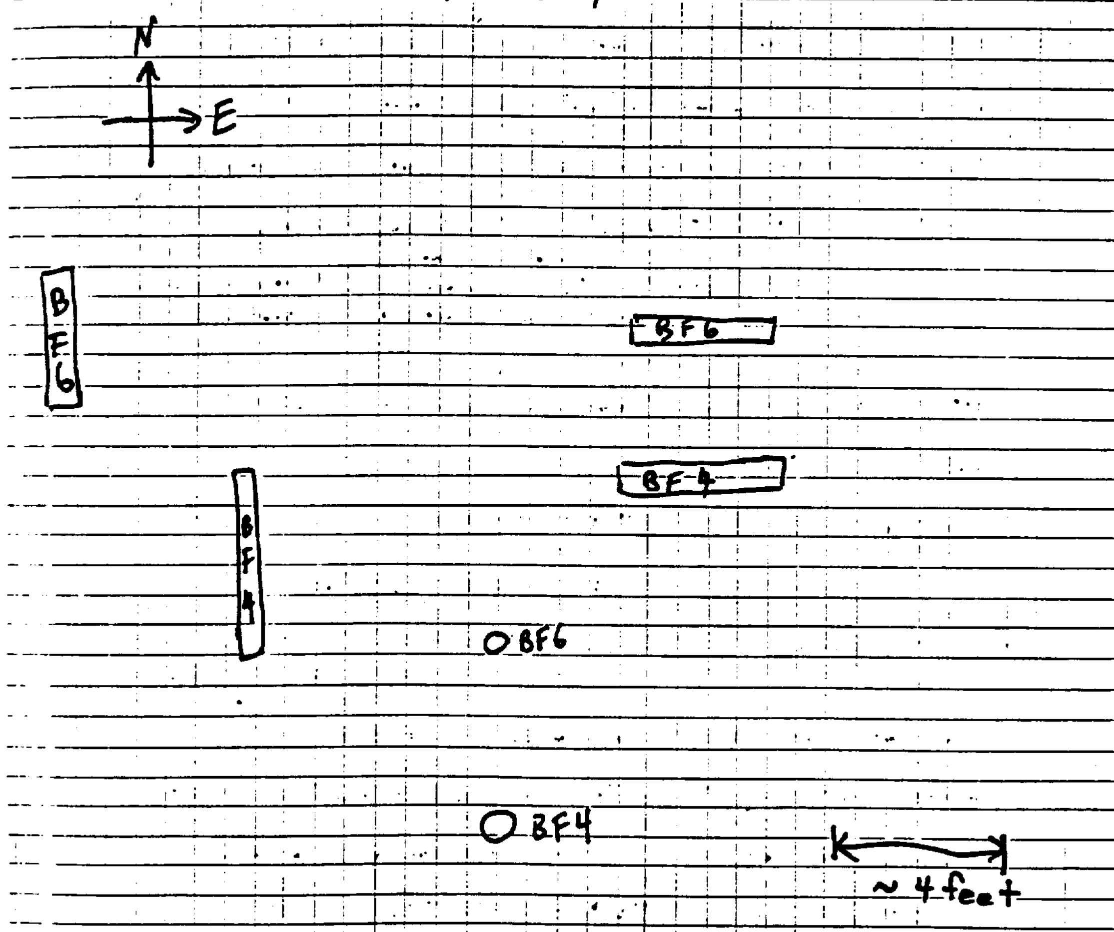

From the Mona Island Log Book: Layout of Sensors

Figure 2.

SIGNAL CONDITIONER WIRING DIAGRAM-STANDARD SETUP
SINGLE POLARIZATION

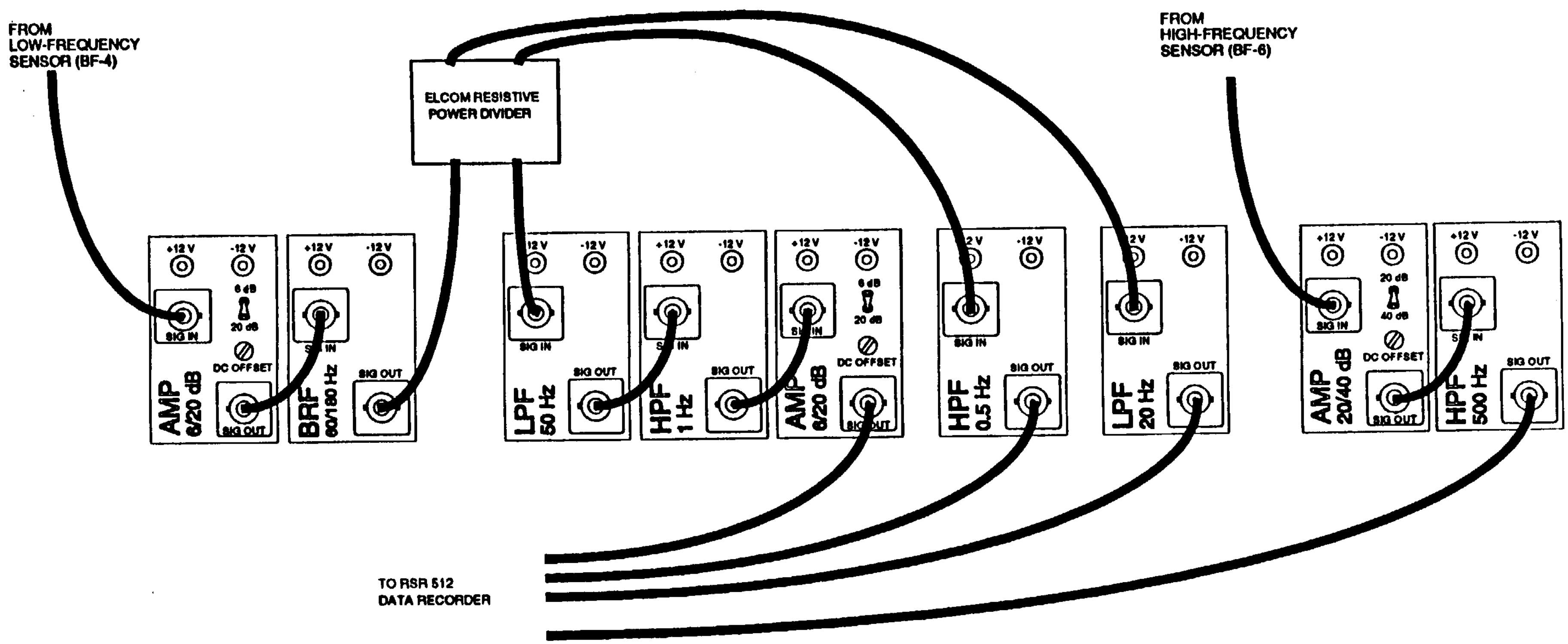

Figure 3.

loss during transfer, we then obtained the loan of a second recorder to make backup copies of all prime data tapes. The copies were then stored off site.

We adapted Fast Fourier Transform (FFT) routines found in *Numerical Recipes in C* (Press, W.H., S. A. Teukolsky, W. T. Vetterling, and B. P. Flannery, Cambridge University Press, 1992) to our purposes. This software enabled us to perform Fourier analyses on data samples of arbitrary start time and size (512 K points in some cases) in whichever channels we wished. Software for demultiplexing the data, which incorporated routines supplied by the manufacturer of the recorder, was written to convert the binary data on the Jaz cartridges into data segregated by channel in ascii format suitable for input to the FFT software.

Some samples of averaged spectra obtained from data taken at Mona island are shown in Figures 4-7. The well-known Schumann resonances of the Earth-ionosphere spherical waveguide are clearly visible in the data for the bands 0.5 Hz<f<50 Hz and f>1.0Hz. Such details tend to be lost in the f<20 Hz data, where the recording scale is set by the large signals at the lowest frequencies. Note also how closely matched the NS and EW spectra are. This was striking in the Mona Island data, about which we will say more in a later section.

Figure 8 shows the Shuttle orbital track (latitude and longitude separately versus GMT) for the period of time relevant to our observations. Figure 9 displays the track in more detail for the time around the tether break and the unscheduled 1 A current event. Plots for the tether current versus GMT follow in Figures 10-15. Some of the plots show in more detail samples most likely to be of interest. All but Figure 15 show the current as recorded by the SETS monitor on the orbiter. The current immediately before and after the break occurred under supposed open circuit conditions, and was not recorded by SETS. The data in Figure 15 comes from the satellite current monitor. By referring to the current and Shuttle position time histories, one can see what was happening and where for any time during the TSS-1R deployed phase of operation.

The data most likely to be of interest were those taken during earlier (pre-break) closest approaches to the ground stations, even though they occurred before full tether deployment and without our special current profile. Of particular interest were the data taken around the time of the break, which

Example 1 of Mona background: 0.5 < f < 50Hz channels

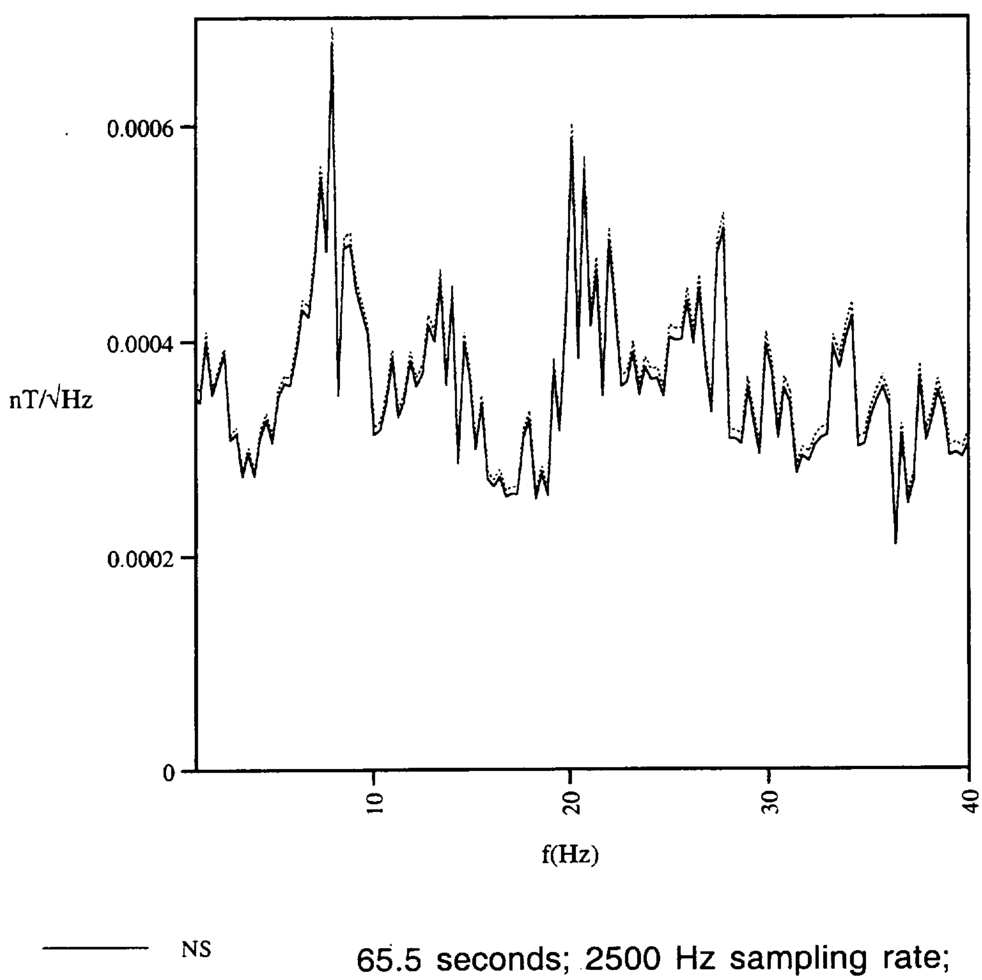

65.5 seconds; 2500 Hz sampling rate;
Avg. over 20 FFT; 8K points per FFT

Figure 4.

Example 2 of Mona background: 0.5 < f < 50Hz channels

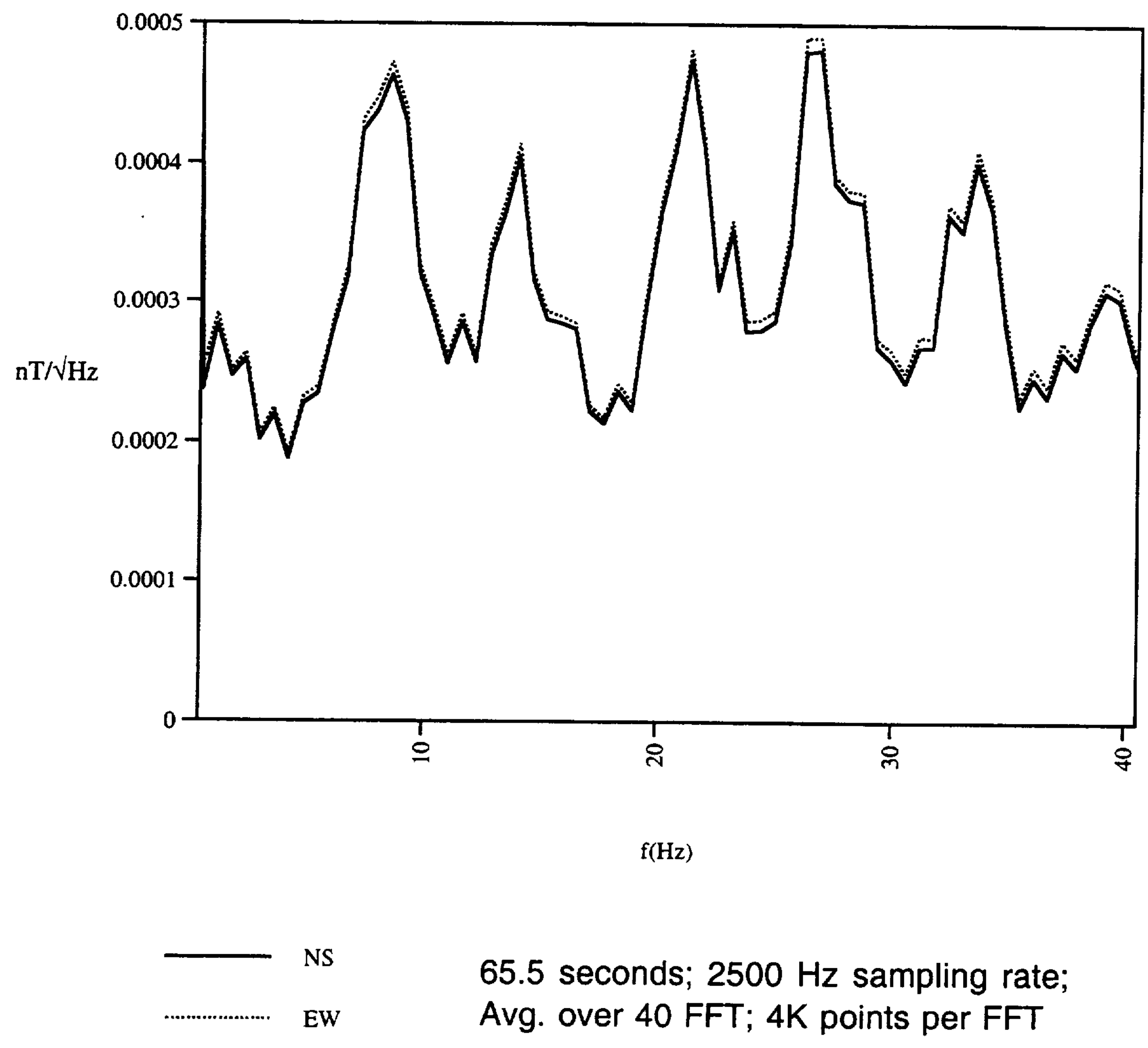

Figure 5.

Example 1 of Mona background: f<20Hz channels

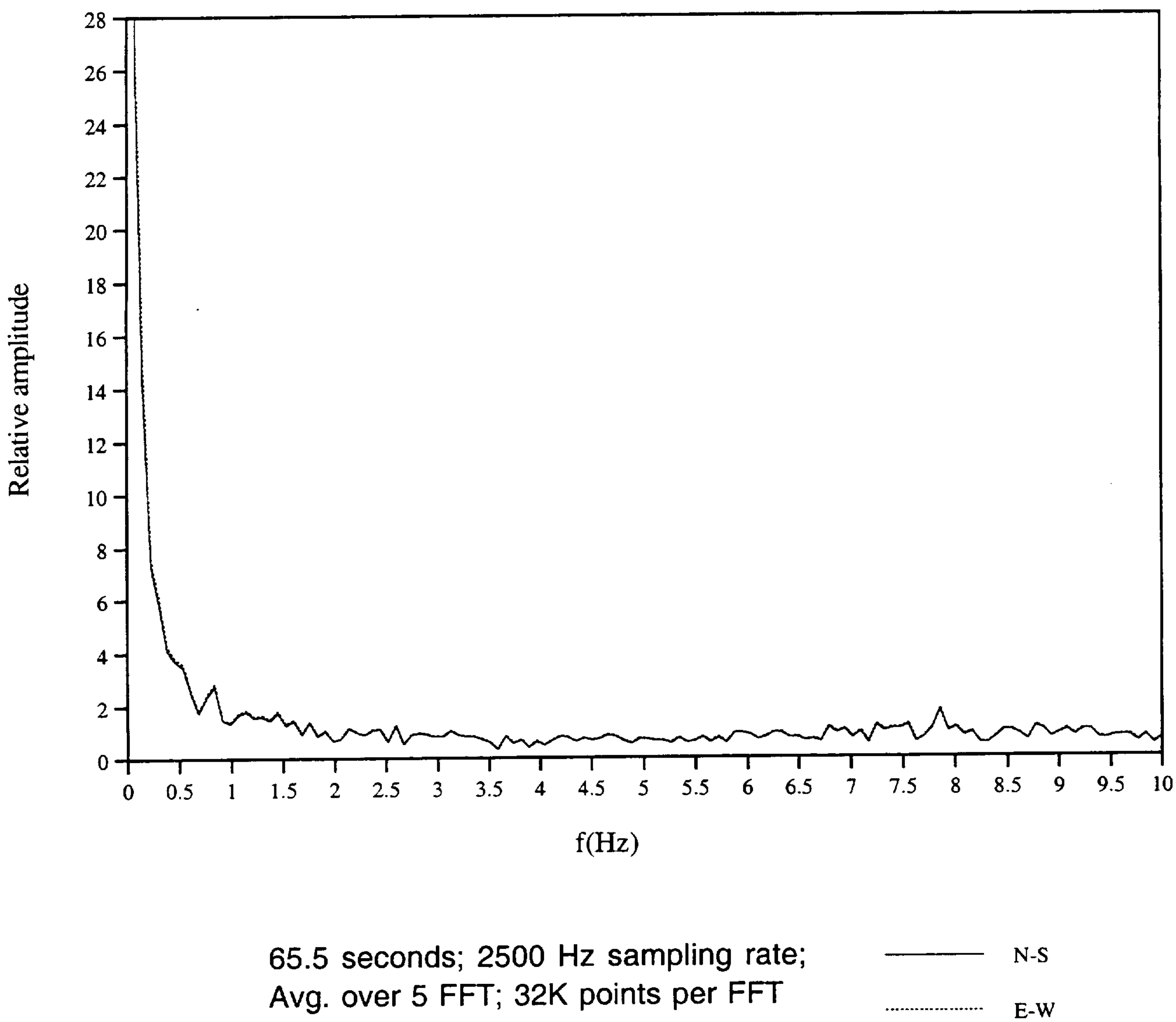

Figure 6.

Example 1 of Mona background: BF-4 sensors; f > 1 Hz channels

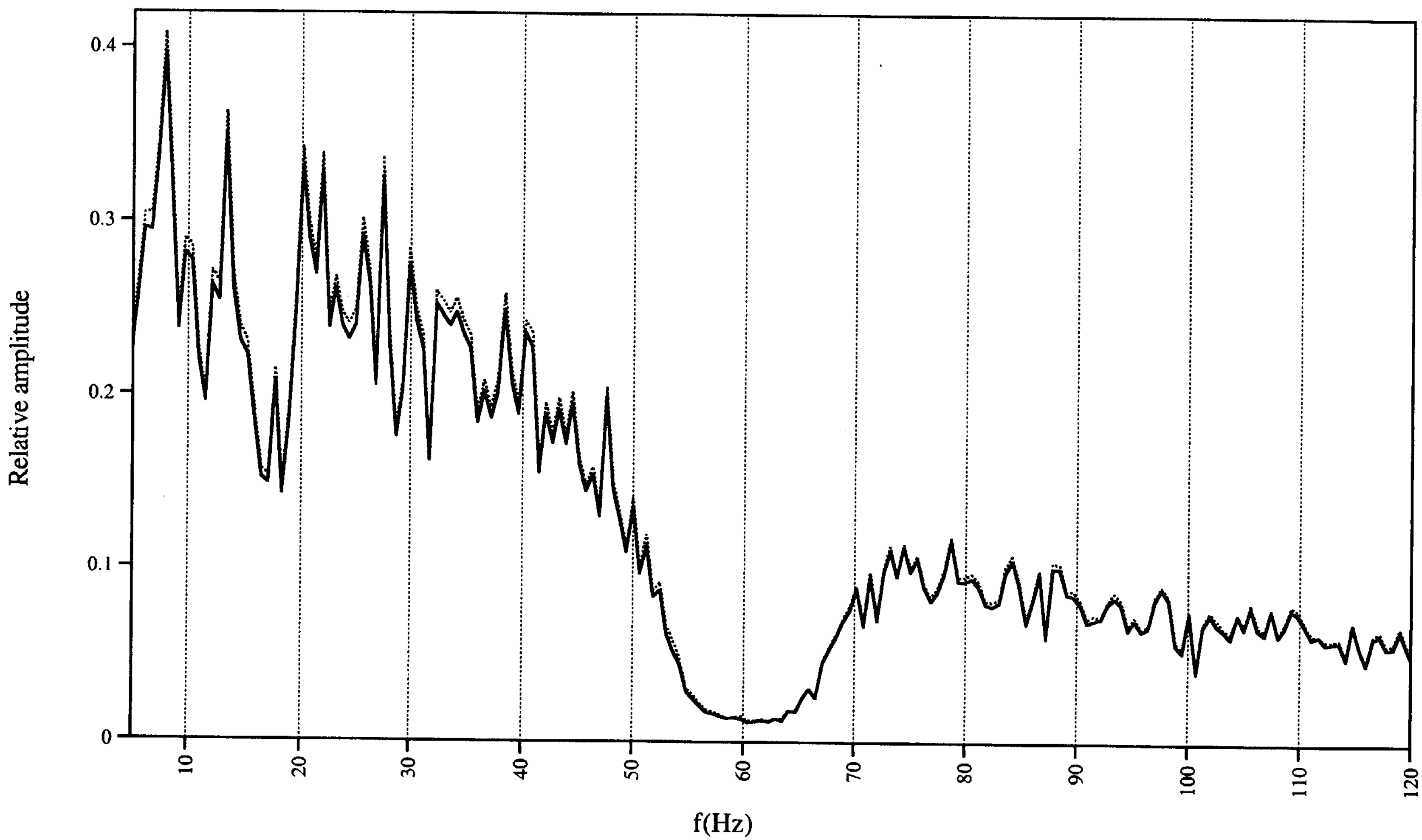

65.5 seconds; 5000 Hz sampling rate;
Avg. over 40 FFT; 8K points per FFT

N-S
E-W

Figure 7.

TSS-1R Orbital Path Data relevant to EMET Observations
GMT for February 25 and 26, 1996

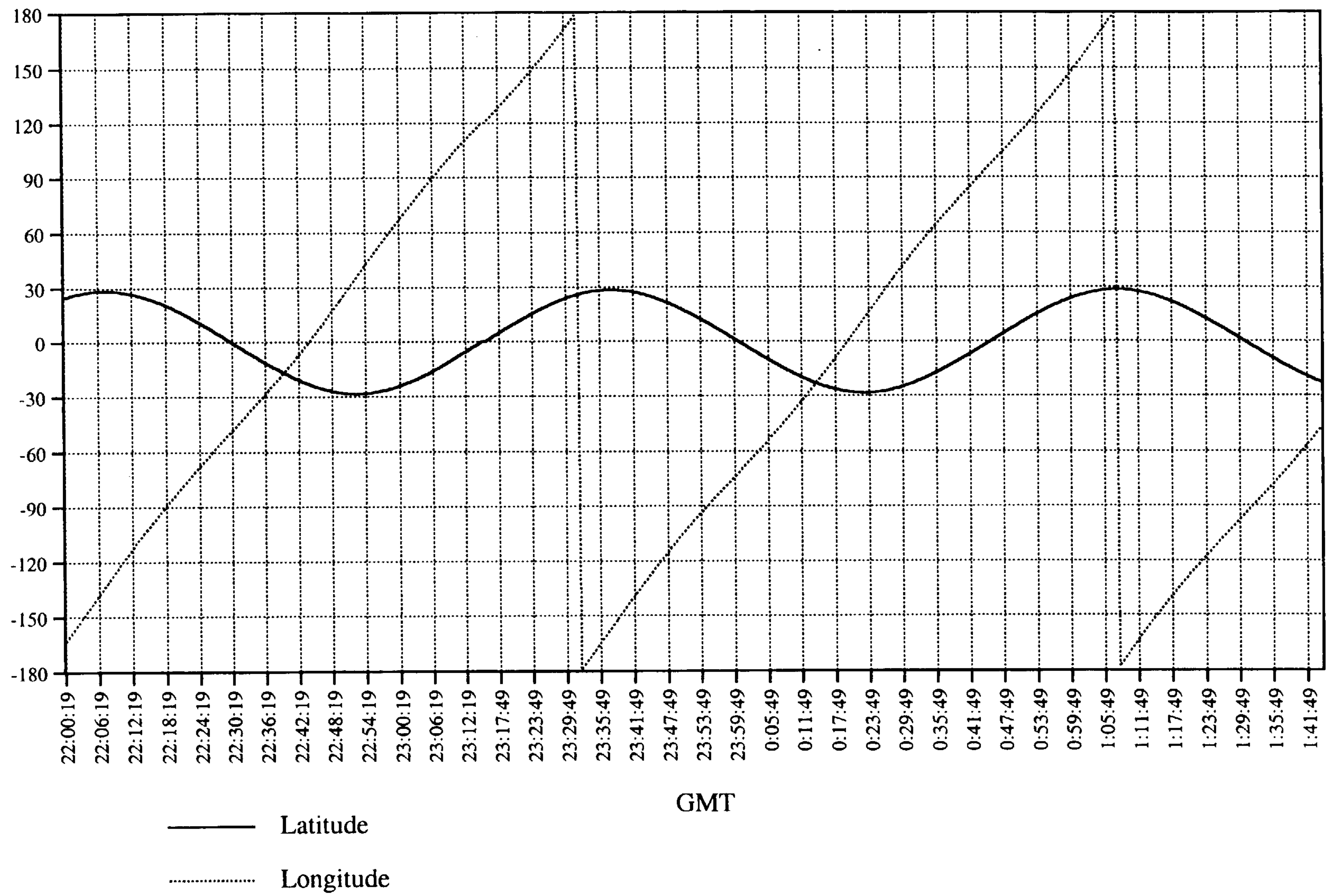

Figure 8.

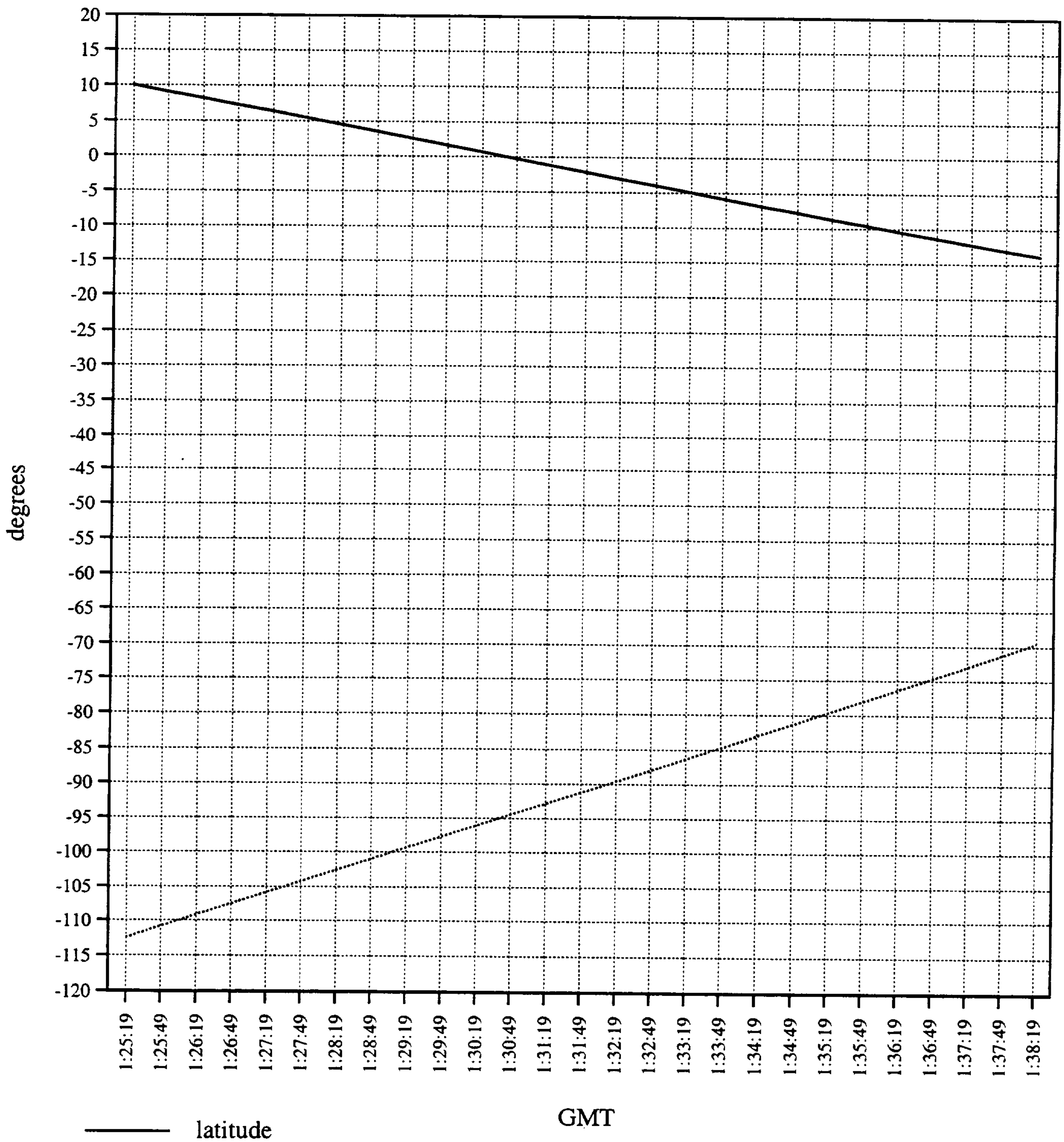

Orbital Track Around Time of Break

Figure 9.

Tether Current (DEP101 Mona Pass)

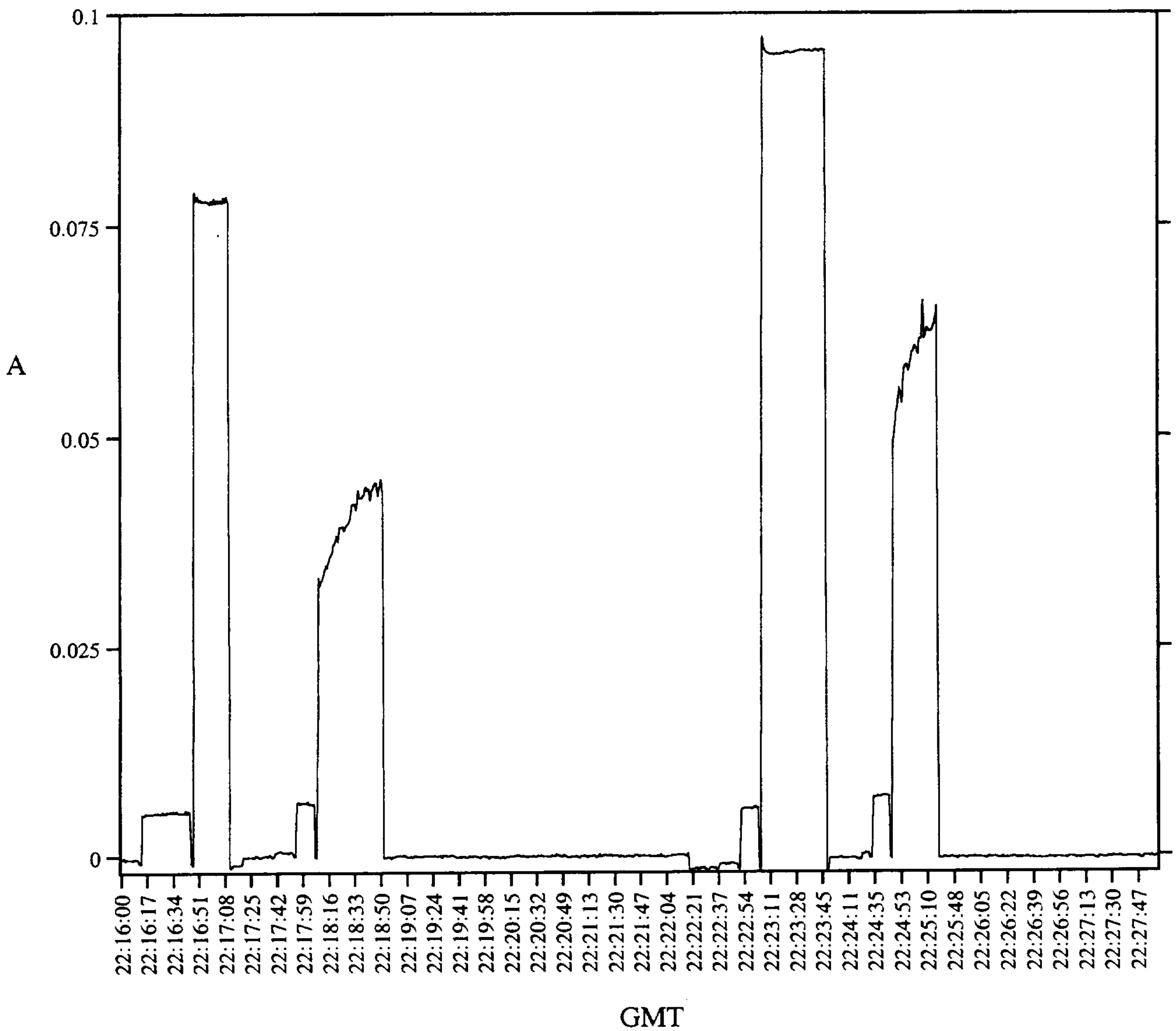

Figure 10.

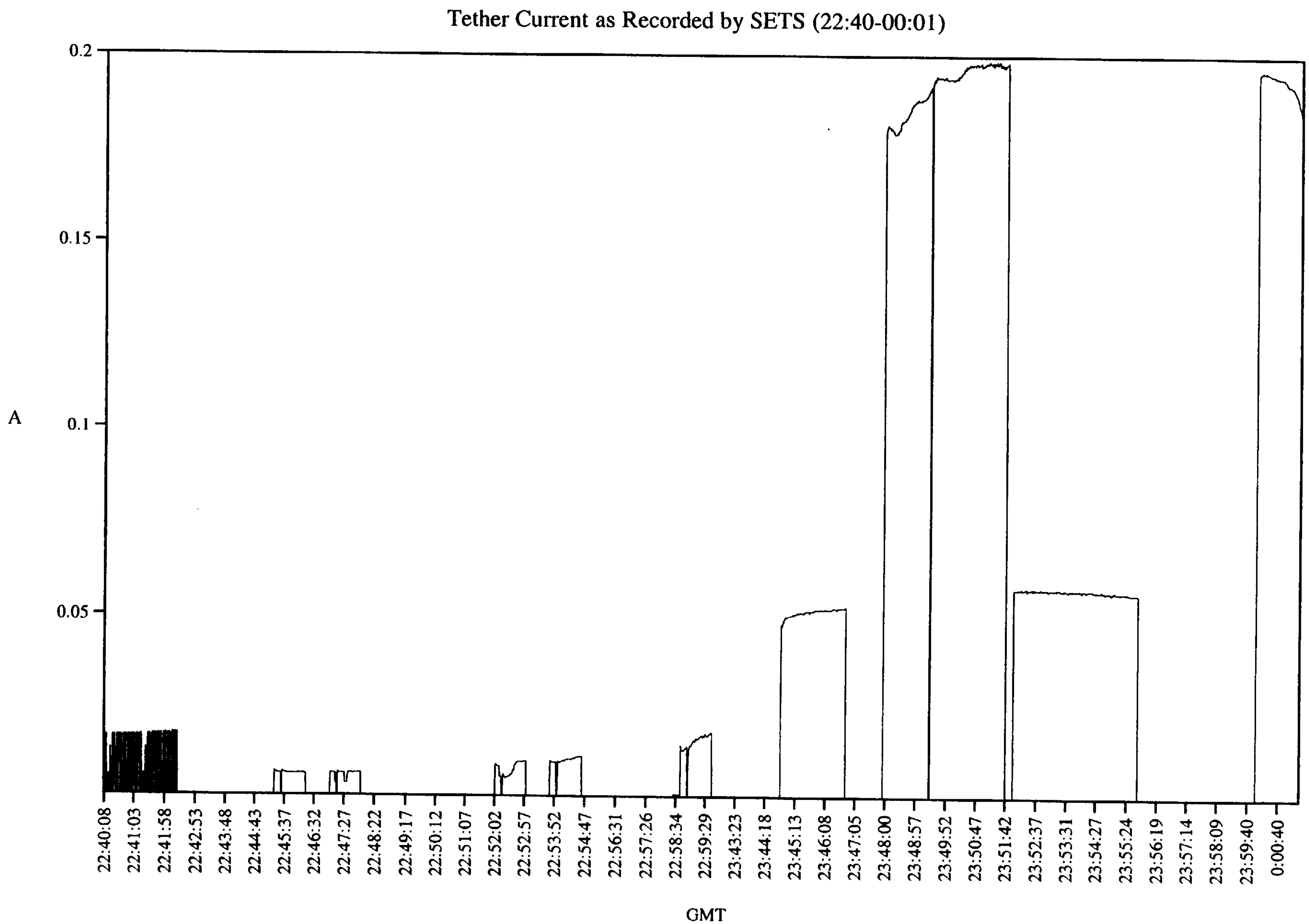
Tether Current as Recorded by SETS (22:40-00:01)
A
0.2
0.15
0.1
0.05
22:40:08
22:41:03
22:41:58
22:42:53
22:43:48
22:44:43
22:45:37
22:46:32
22:47:27
22:48:22
22:49:17
22:50:12
22:51:07
22:52:02
22:52:57
22:53:52
22:54:47
22:56:31
22:57:26
22:58:34
22:59:29
23:43:23
23:44:18
23:45:13
23:46:08
23:47:05
23:48:00
23:48:57
23:49:52
23:50:47
23:51:42
23:52:37
23:53:31
23:54:27
23:55:24
23:56:19
23:57:14
23:58:09
23:59:40
0:00:40
GMT

Figure 11.

Tether Current as recorded by SETS (23:43:00-01:29:59)

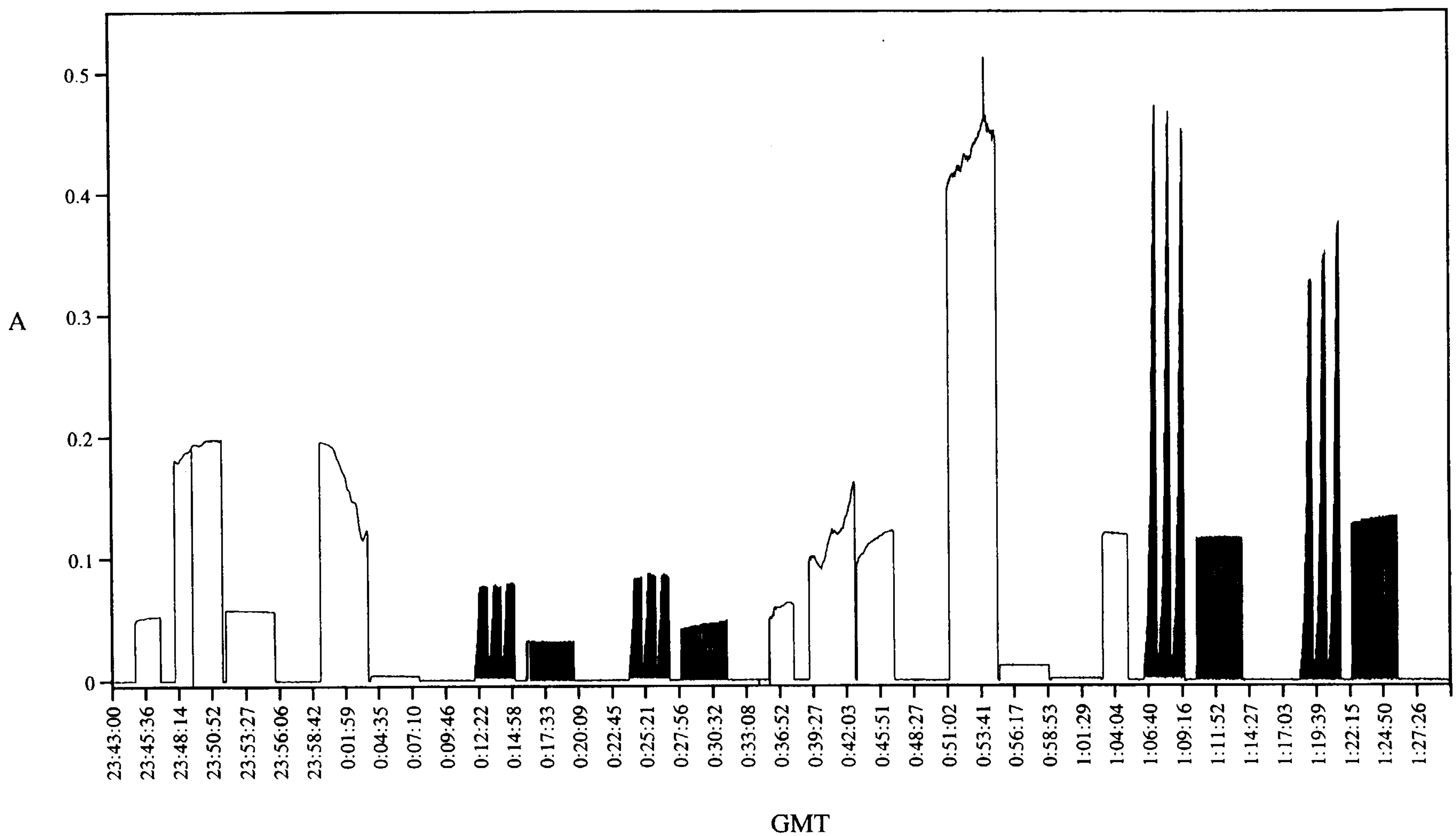

Figure 12.

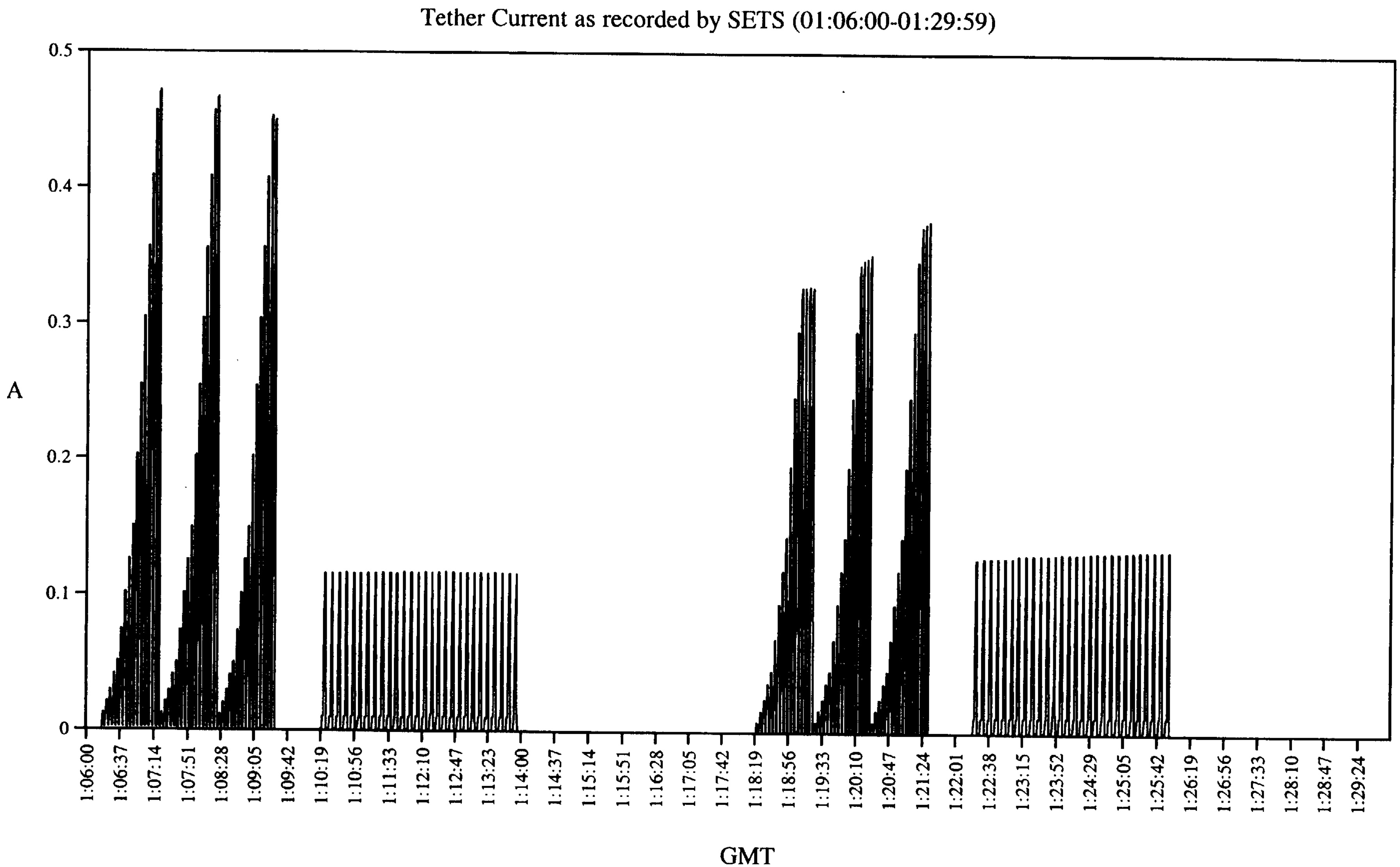
Tether Current as recorded by SETS (01:06:00-01:29:59)
A
0.5
0.4
0.3
0.2
0.1
0
1:06:00
1:06:37
1:07:14
1:07:51
1:08:28
1:09:05
1:09:42
1:10:19
1:10:56
1:11:33
1:12:10
1:12:47
1:13:23
1:14:00
1:14:37
1:15:14
1:15:51
1:16:28
1:17:05
1:17:42
1:18:19
1:18:56
1:19:33
1:20:10
1:20:47
1:21:24
1:22:01
1:22:38
1:23:15
1:23:52
1:24:29
1:25:05
1:25:42
1:26:19
1:26:56
1:27:33
1:28:10
1:28:47
1:29:24
GMT

Figure 13.

Tether Current as recorded by SETS (01:18:00-01:26:00)

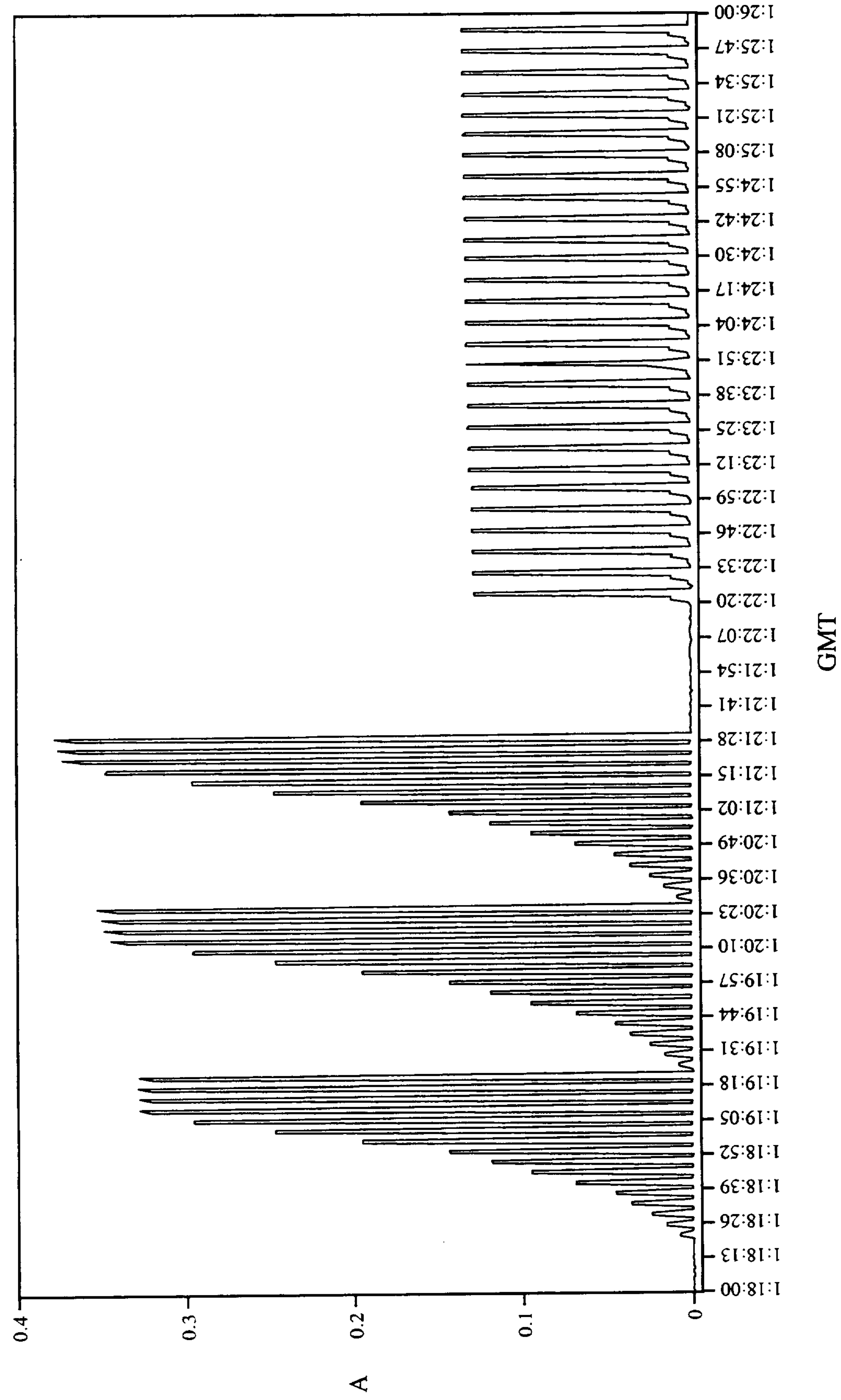

Figure 14.

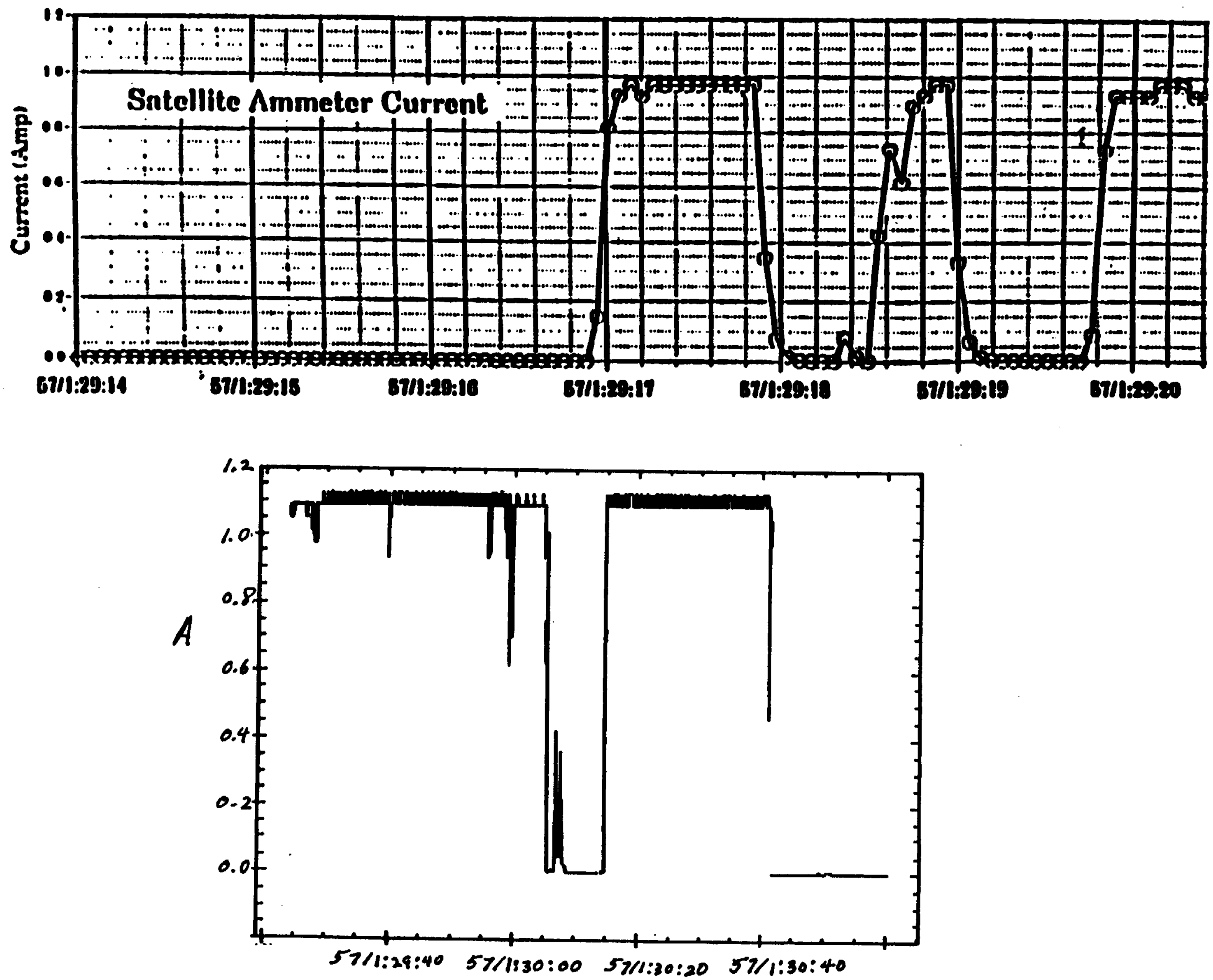

Tether Current Before and After Break

Figure 15.

coincided with the unscheduled and unpredicted one minute of 1 A current in the tether.

Figure 16 shows the TSS-1R passes by the EMET Mona Island site. The dark circle to the south of Mona Island indicates the point from which tracking the geomagnetic field lines at the Shuttle orbital height (300 km) down to 100 km arrives at point directly above Mona. This might be considered the location from which to obtain a "direct hit" of Mona with Alfvén waves from the Shuttle. Ground tracks of the Shuttle orbit are shown by dashed lines, with the orbital revolution since launch shown in bold numerals (49-52). Times in GMT and Mission Elapsed Times (MET) are indicated for a few points along the orbital trajectory, along with the corresponding tether currents and deployed tether lengths. The operating cycles (J2CYCLE, DEP101, and DC24) are also noted. The general location of the Shuttle at the time of the tether break (2° N, 100.4° W) is also indicated. The current reached 1 A with a deployed length of 19.6 km at this point. The opportunities did not look promising.

A similar plot for the Bribie Island (Australia) site is shown in Figure 17. The dark circle to the north of Bribie has the same "direct hit" significance as the one to the south of Mona. Since all of the passes through Bribie's longitude after tether deployment had begun occurred for ground tracks in the northern hemisphere, the Bribie "passes" have to be taken in the magnetoconjugate sense. Even the magnetoconjugate tracks lie far to the north of Bribie. Worse still, all of these "passes" occurred during minutes-long stretches of dead time for the tether current. The chance of seeing anything at Bribie, except for some global effect of the tether current thus seemed to be even smaller than for Mona Island. The largest scheduled tether current (0.4-0.5 A) was achieved while the system was at least on the same side of the Earth as Bribie. In Figure 17 this occurs between 105° E and 126° E on revolution 52 (top track) of the orbit.

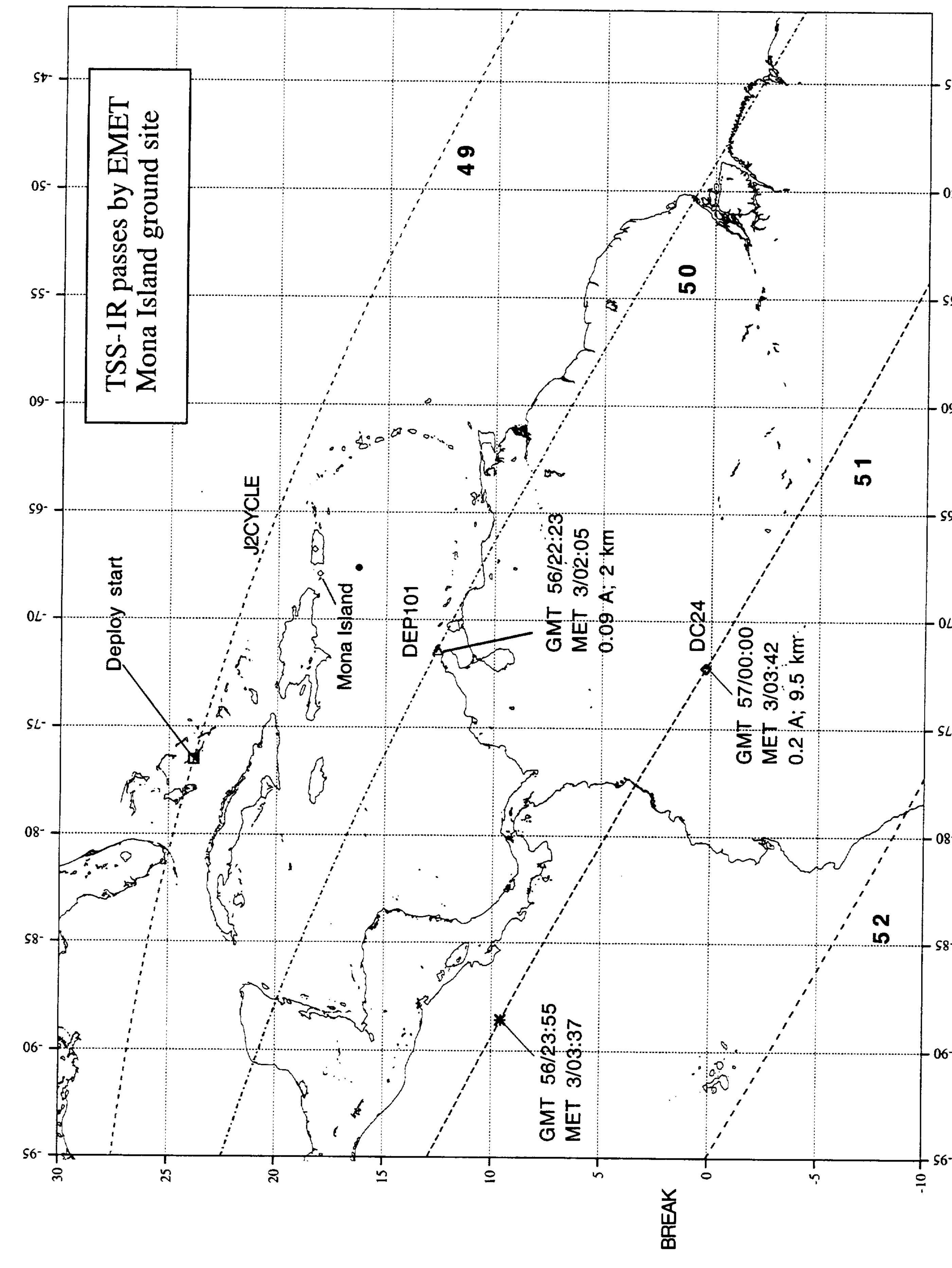

TSS-1R passes by EMET
Mona Island ground site
Deploy start
J2CYCLE
Mona Island
DEP101
GMT 56/22:23
MET 3/02:05
0.09 A; 2 km
DC24
GMT 57/00:00
MET 3/03:42
0.2 A; 9.5 km
GMT 56/23:55
MET 3/03:37
49
50
51
52
-95
-90
-85
-80
-75
-70
-65
-60
-55
-50
-45
30
25
20
15
10
5
0
-5
-10
BREAK

Figure 16.

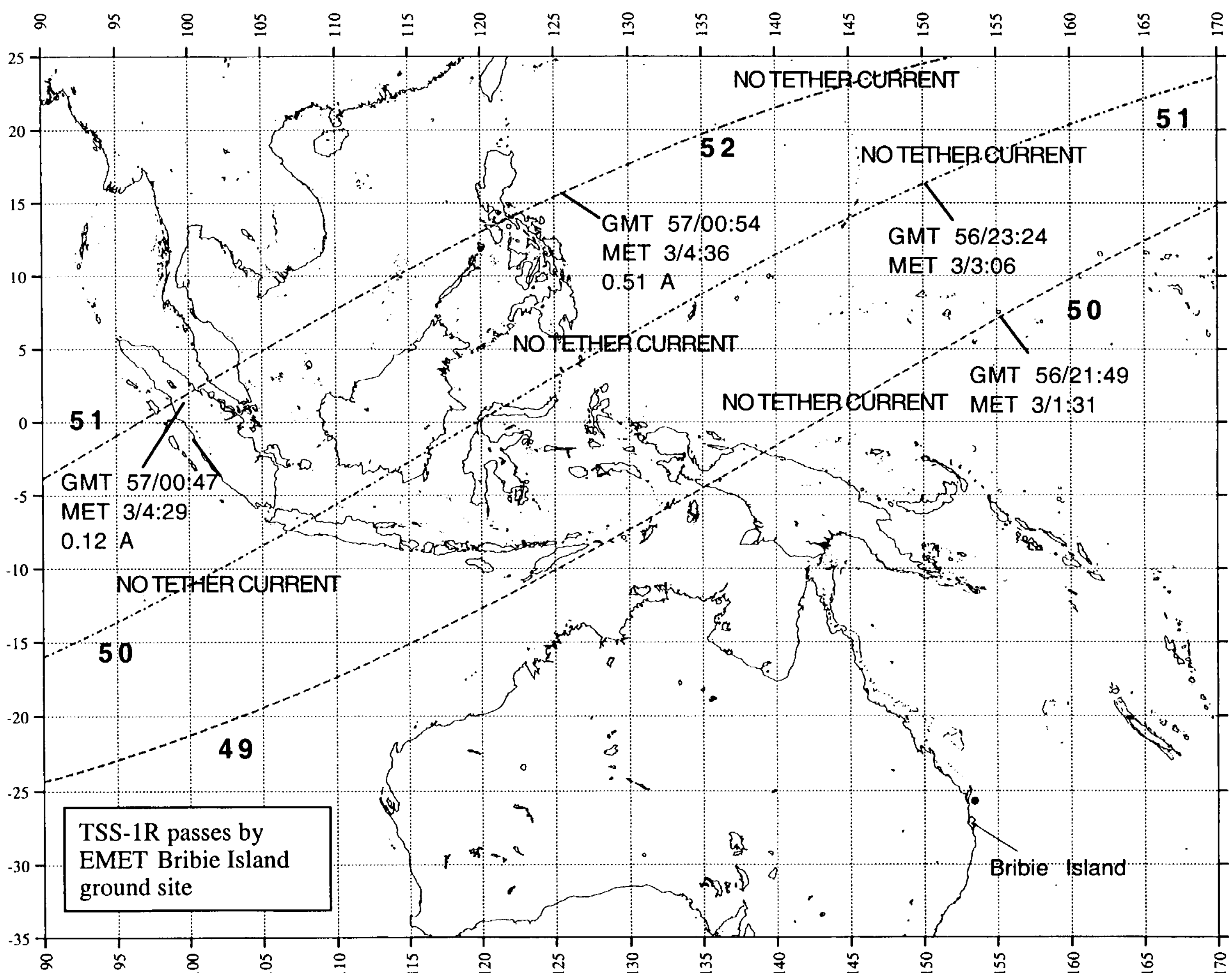

NO TETHER CURRENT
52
51
NO TETHER CURRENT
GMT 57/00:54
MET 3/4:36
0.51 A
GMT 56/23:24
MET 3/3:06
50
NO TETHER CURRENT
GMT 56/21:49
MET 3/1:31
NO TETHER CURRENT
51
GMT 57/00:47
MET 3/4:29
0.12 A
NO TETHER CURRENT
50
49
TSS-1R passes by
EMET Bribie Island
ground site
Bribie Island

Figure 17.

PLOTS FROM THE DIGITAL SIGNAL ANALYZER

We looked at ELF spectra from Mona and Bribie to get a feel for the data and to scan for implausibly strong signals that might show up in such a scan. This was done by playing the data from the Metrum into the Hewlett Packard 3561A Dynamic Signal Analyzer (DSA), concentrating on low frequency data taken around times of crossings of ground-site meridians and at the time of maximum current immediately before and after the break.

Plots obtained from DSA scans of data collected on Mona Island are shown in the following pages (no Figure numbers) for the time periods indicated below. The sample times are all one minute, but spectra shown are averaged over several computed for each period.

pp. 25-26: Mona series 1: DEP101 pass from GMT 56/22:17 to 56/22:28 (MET 3/01:59 to 3/02:10);

pp. 27-29: Mona series 2: passfrom GMT 56/23:43 to 57/00:13 (MET 3/03:25 to 3/03:55);

pp. 30-35: Mona series 3: around time of break from GMT 57/01:00:00 to 57/01:45:00 (MET 3/04:42 to 3/05:/27)

There is nothing remarkable about these spectra, and they are shown here only for completeness. Schumann resonances are of course visible much of the time. The next section will discuss an event whose existence was discovered in the Mona data with the aid of the DSA, but which was of such brief duration that it did not show up in these scans.

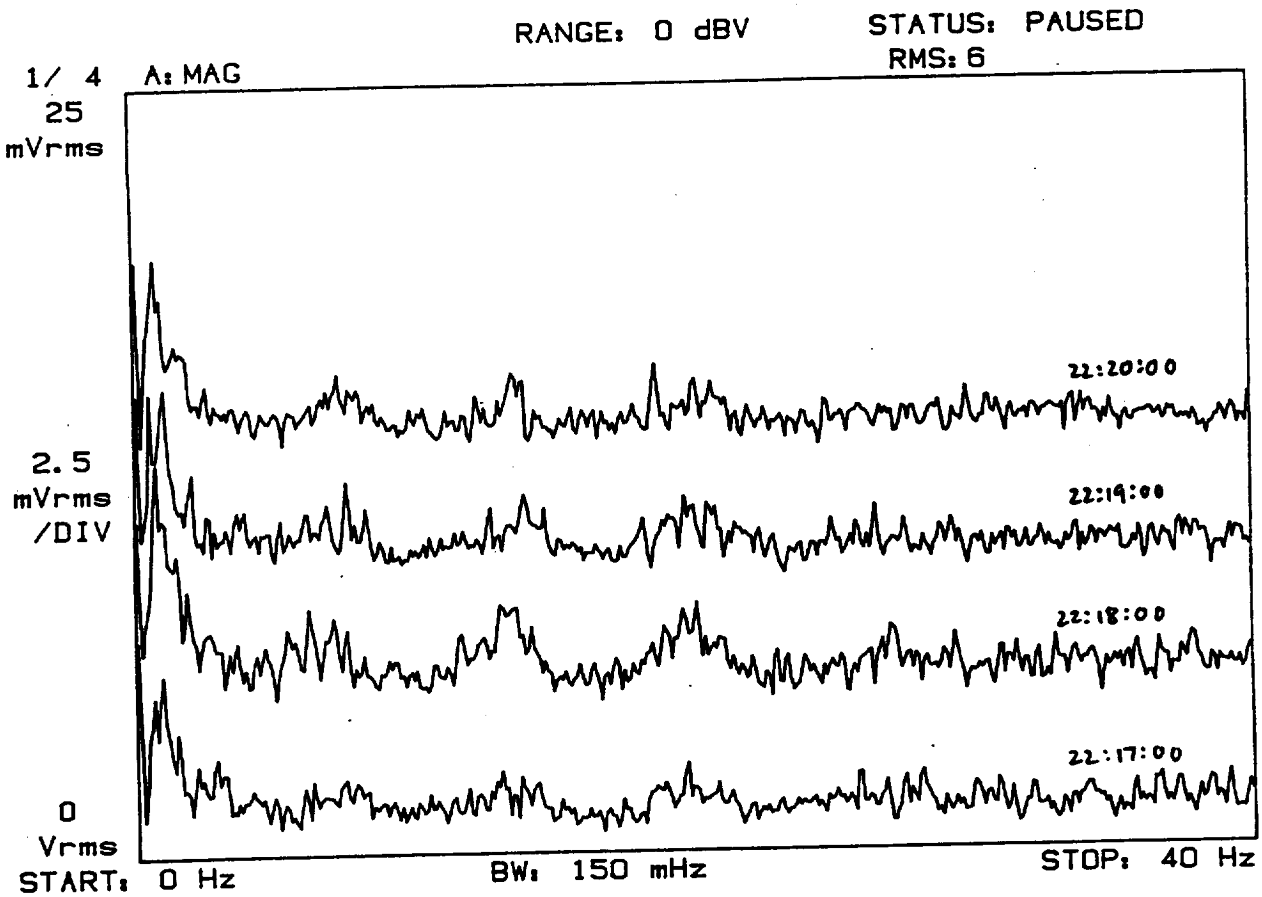

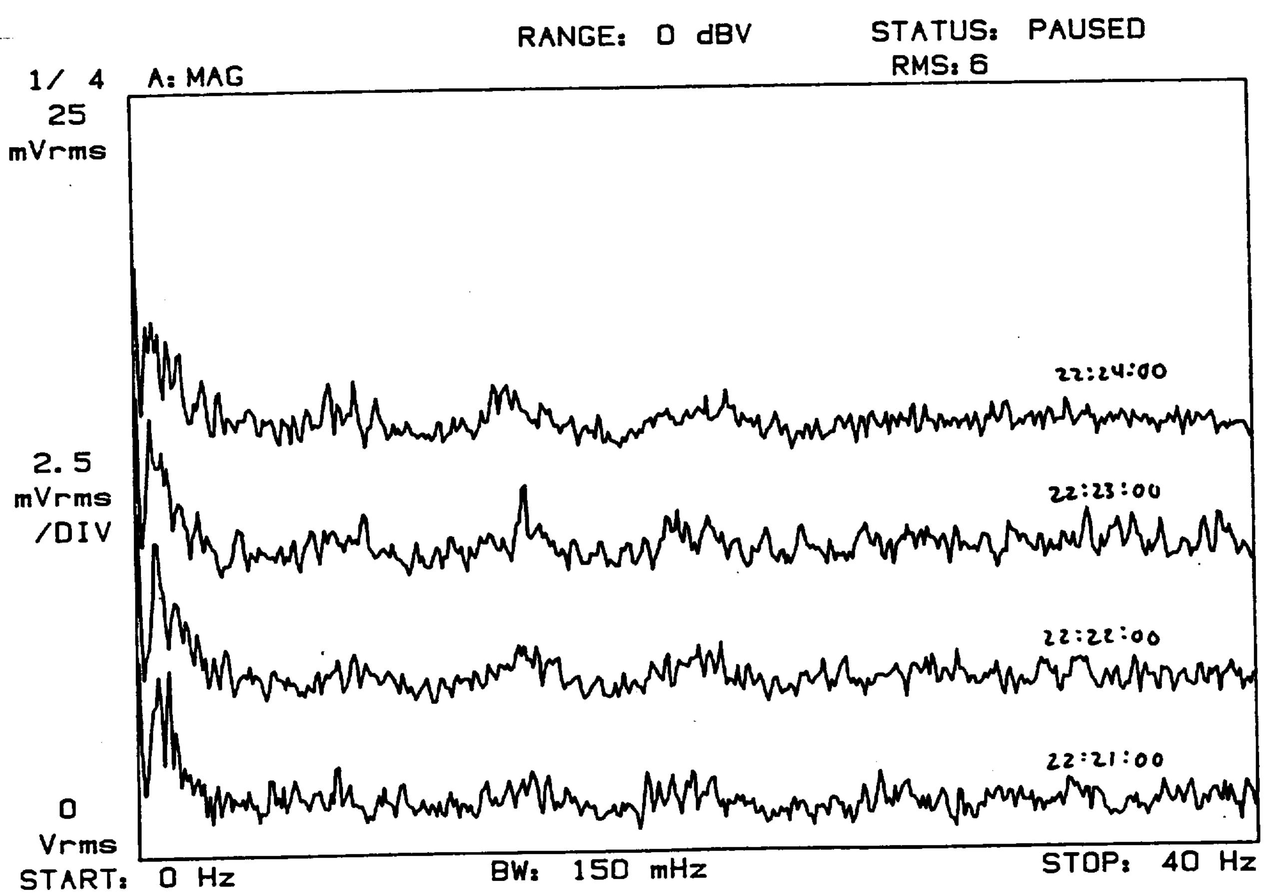

Mona series 1(a)-(b): 0.5-50 Hz NS channel, 0-40 Hz shown, integration time of 1 minute, end of period indicated in GMT

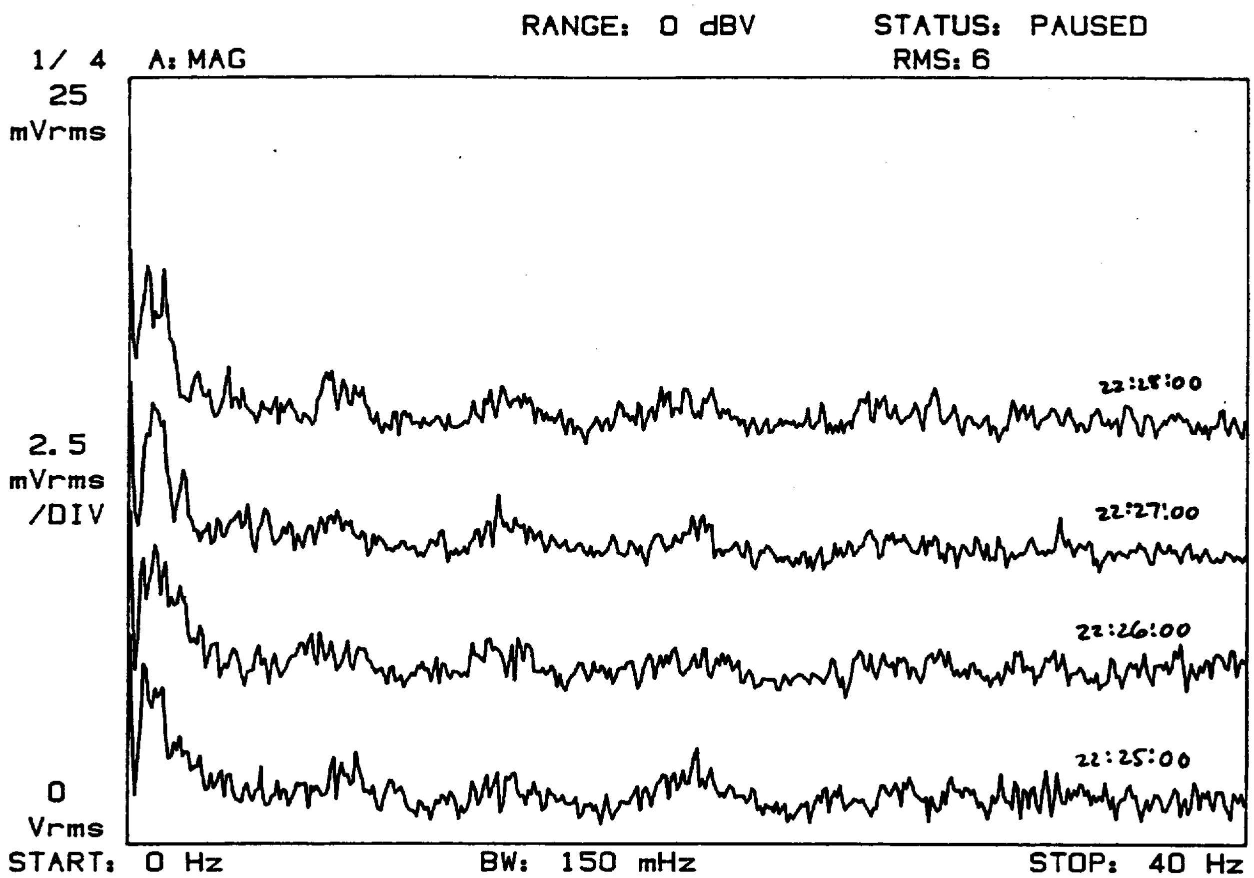

Mona series 1(c): 0.5-50 Hz NS channel, 0-40 Hz shown, integration time of 1 minute, end of period indicated in GMT

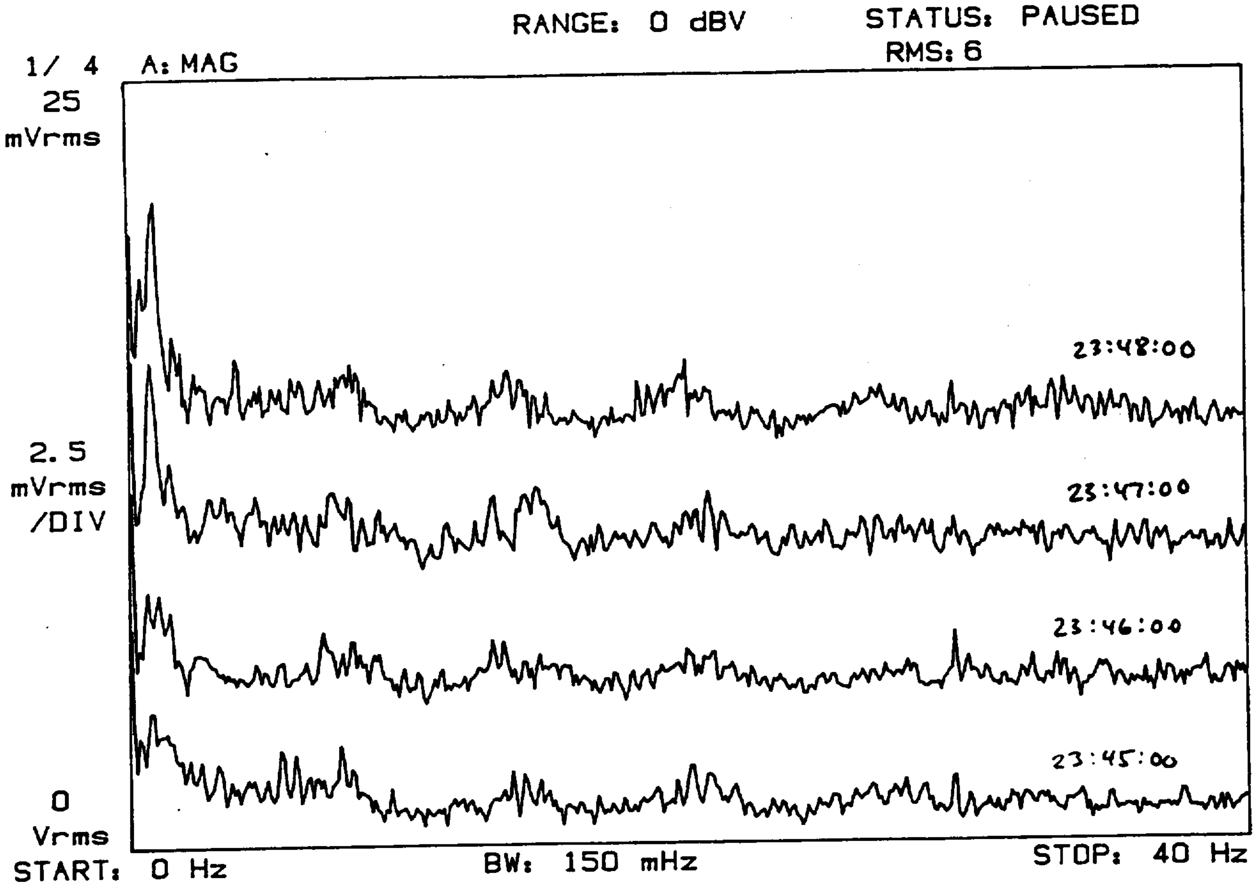

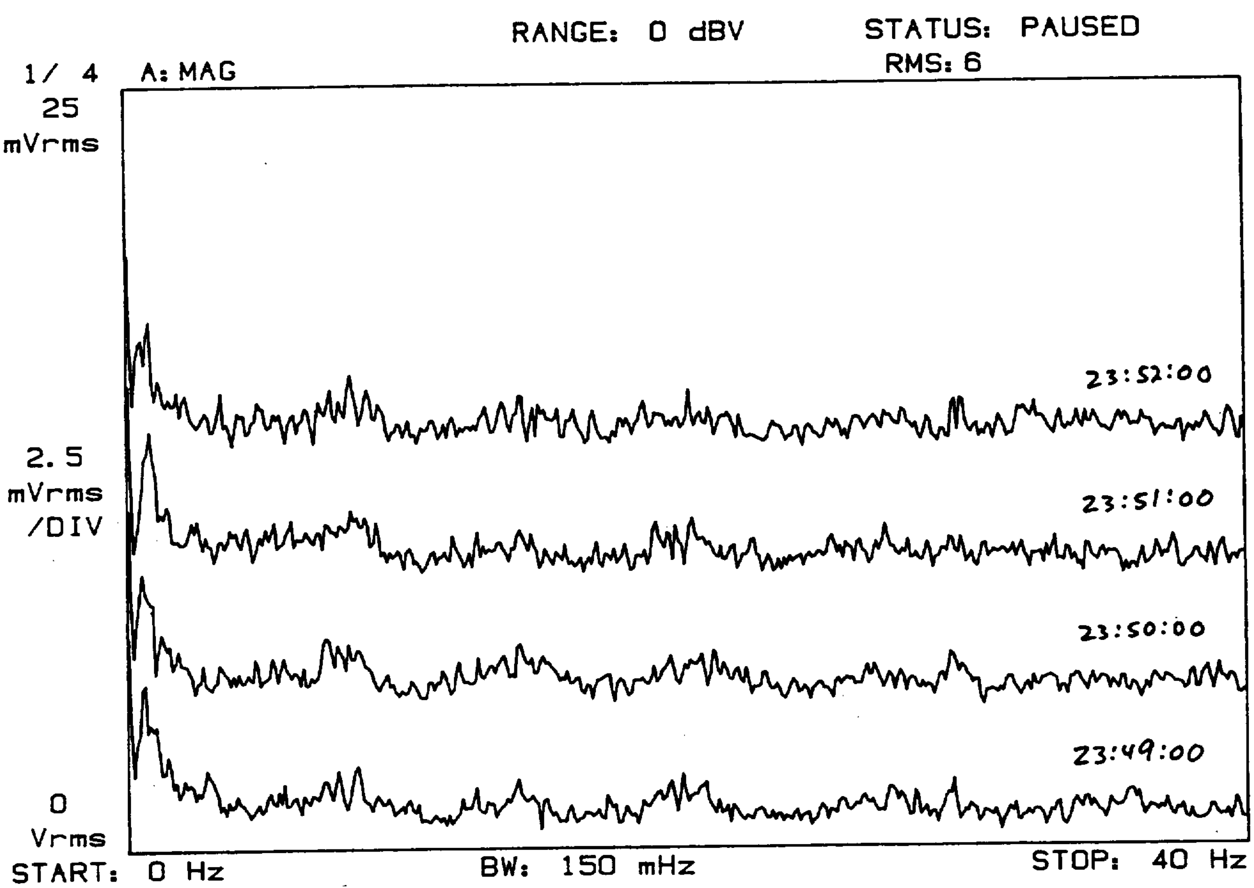

Mona series 2(a)-(b): 0.5-50 Hz NS channel, 0-40 Hz shown, integration time of 1 minute, end of period indicated in GMT

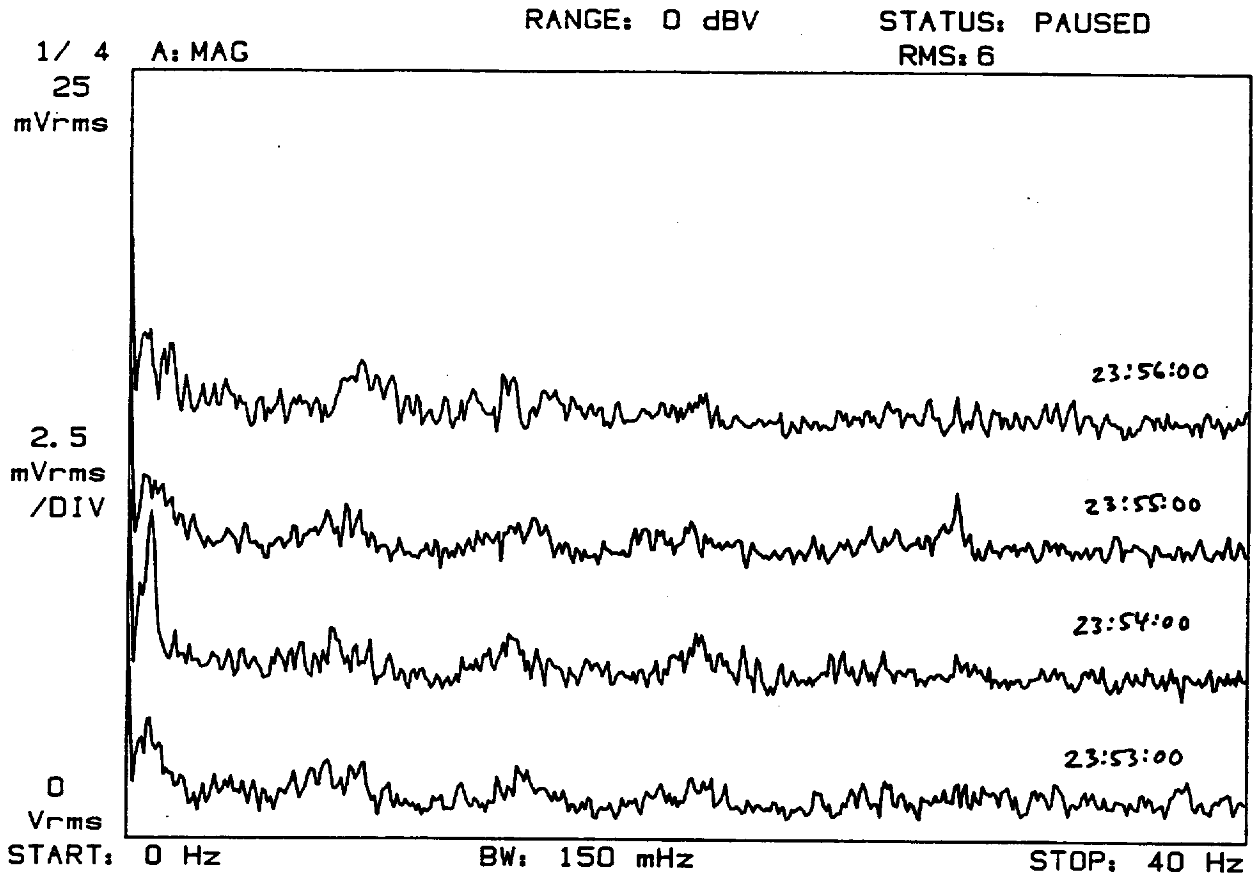

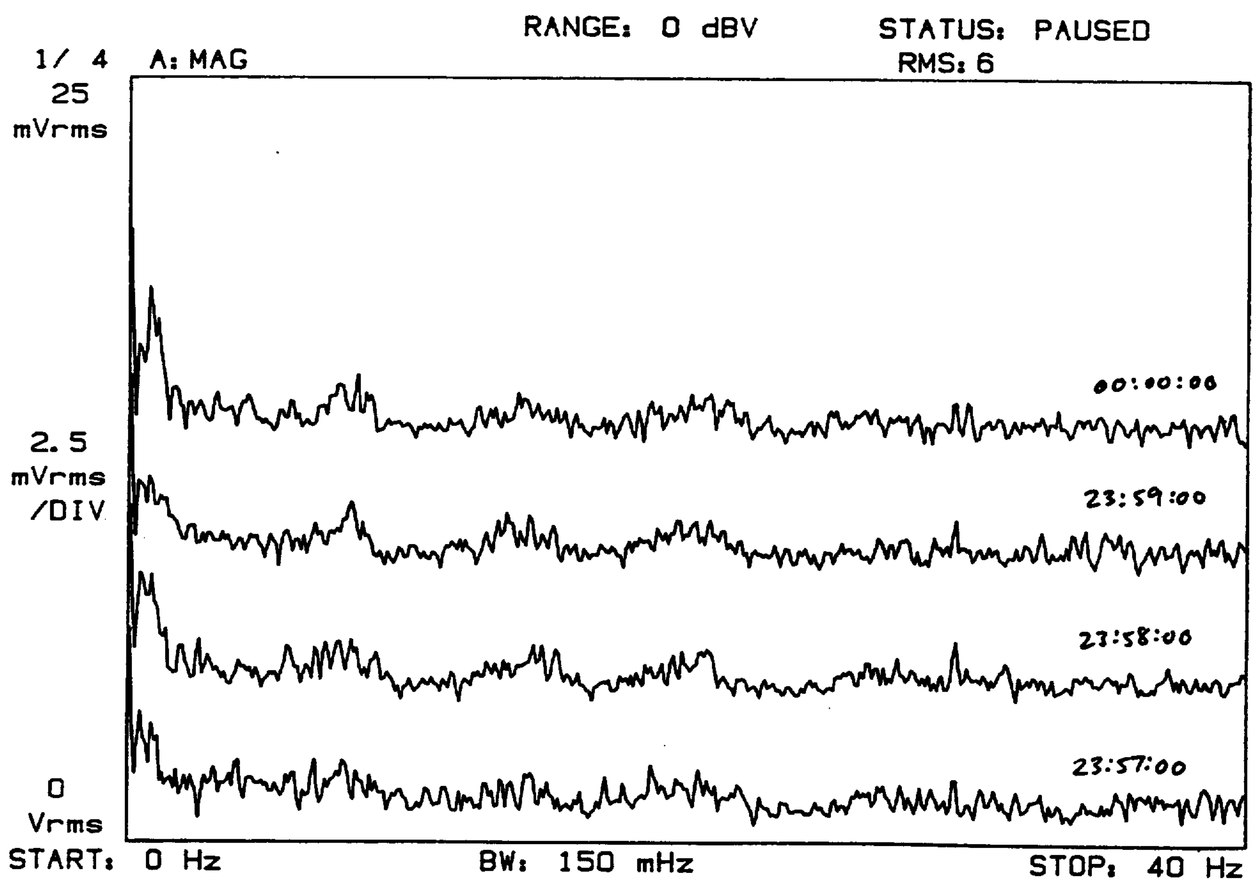

Mona series 2(c)-(d): 0.5-50 Hz NS channel, 0-40 Hz shown, integration time of 1 minute, end of period indicated in GMT

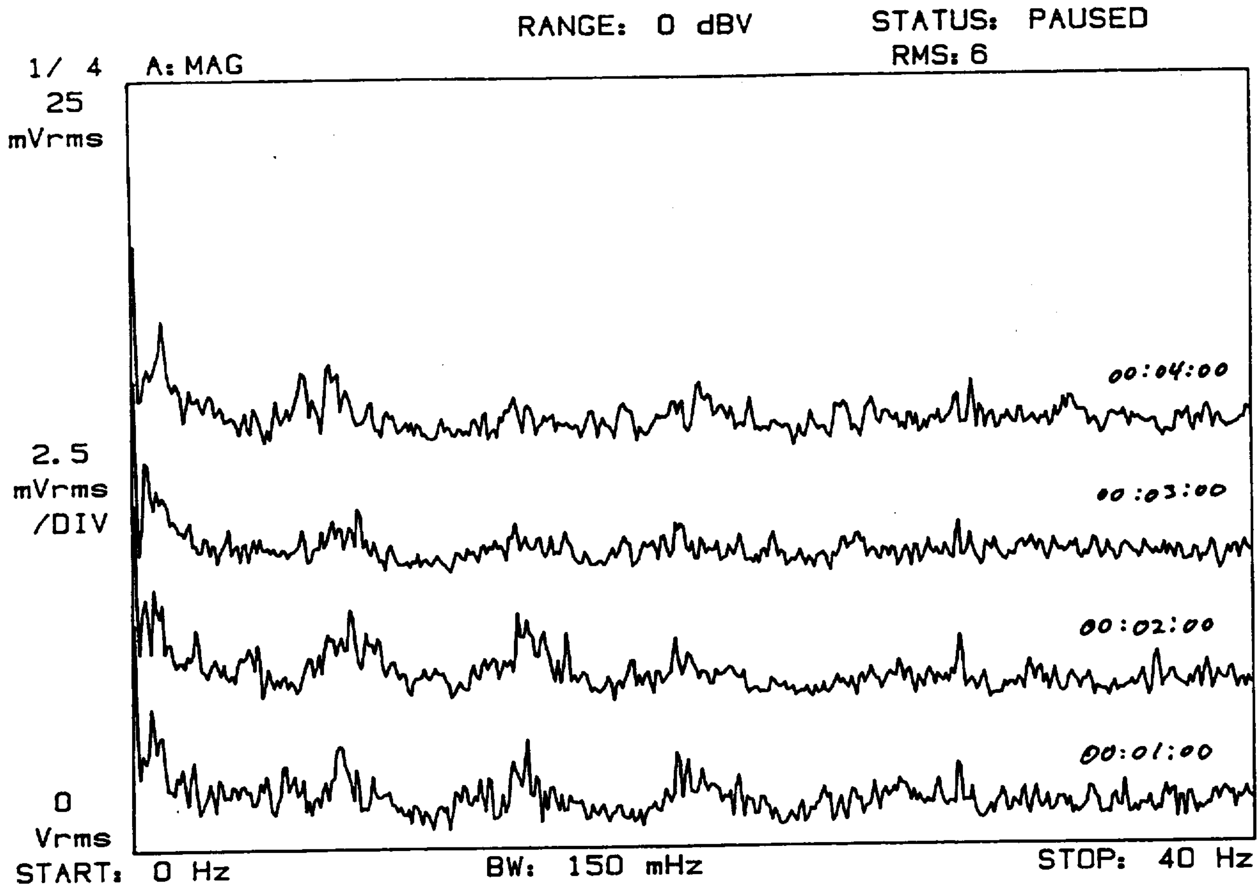

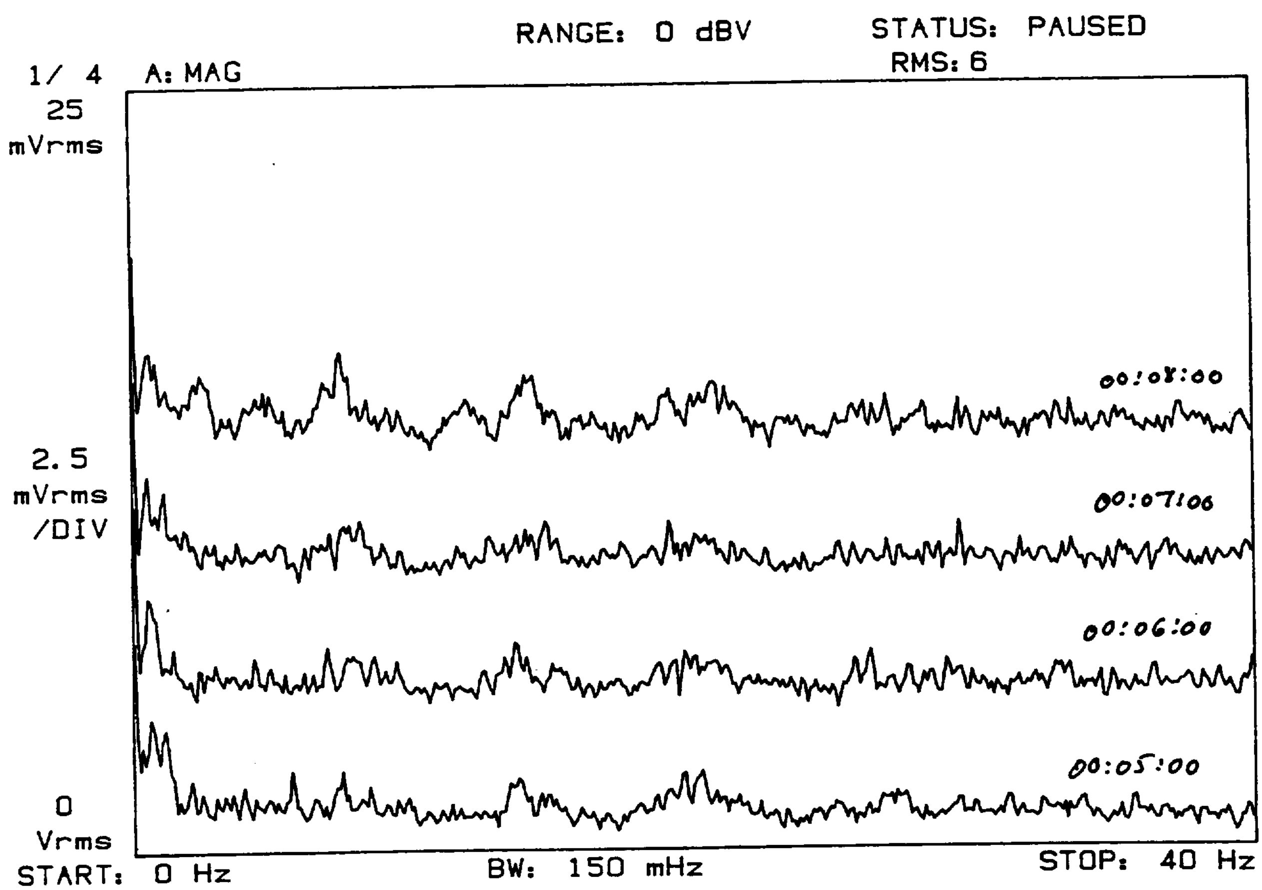

Mona series 2(e)-(f): 0.5-50 Hz NS channel, 0-40 Hz shown, integration time of 1 minute, end of period indicated in GMT

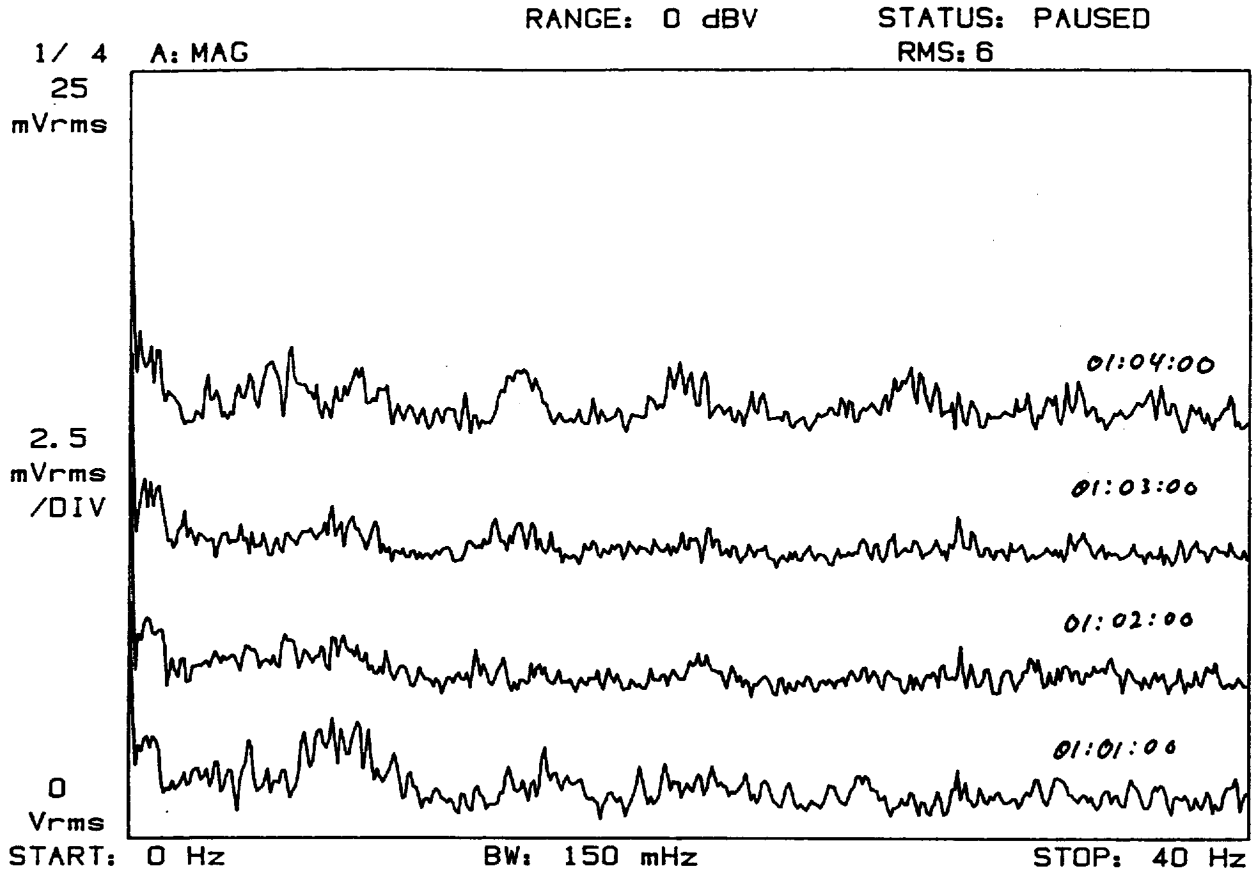

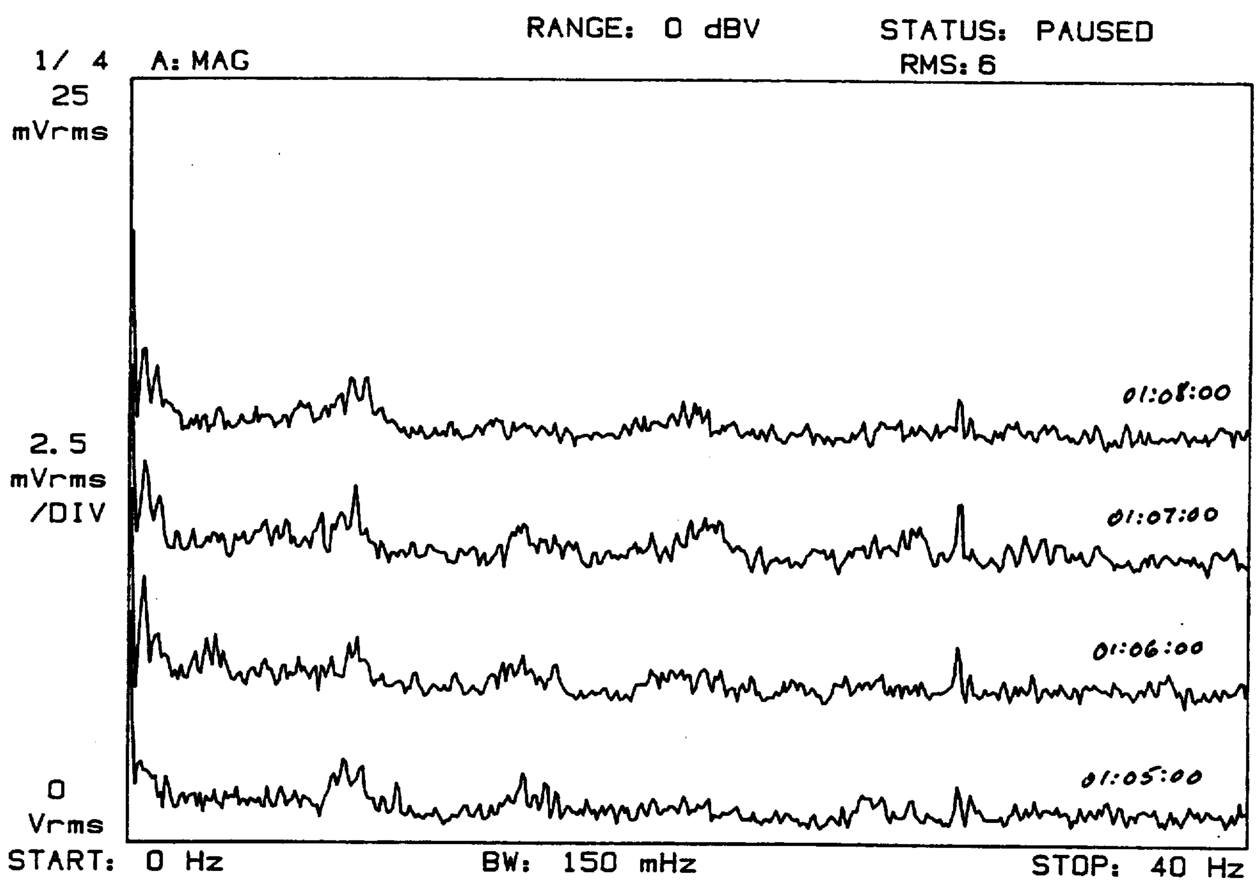

Mona series 3(a)-(b): 0.5-50 Hz NS channel, 0-40 Hz shown, integration time of 1 minute, end of period indicated in GMT

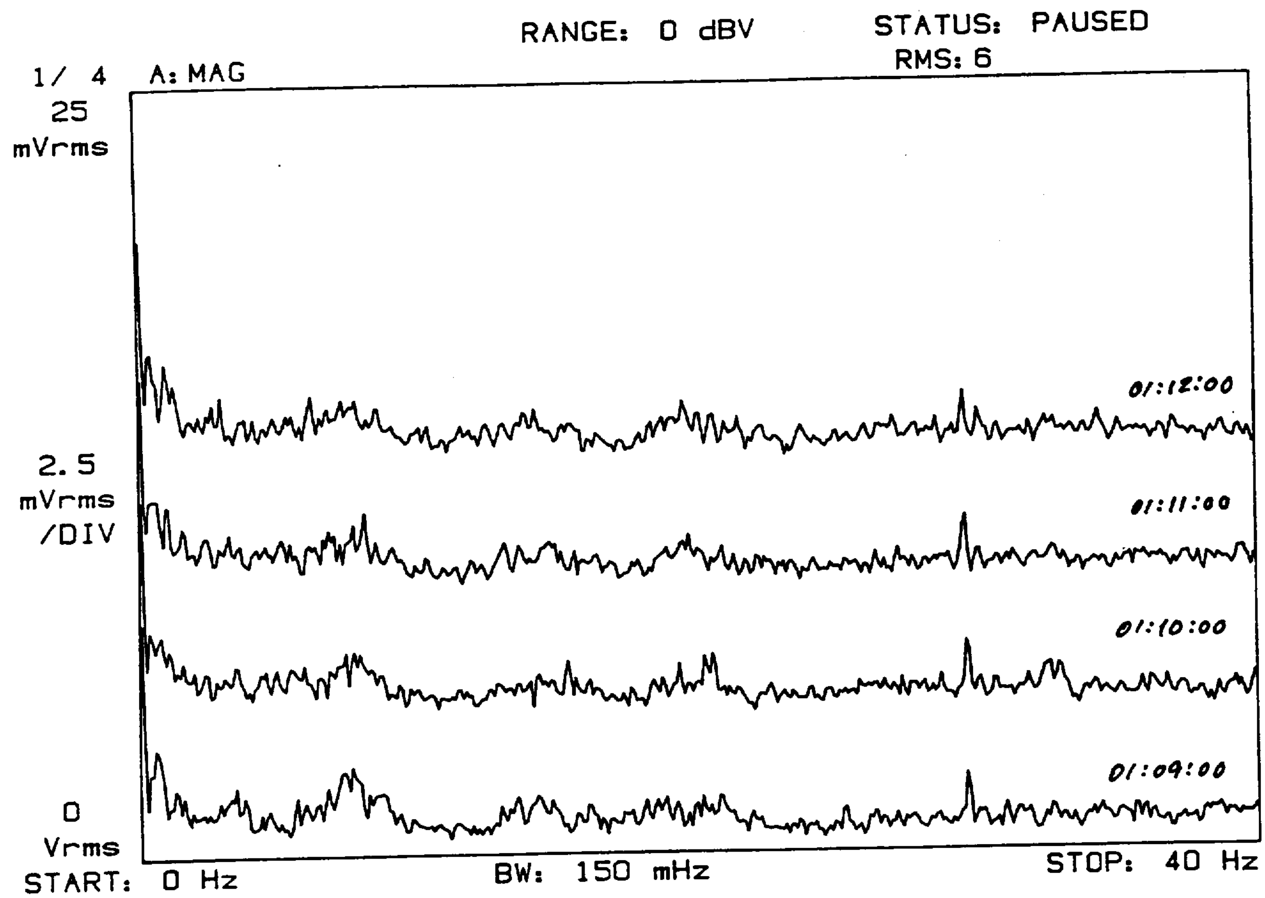

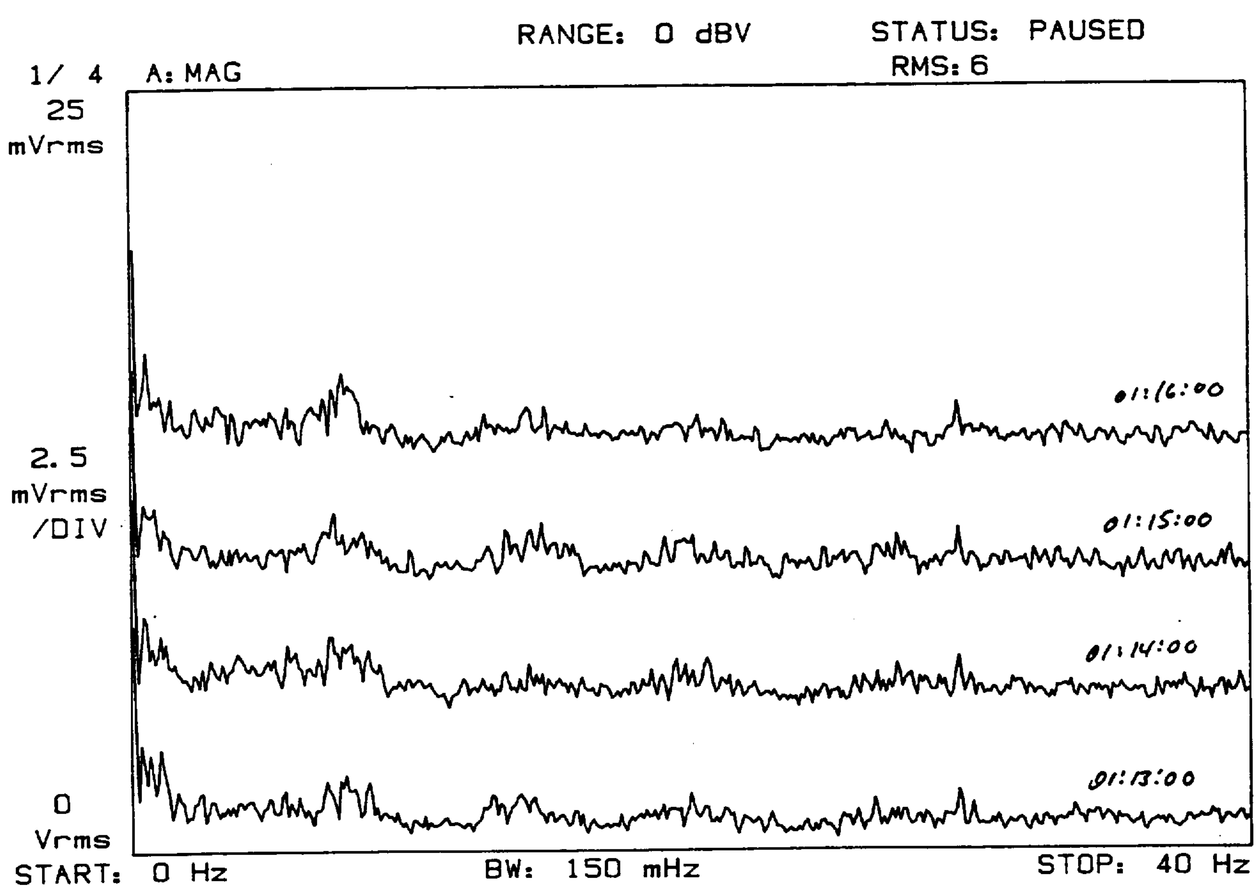

Mona series 3(c)-(d): 0.5-50 Hz NS channel, 0-40 Hz shown, integration time of 1 minute, end of period indicated in GMT

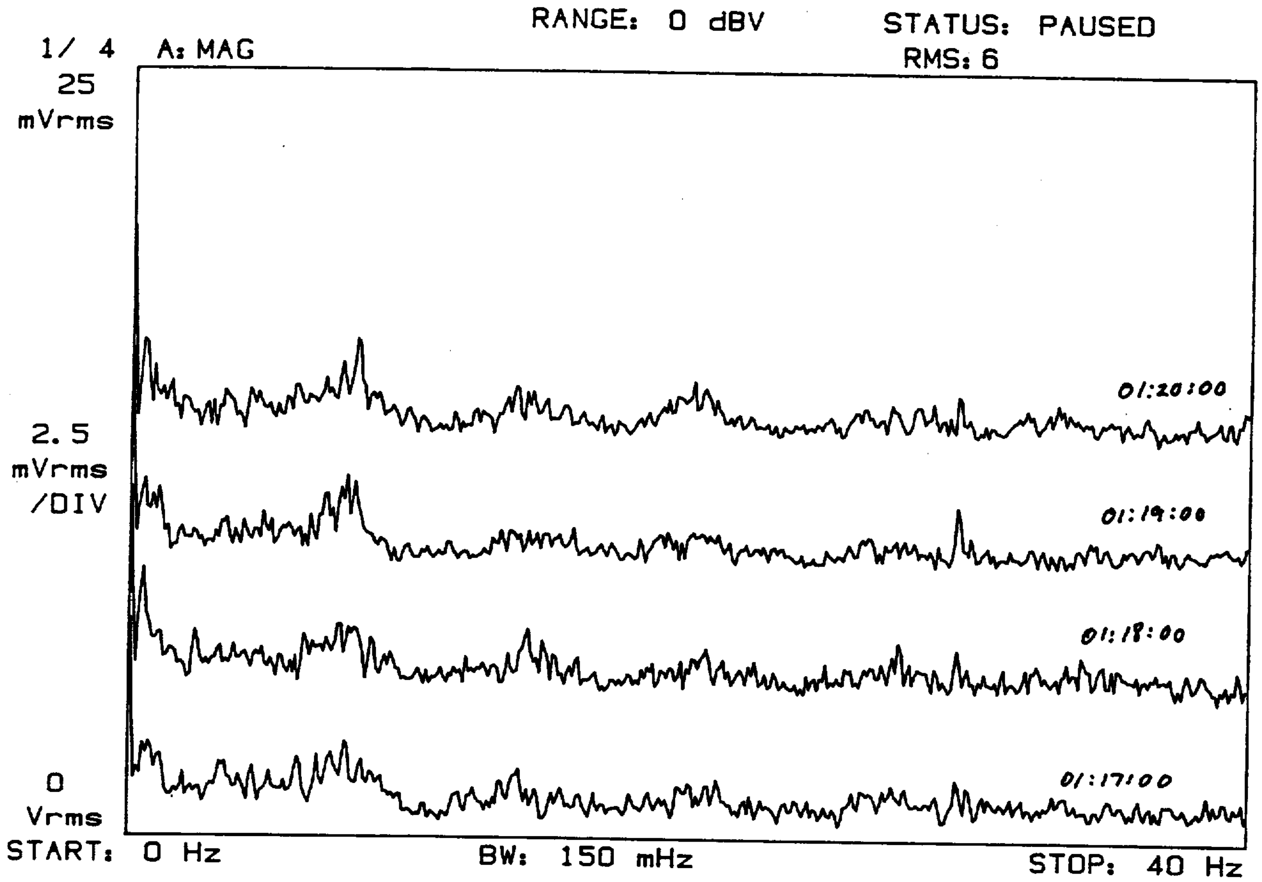

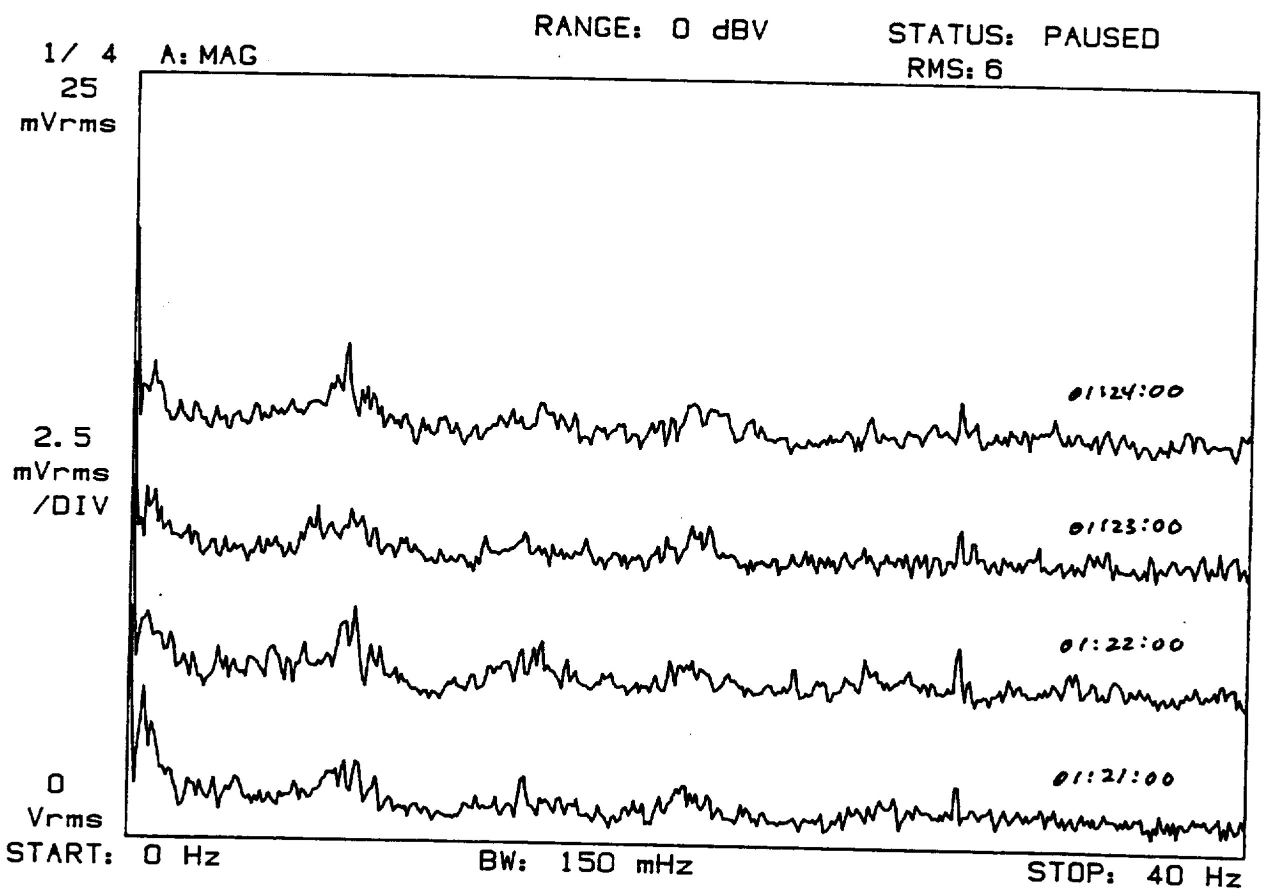

Mona series 3(e)-(f): 0.5-50 Hz NS channel, 0-40 Hz shown, integration time of 1 minute, end of period indicated in GMT

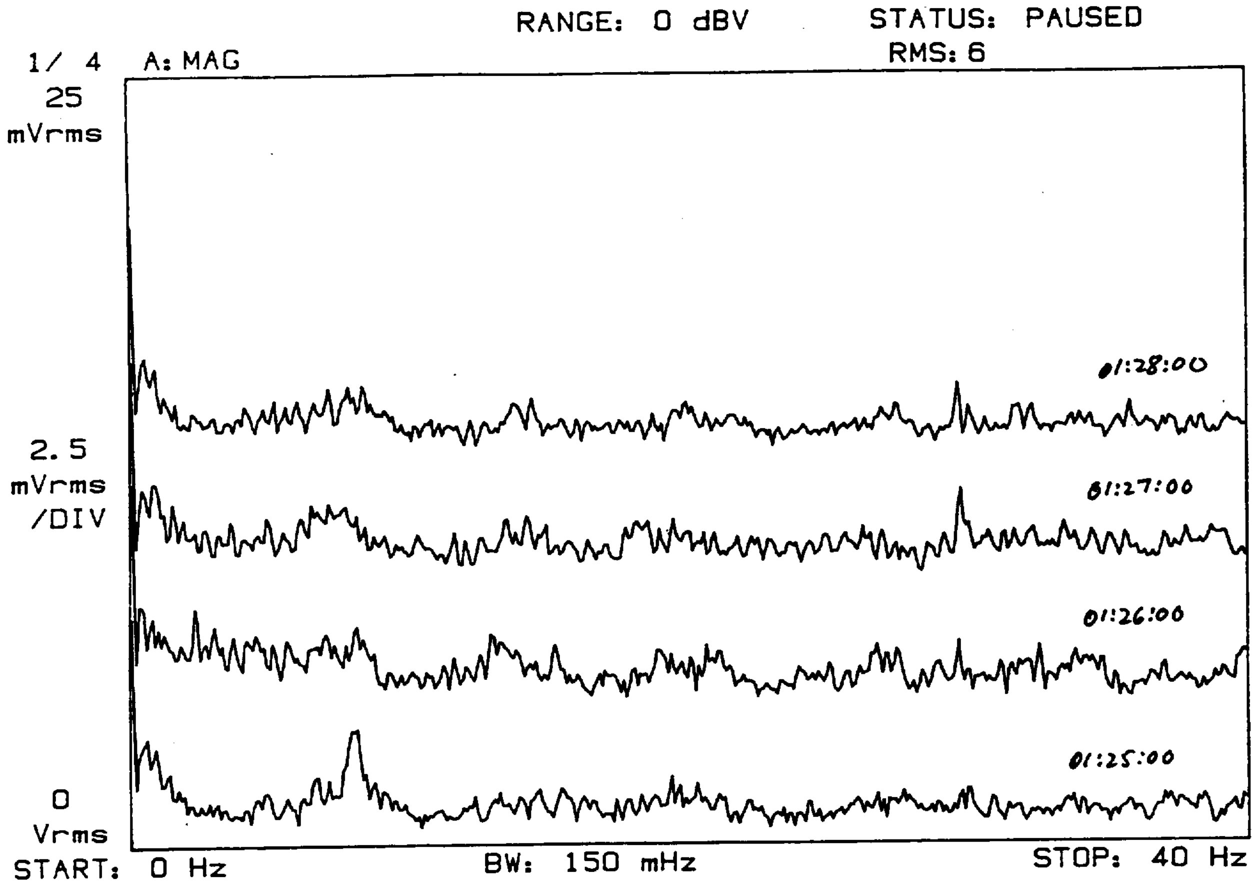

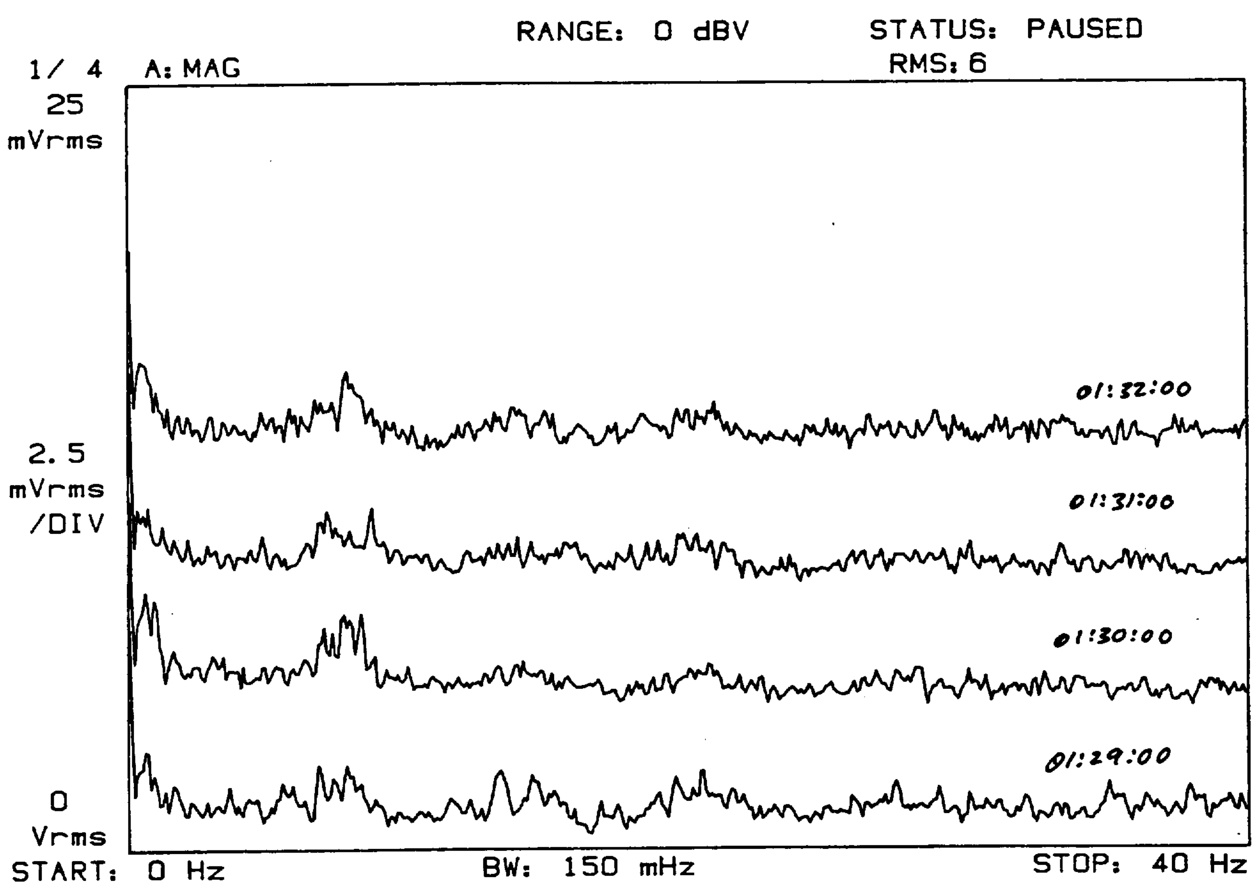

Mona series 3(g)-(h): 0.5-50 Hz NS channel, 0-40 Hz shown, integration time of 1 minute, end of period indicated in GMT

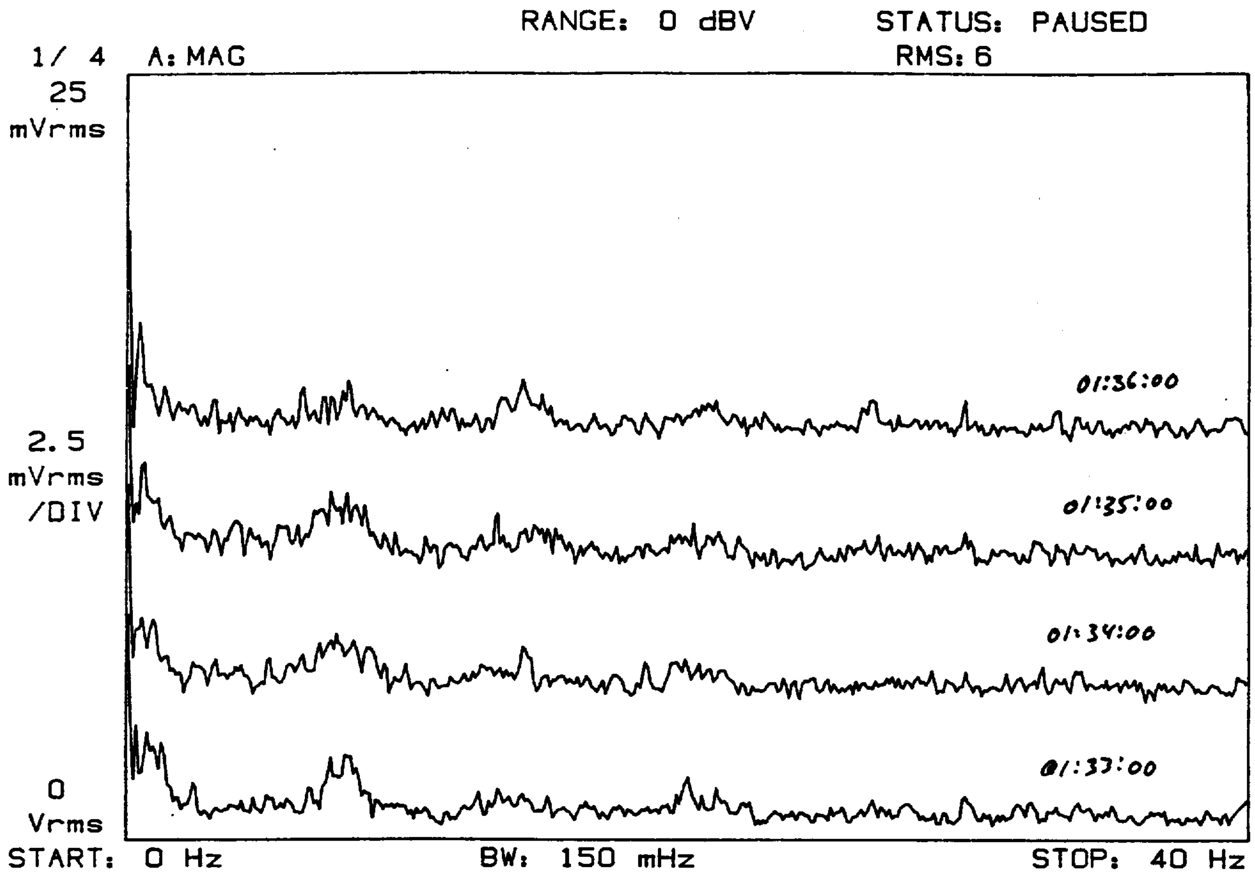

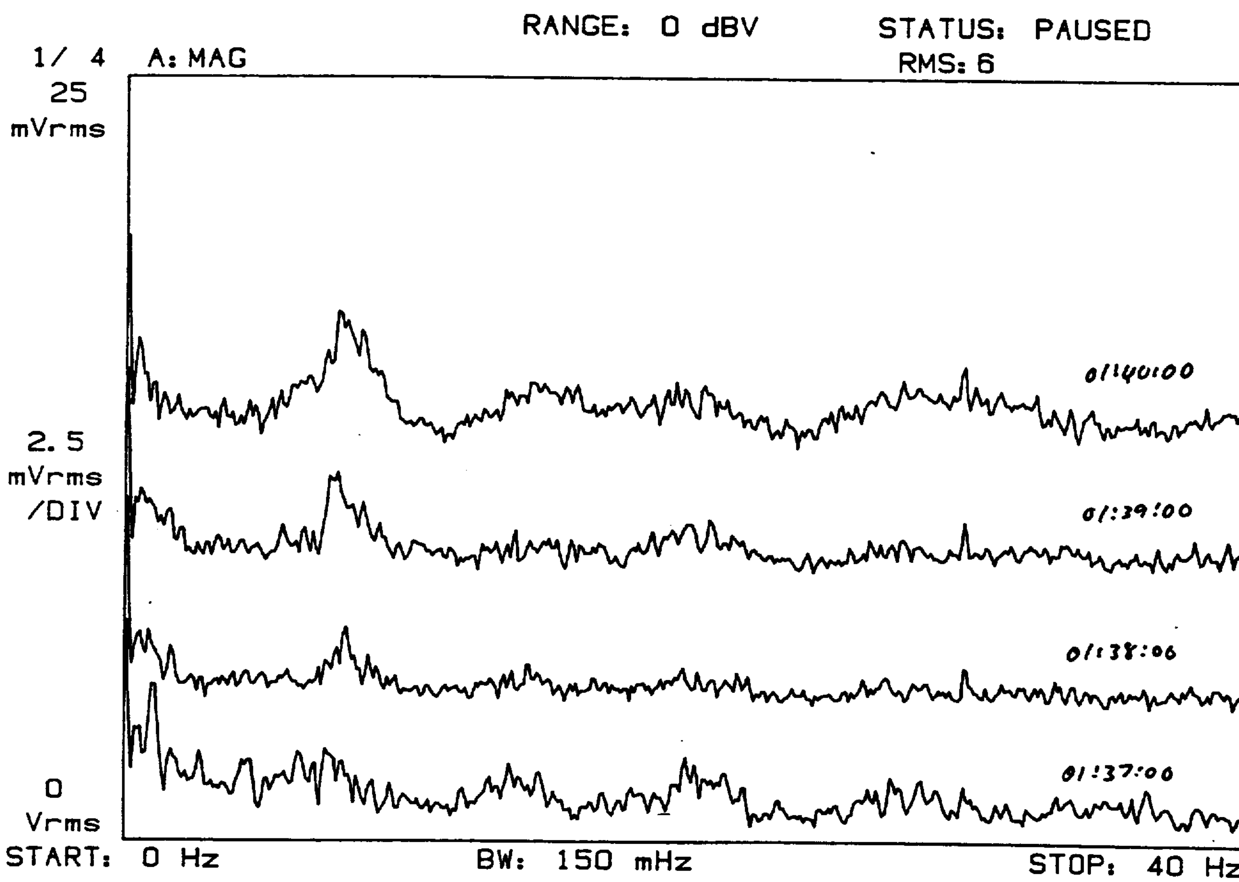

Mona series 3(i)-(j): 0.5-50 Hz NS channel, 0-40 Hz shown, integration time of 1 minute, end of period indicated in GMT

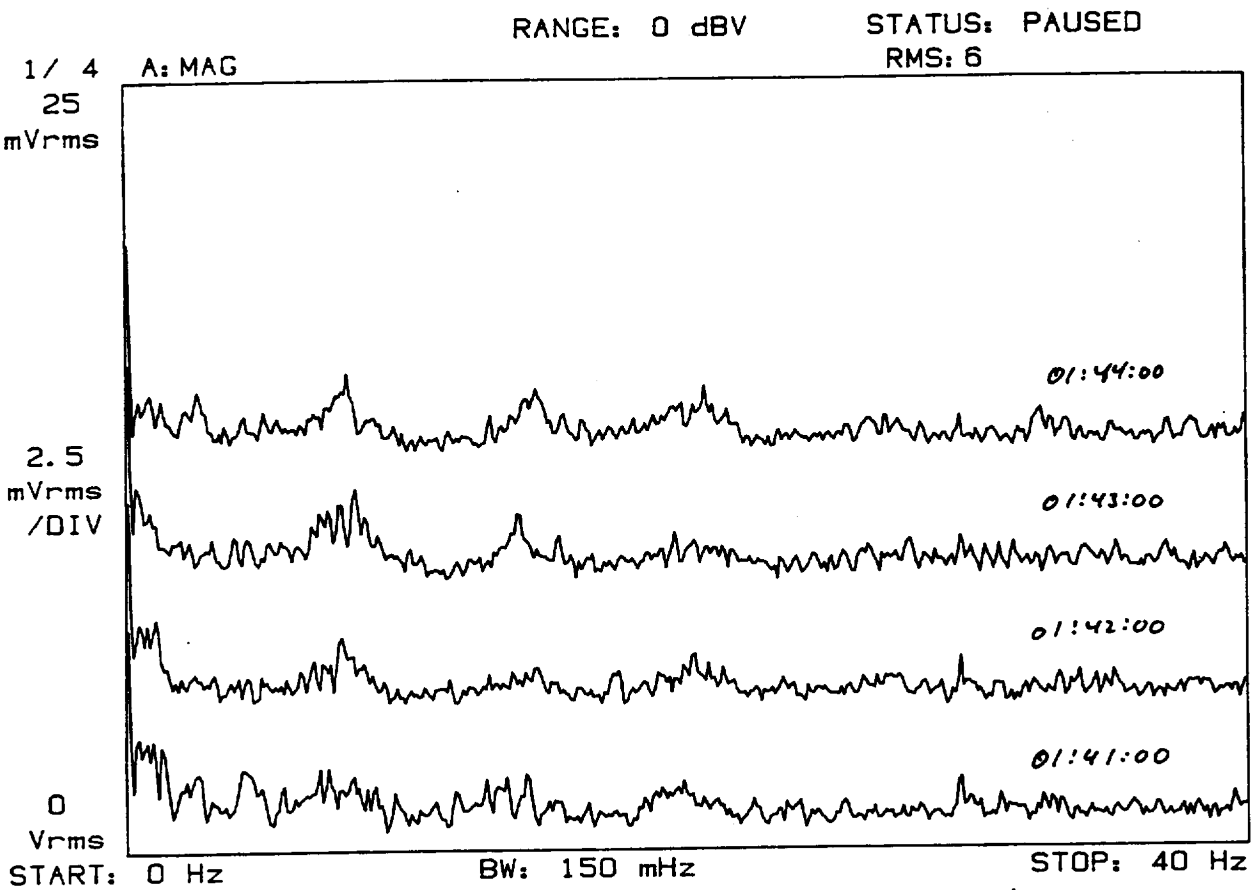

Mona series 3(k): 0.5-50 Hz NS channel, 0-40 Hz shown, integration time of 1 minute, end of period indicated in GMT

Figures 18-20 show the integrated signal for Bribie Island (obtained with the DSA) over the range 0.5-50Hz for 20 second intervals from GMT 57/00:45:00 to 57/01:45:00 (MET 3/04:27 to 3/05:27) for the NS, EW, and vertically aligned sensors. The Bribie DSA spectral plots (NS) at one minute intervals for the same time period follow (no Figure numbers) on pp.40-47. There is evidence for some 30-35 Hz disturbance on Bribie which showed up in the integrated spectra of Figures 18-20. This especially caught our attention because we also saw an even narrower, strong peak in the Mona integrated data (see Figures 21-23) from a few minutes earlier. This Mona event is discussed in the next section. The Bribie disturbance, however, can be seen over several minutes (Bribie series k-o). There is no reason to think that this was due to tether currents, since it began at a time when no current was flowing and continued for some 13 minutes after tether currents had ceased after the break.

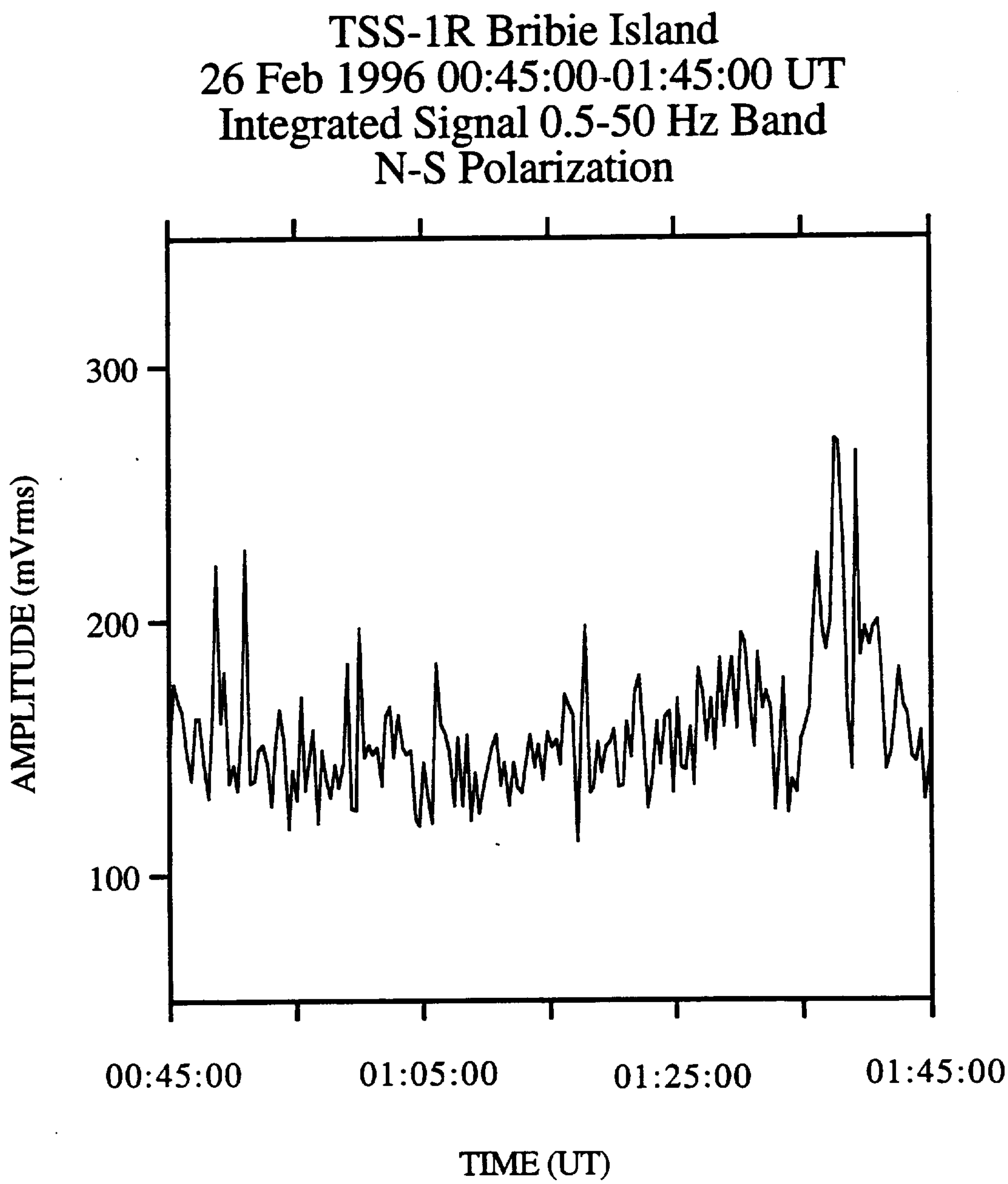
TSS-1R Bribie Island
26 Feb 1996 00:45:00-01:45:00 UT
Integrated Signal 0.5-50 Hz Band
N-S Polarization
300
200
100
AMPLITUDE (mVrms)
00:45:00
01:05:00
01:25:00
01:45:00
TIME (UT)

Figure 18.

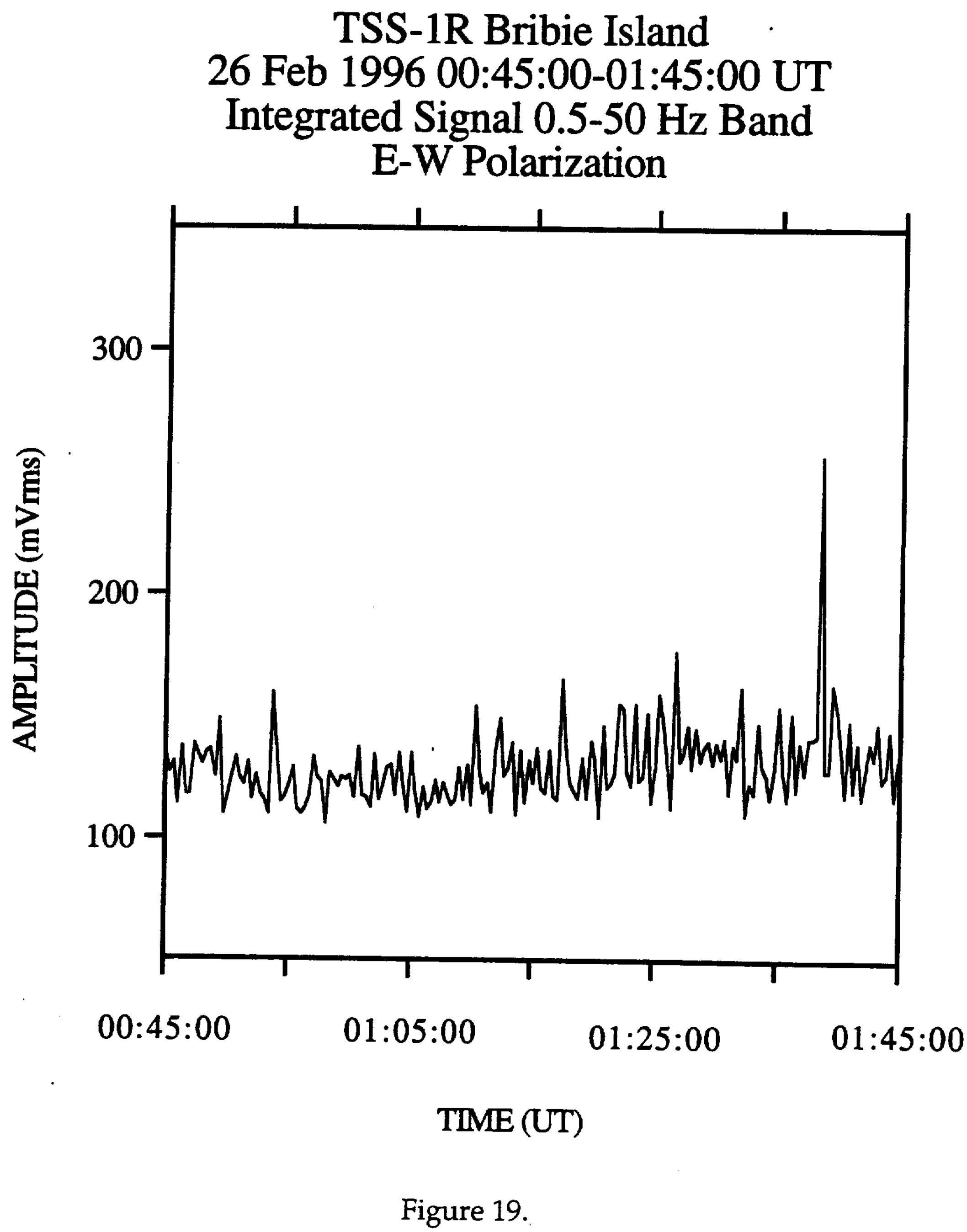

TSS-1R Bribie Island
26 Feb 1996 00:45:00-01:45:00 UT
Integrated Signal 0.5-50 Hz Band
E-W Polarization
300
200
100
AMPLITUDE (mVrms)
00:45:00
01:05:00
01:25:00
01:45:00
TIME (UT)

Figure 19.

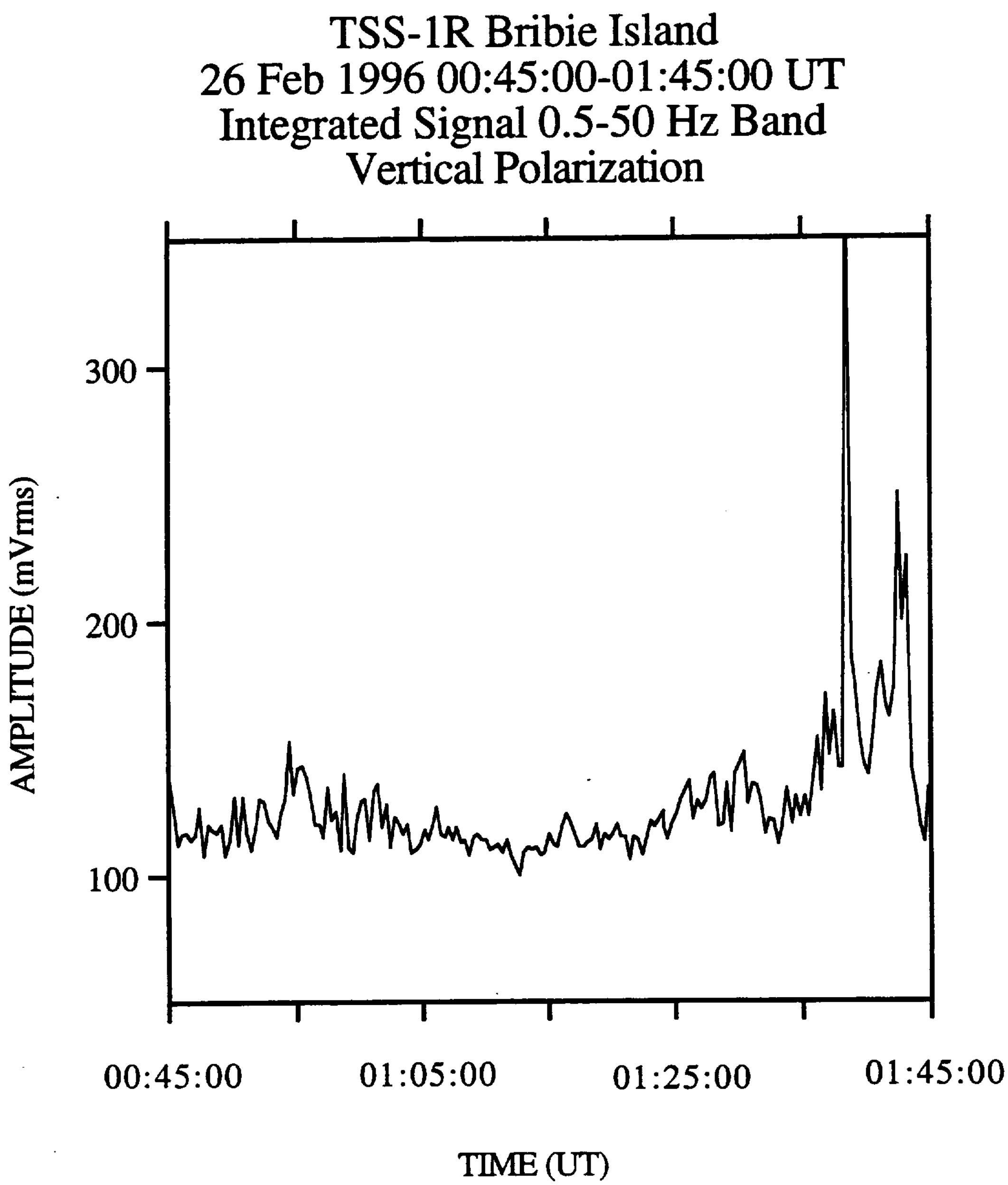
TSS-1R Bribie Island
26 Feb 1996 00:45:00-01:45:00 UT
Integrated Signal 0.5-50 Hz Band
Vertical Polarization
AMPLITUDE (mVrms)
300
200
100
00:45:00
01:05:00
01:25:00
01:45:00
TIME (UT)

Figure 20.

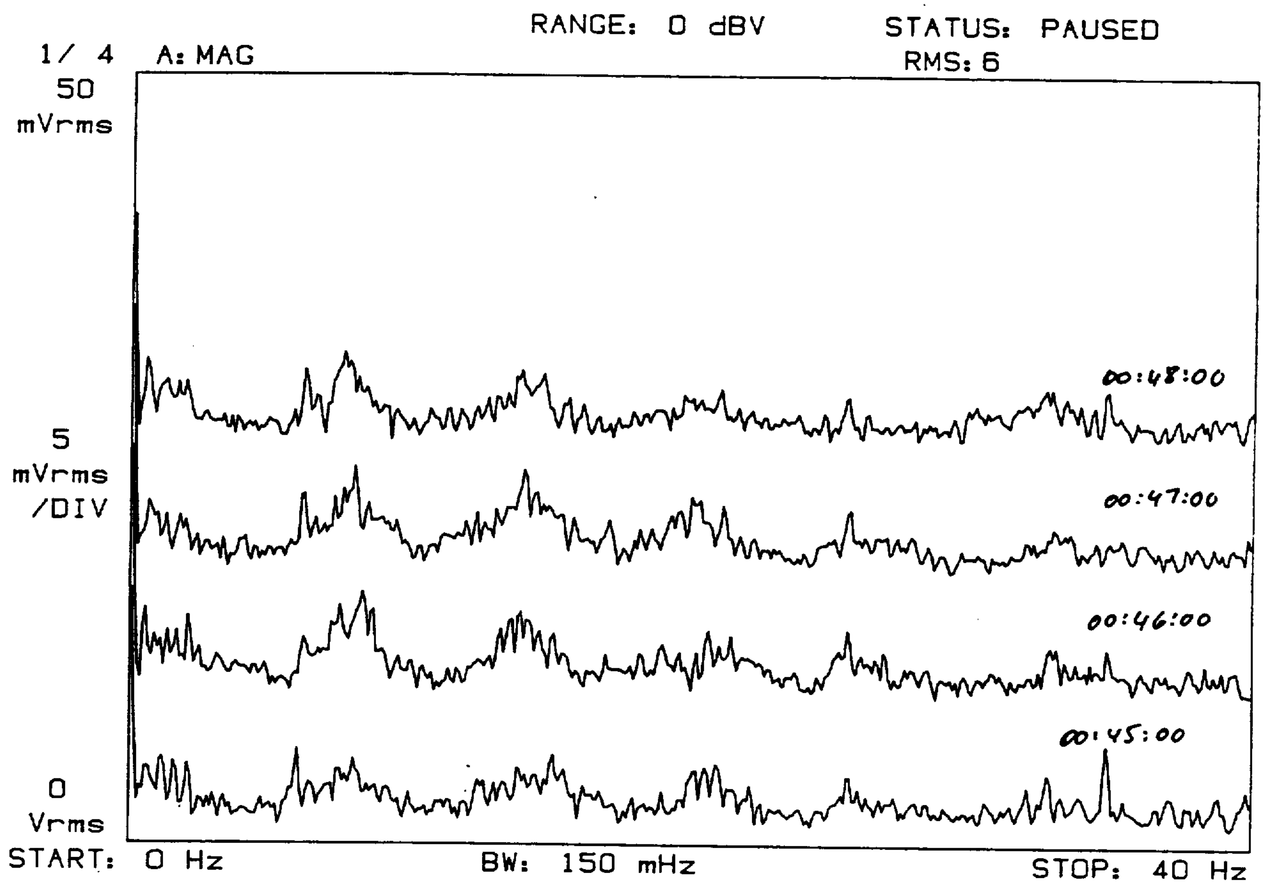

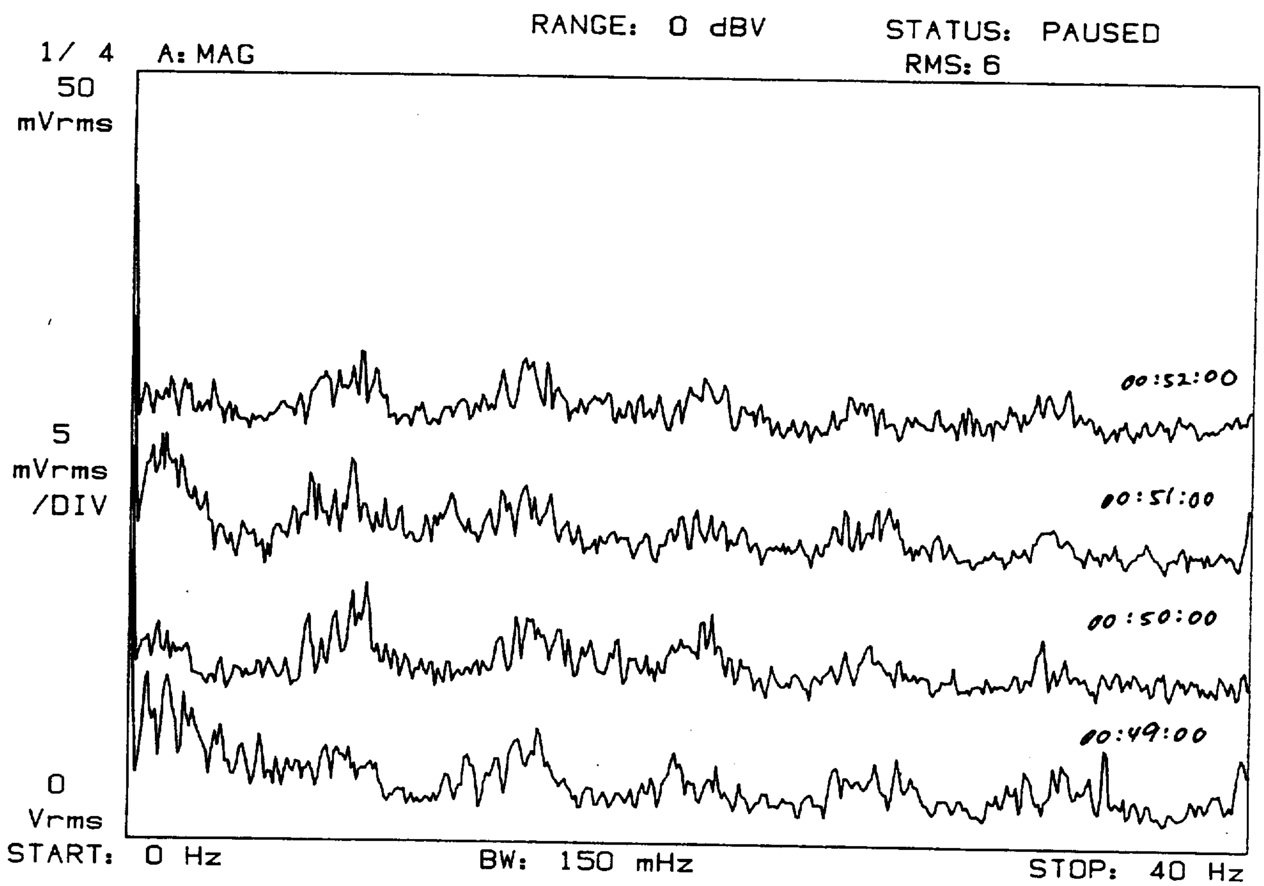

Bribie series (a)-(b): 0.5-50 Hz NS channel, 0-40 Hz shown, integration time of 1 minute, end of period indicated in GMT

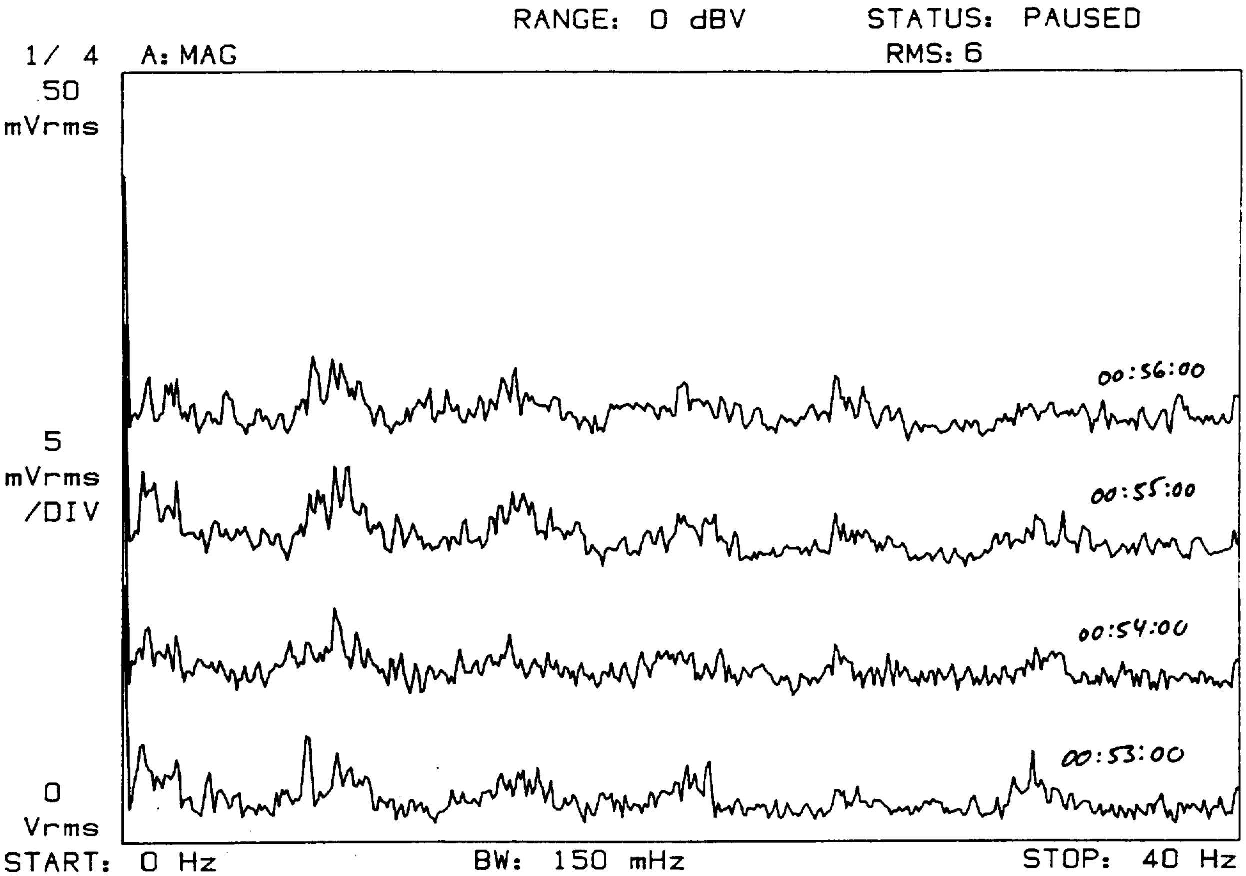

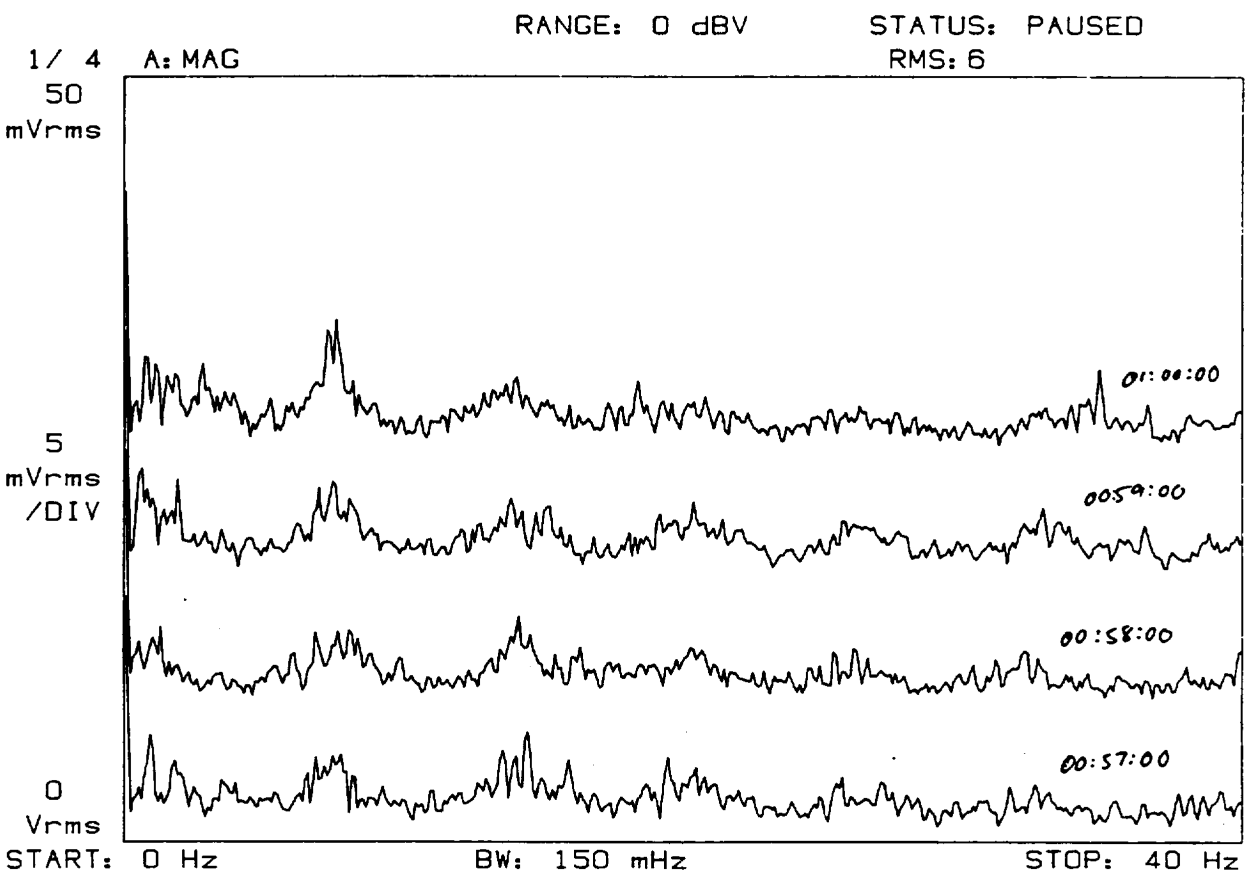

Bribie series (c)-(d): 0.5-50 Hz NS channel, 0-40 Hz shown, integration time of 1 minute, end of period indicated in GMT

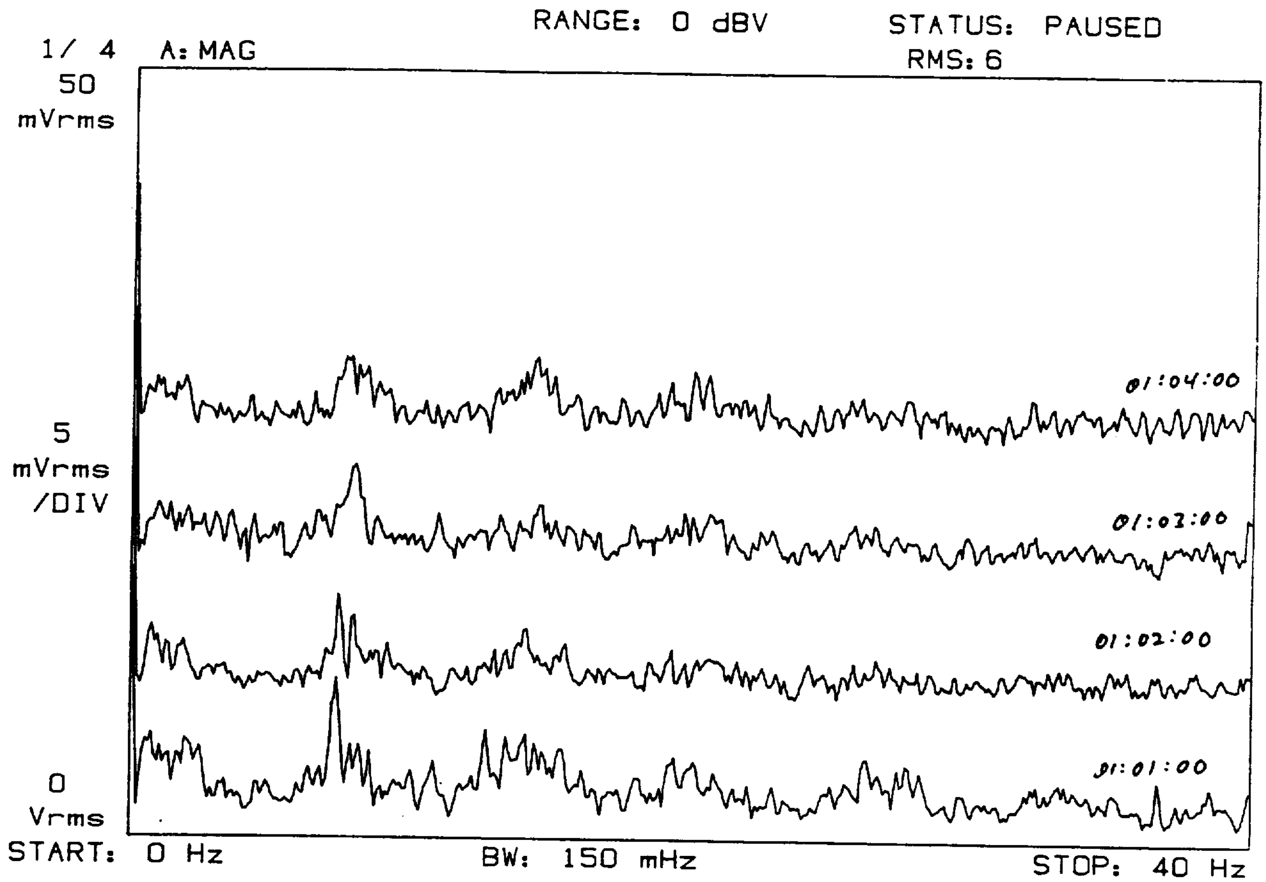

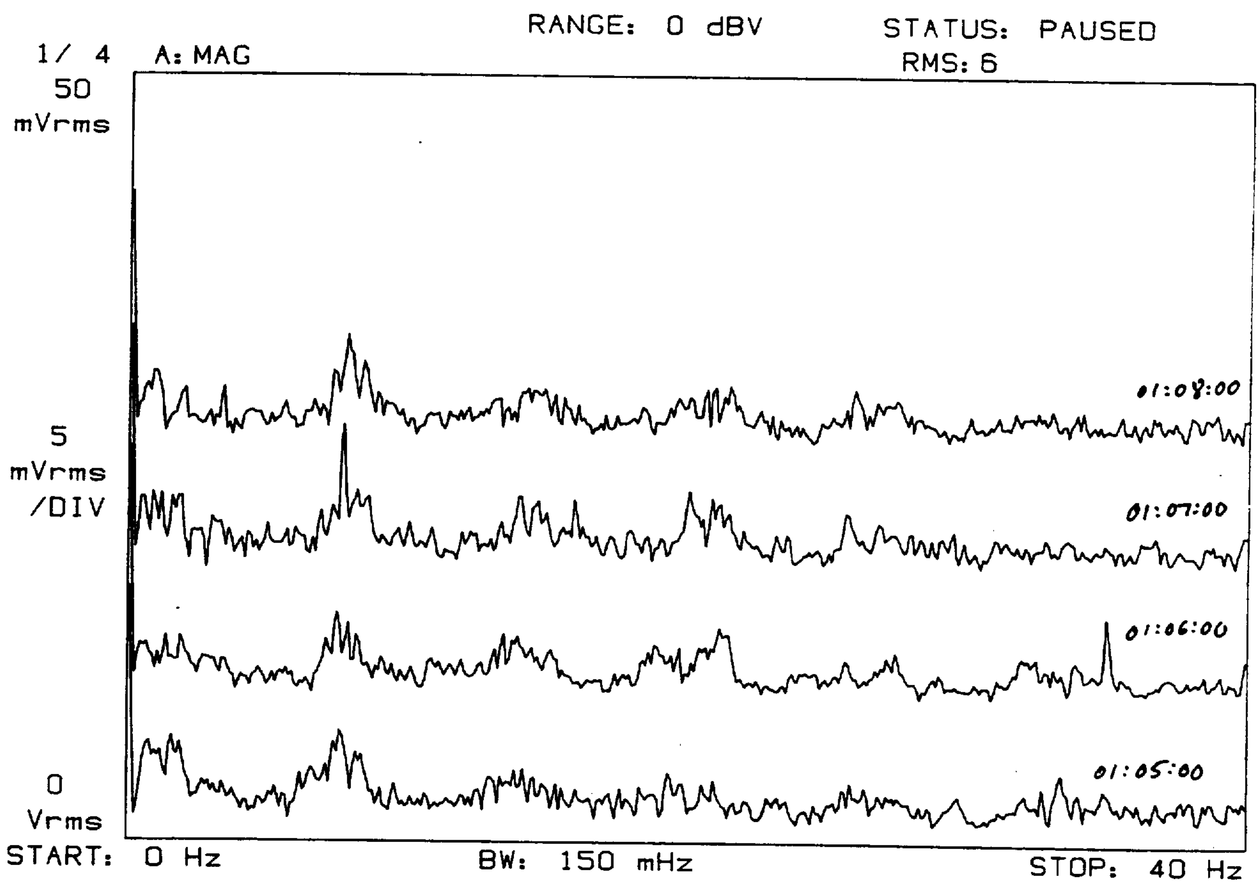

Bribie series (e)-(f): 0.5-50 Hz NS channel, 0-40 Hz shown, integration time of 1 minute, end of period indicated in GMT

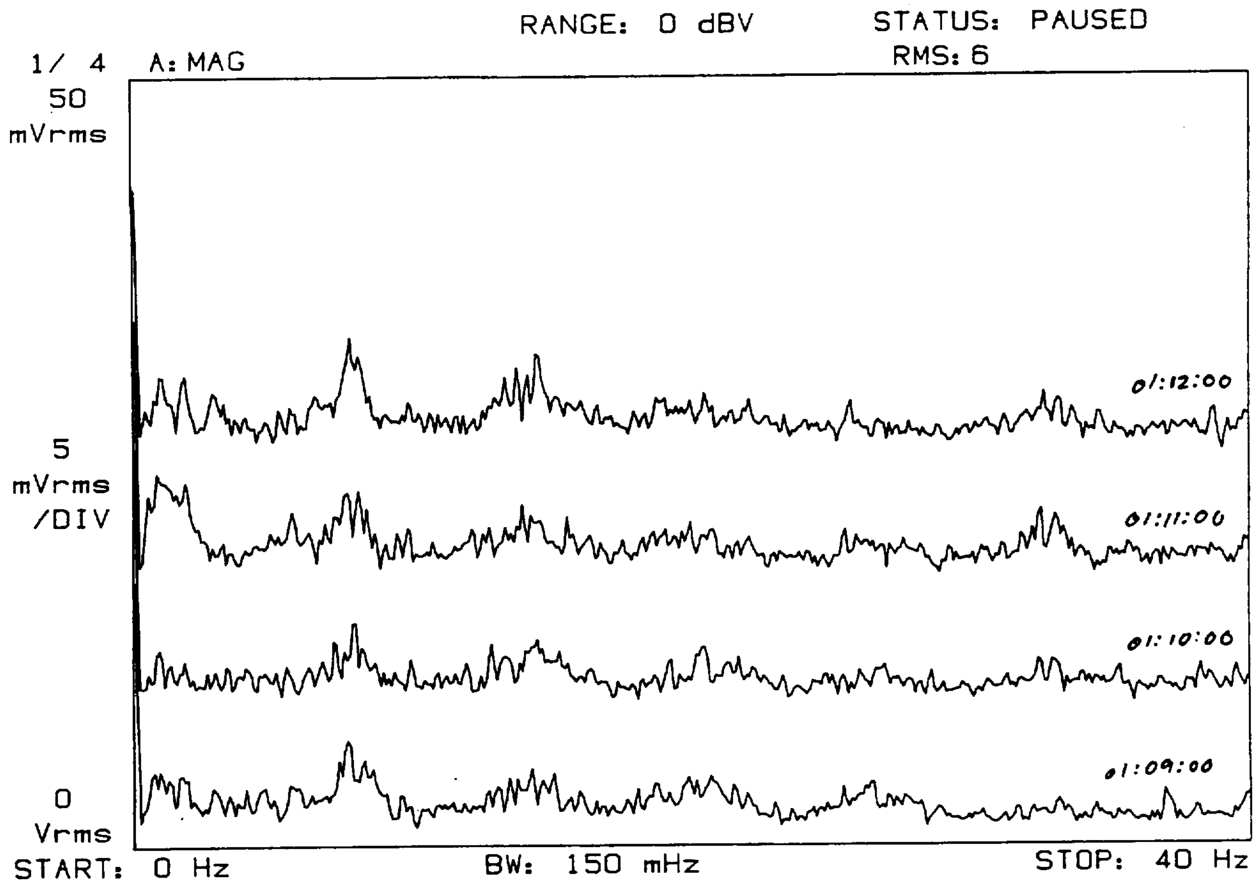

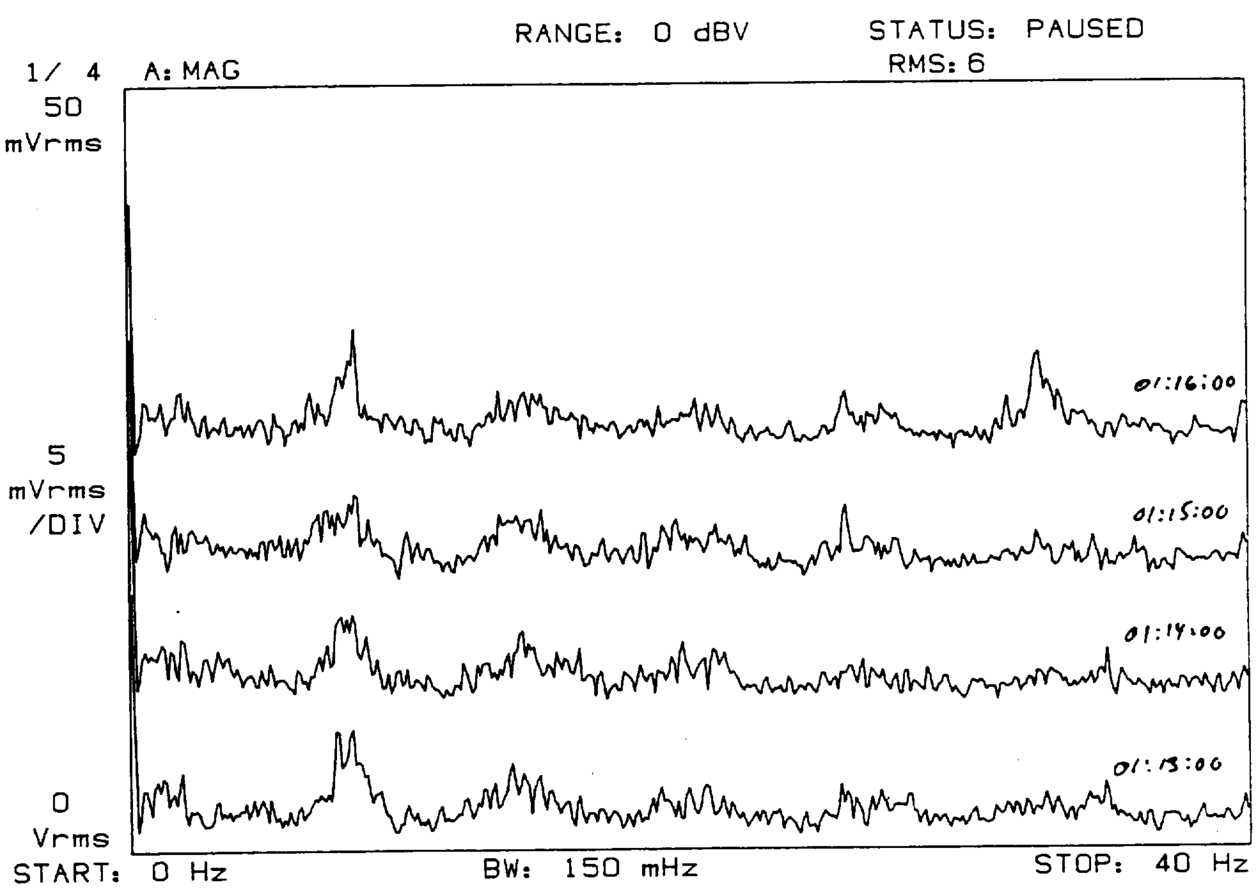

Bribie series (g)-(h): 0.5-50 Hz NS channel, 0-40 Hz shown, integration time of 1 minute, end of period indicated in GMT

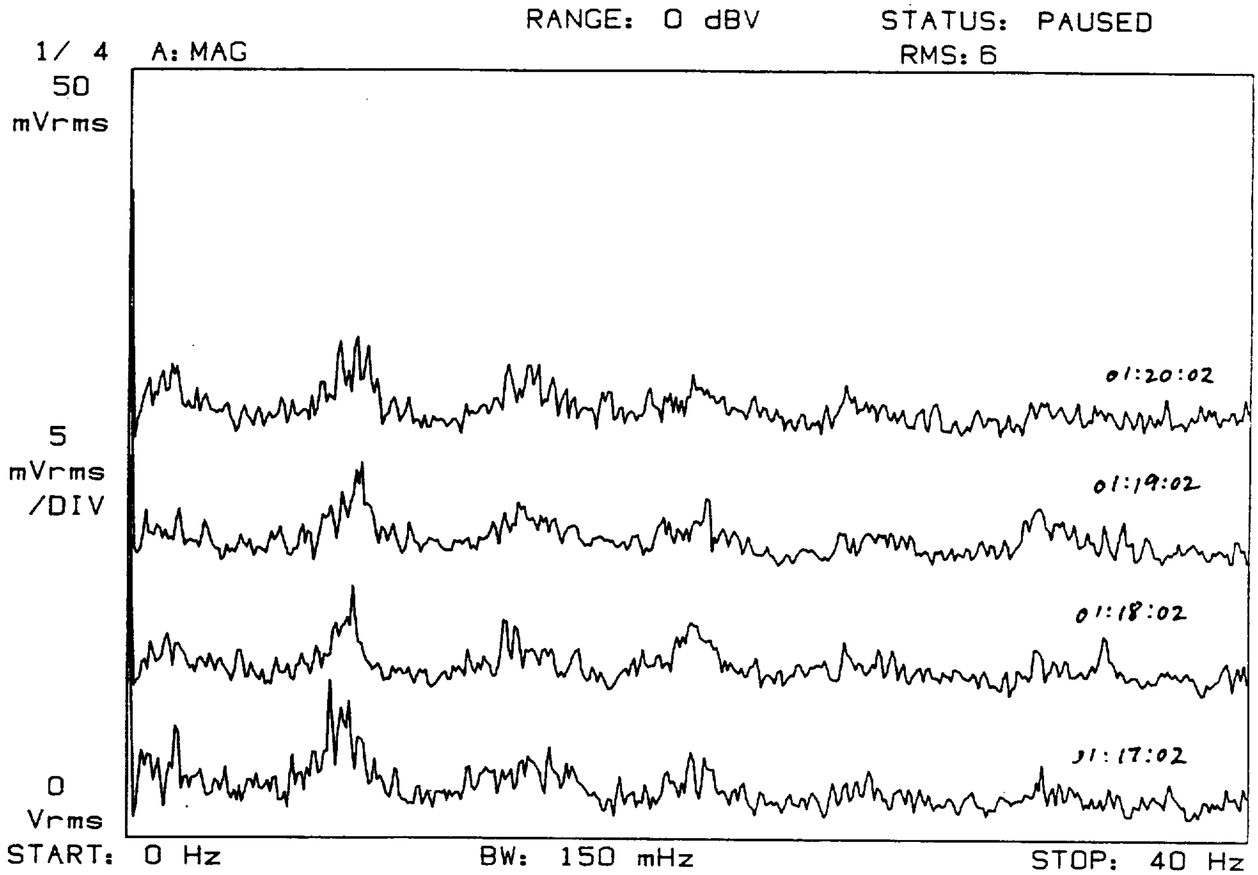

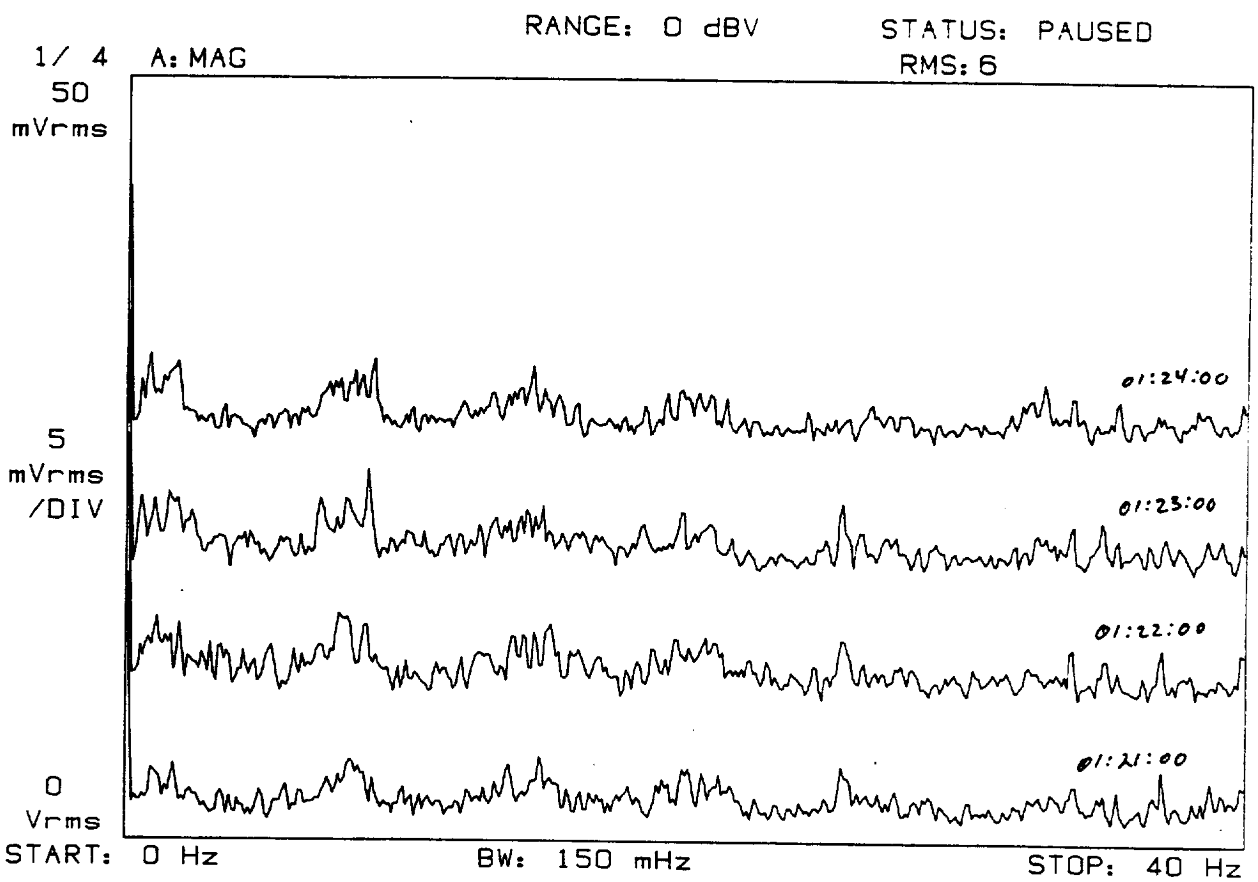

Bribie series (i)-(j): 0.5-50 Hz NS channel, 0-40 Hz shown, integration time of 1 minute, end of period indicated in GMT

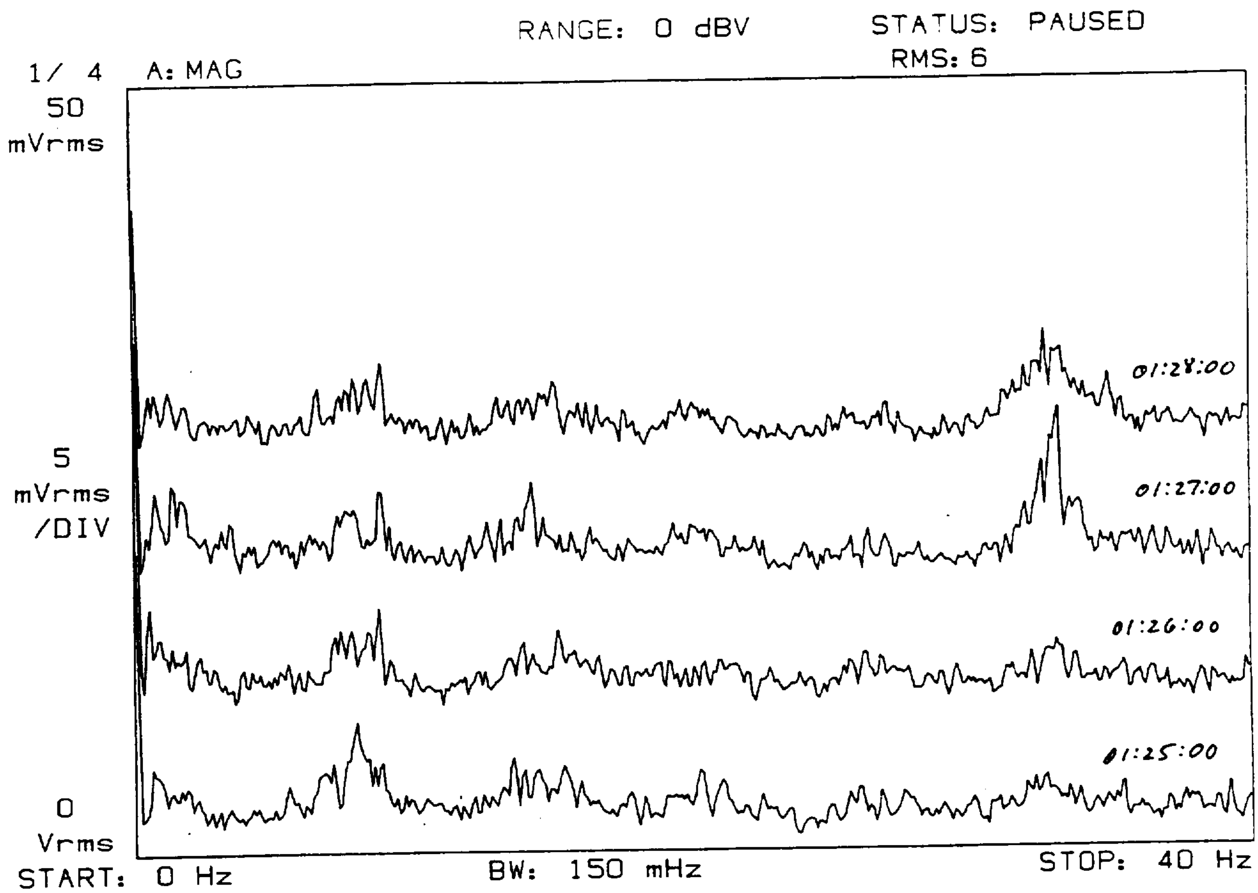

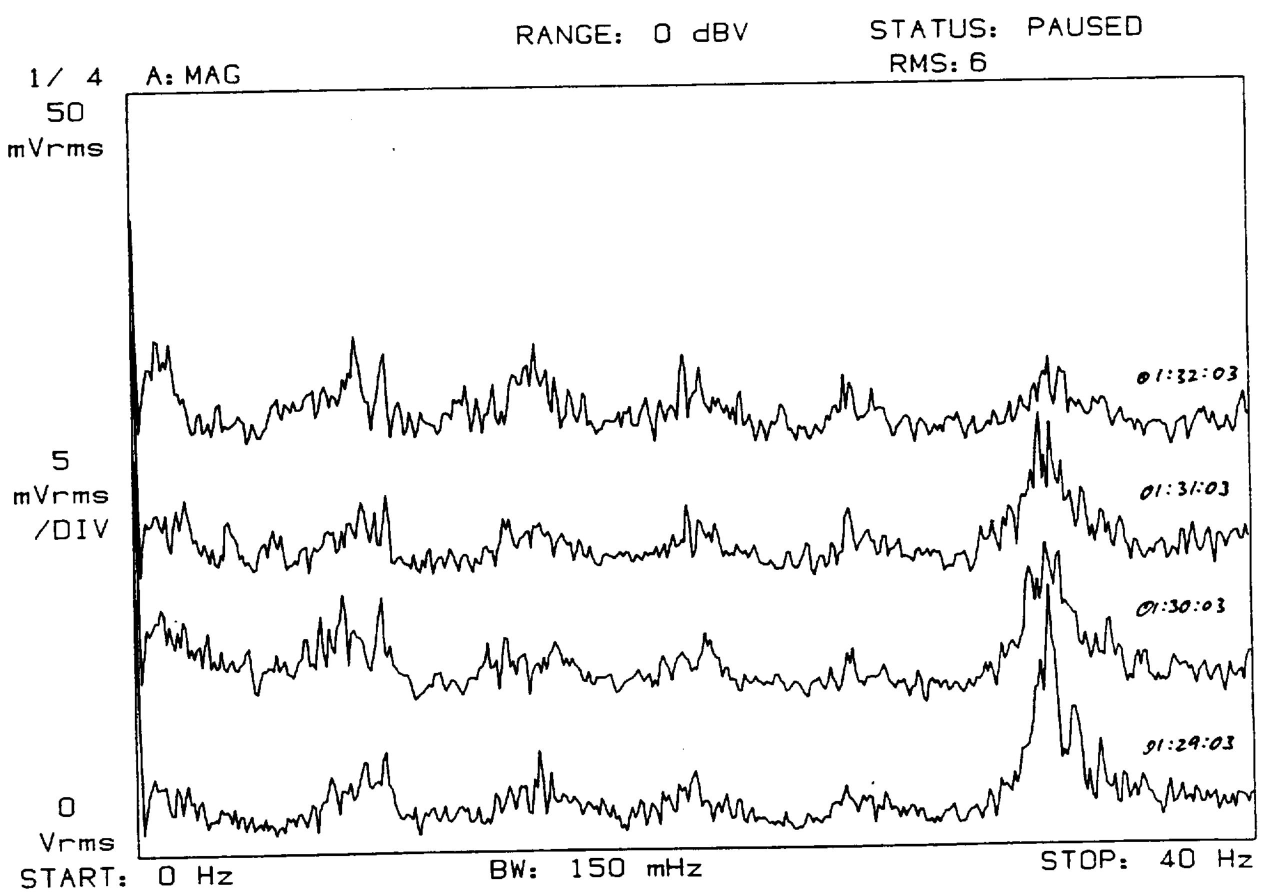

Bribie series (k)-(l): 0.5-50 Hz NS channel, 0-40 Hz shown, integration time of 1 minute, end of period indicated in GMT

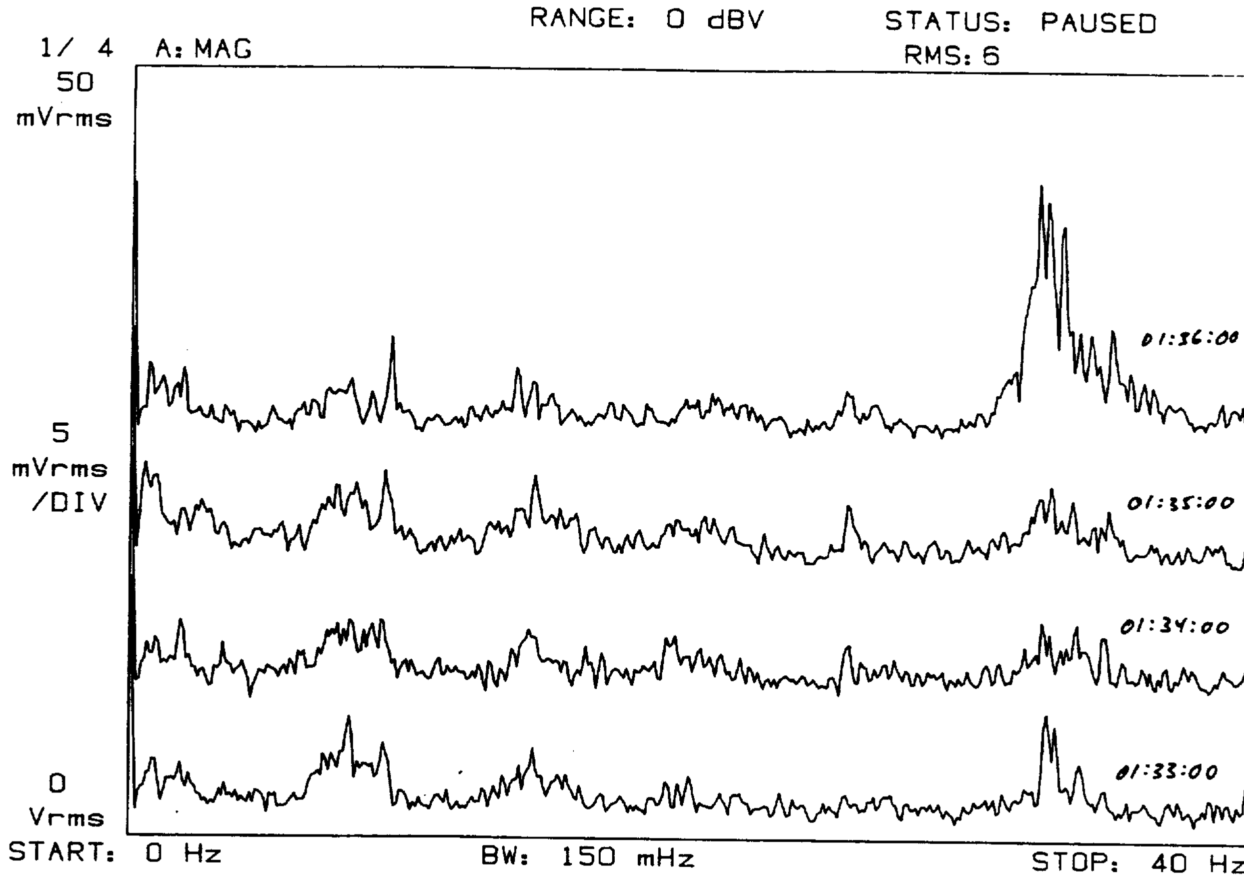

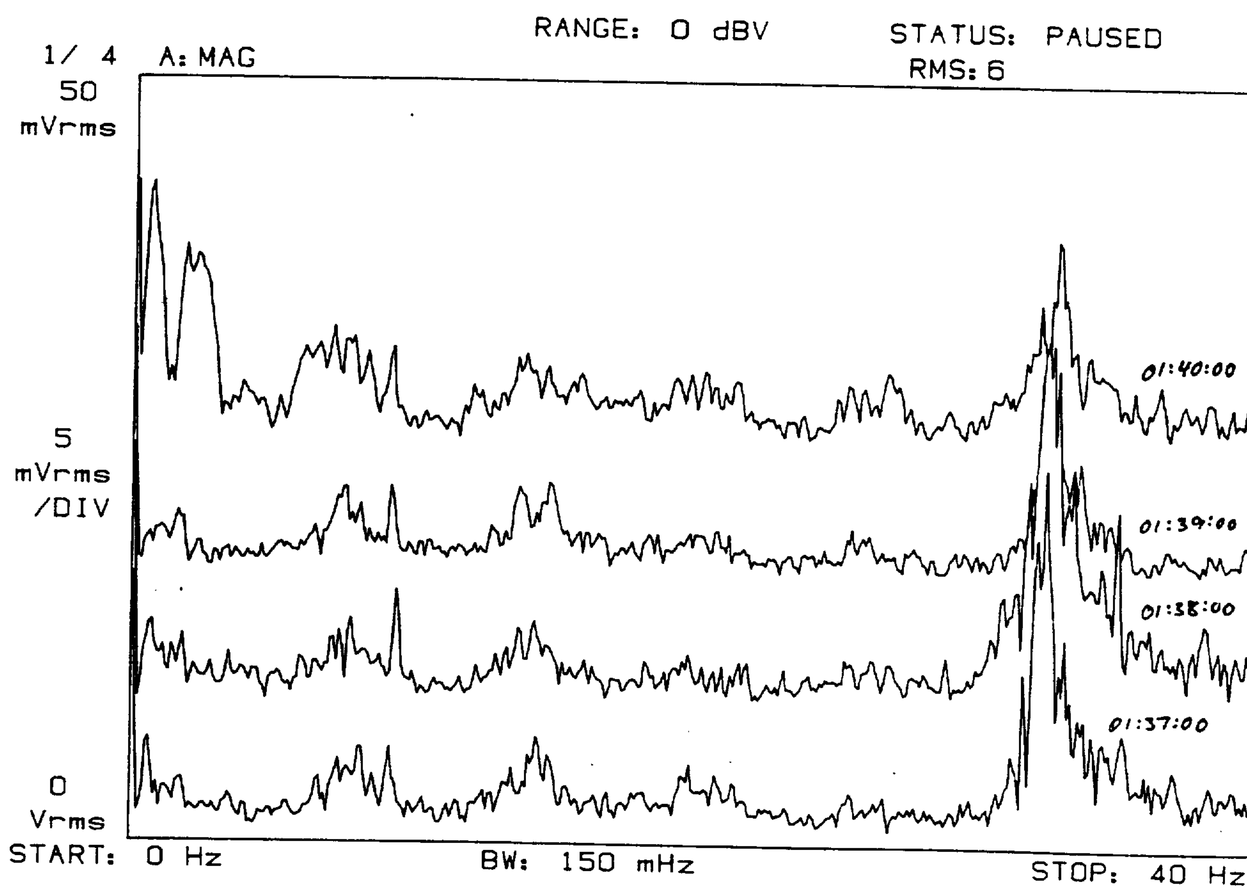

Bribie series (m)-(n): 0.5-50 Hz NS channel, 0-40 Hz shown, integration time of 1 minute, end of period indicated in GMT

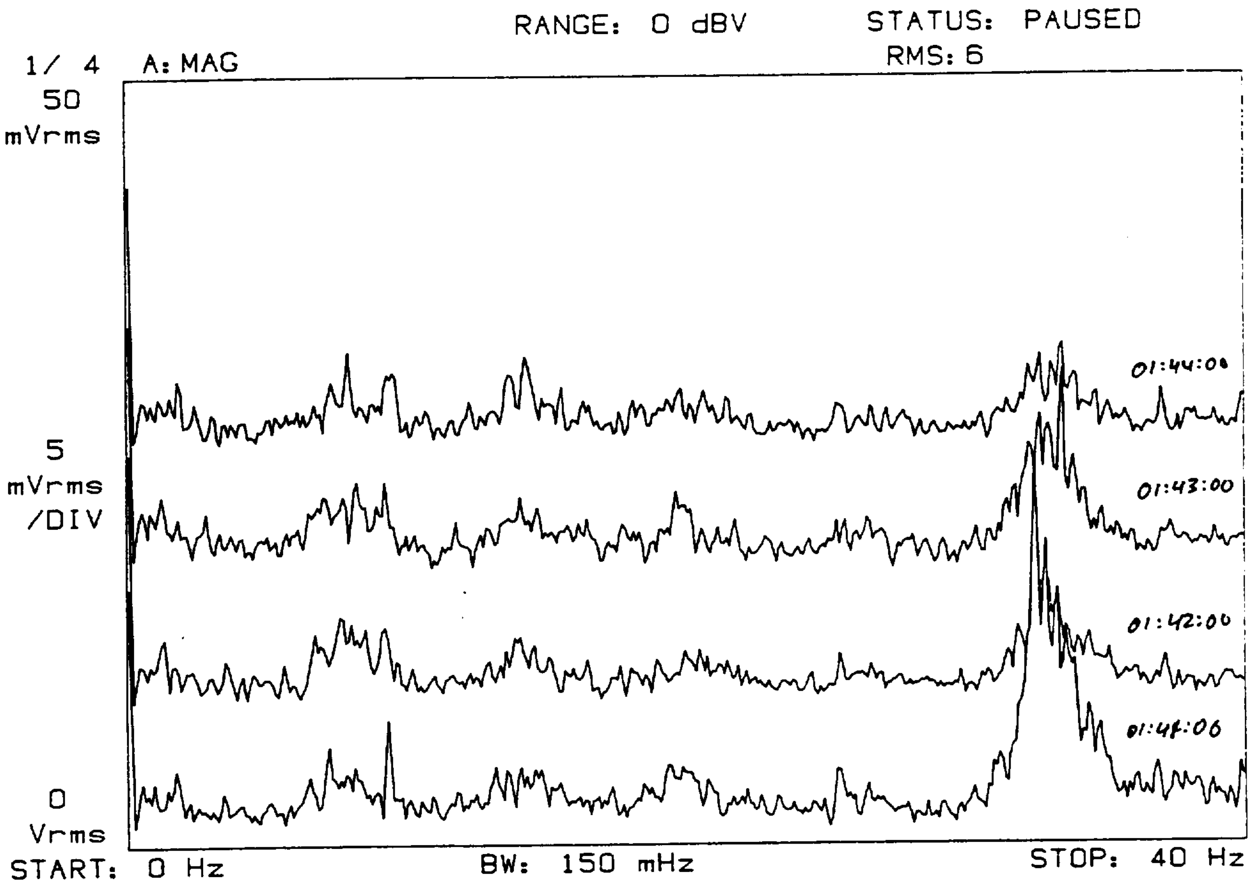

Bribie series (o): 0.5-50 Hz NS channel, 0-40 Hz shown, integration time of 1 minute, end of period indicated in GMT

A BIG (LOCAL) SIGNAL ON MONA

Although we are convinced that there is a satisfactory explanation in terms of a local perturbation to the magnetic field, we feel obligated to note one strong signal with a well-defined signature which was detected by all three low frequency sensors on Mona Island around five minutes after the break of the tether and the generation of the largest tether currents achieved during the mssion.

Our attention was first gained by a large spike in the integrated signal over the 0.5-50Hz band in a 20 second interval that began at 01:34:03 GMT. This is seen in all three Mona ELF sensors, as Figures 21-23 (plotted from DSA display output) make clear. Whatever its origin, this event was of short duration. A closer examination of the evolution of the spectrum over intervals of 0.8 seconds shows a sudden eruption around 50 Hz. This peak then moves to lower frequencies, gradually decaying as it goes. This time evolution is displayed in Figure 24.

Here is how we explain the observations. There is in operation on Mona Island, in ordinary circumstances, a generator for the electrical power needs of the small group of Puerto Rican police and Interior Department personnel resident on the island. In order to minimize local noise, the Mona EMET team had requested that this generator be turned off during the TSS-1R deployed phase. In addition, the signal was also filtered in the 60 Hz region to avoid contamination from any power sources.

We believe that what the data in Figure 24 show is the shutdown of the Mona Island generator. All 60 Hz signals were filtered out, so the signal due to the generator would not be visible before shutdown. As the generator wound down, it would continue to generate a magnetic signal, but at ever lower frequencies. The shutdown process evidently took about 4 seconds.

A Mona log book entry indicates that the generator was not scheduled to be shut off until 02:30 GMT. The log book also states that the team was planning to observe the shutdown. However, sometime after 01:10 GMT a team member who went to visit the police compound regarding a nearby boat (possible noise from which was a concern) noted that the generator was still running and obtained a shutdown while he was there. Unfortunately, the timing of the shutdown was not recorded.

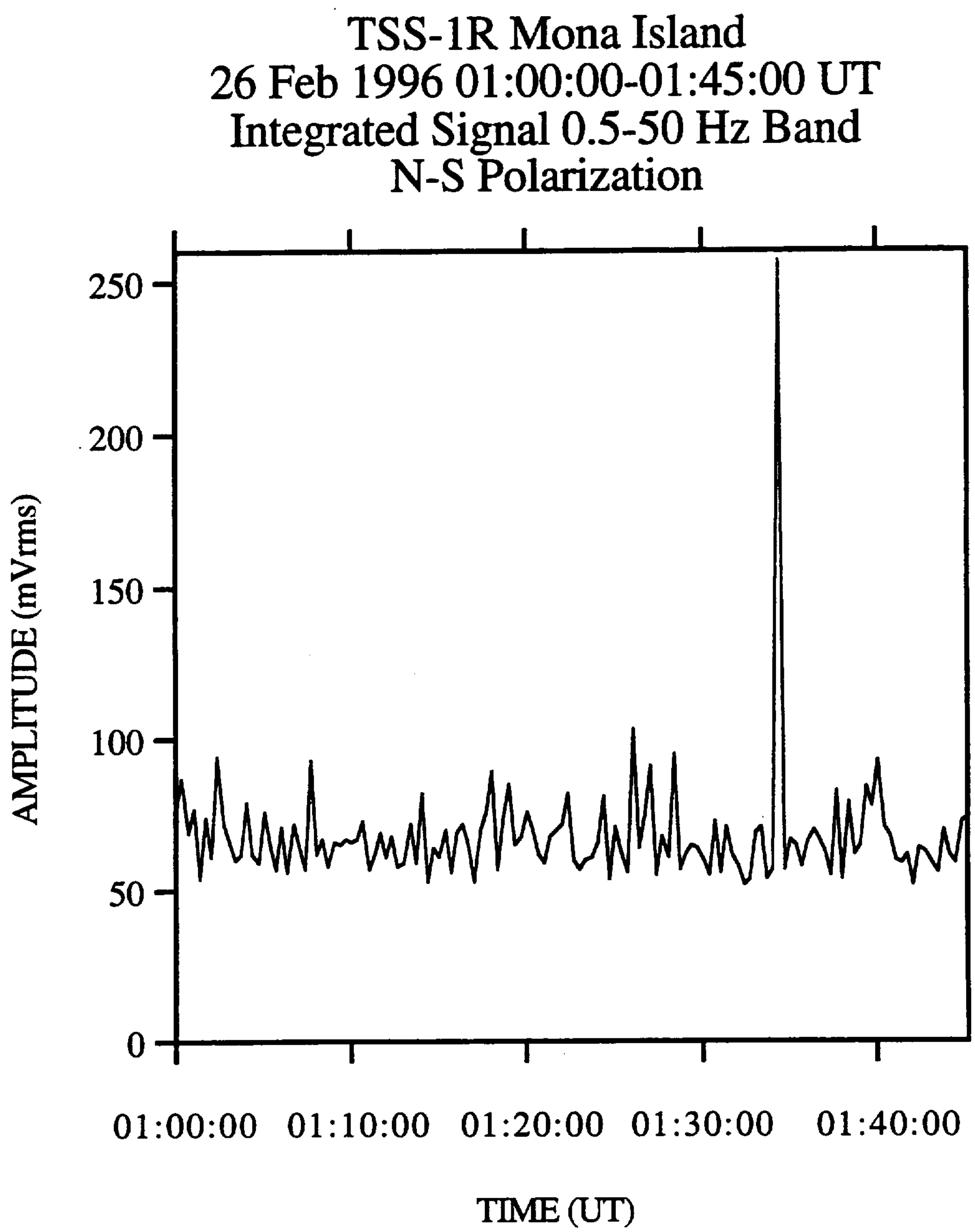
TSS-1R Mona Island
26 Feb 1996 01:00:00-01:45:00 UT
Integrated Signal 0.5-50 Hz Band
N-S Polarization
250
200
150
100
50
0
AMPLITUDE (mVrms)
01:00:00
01:10:00
01:20:00
01:30:00
01:40:00
TIME (UT)

Figure 21.

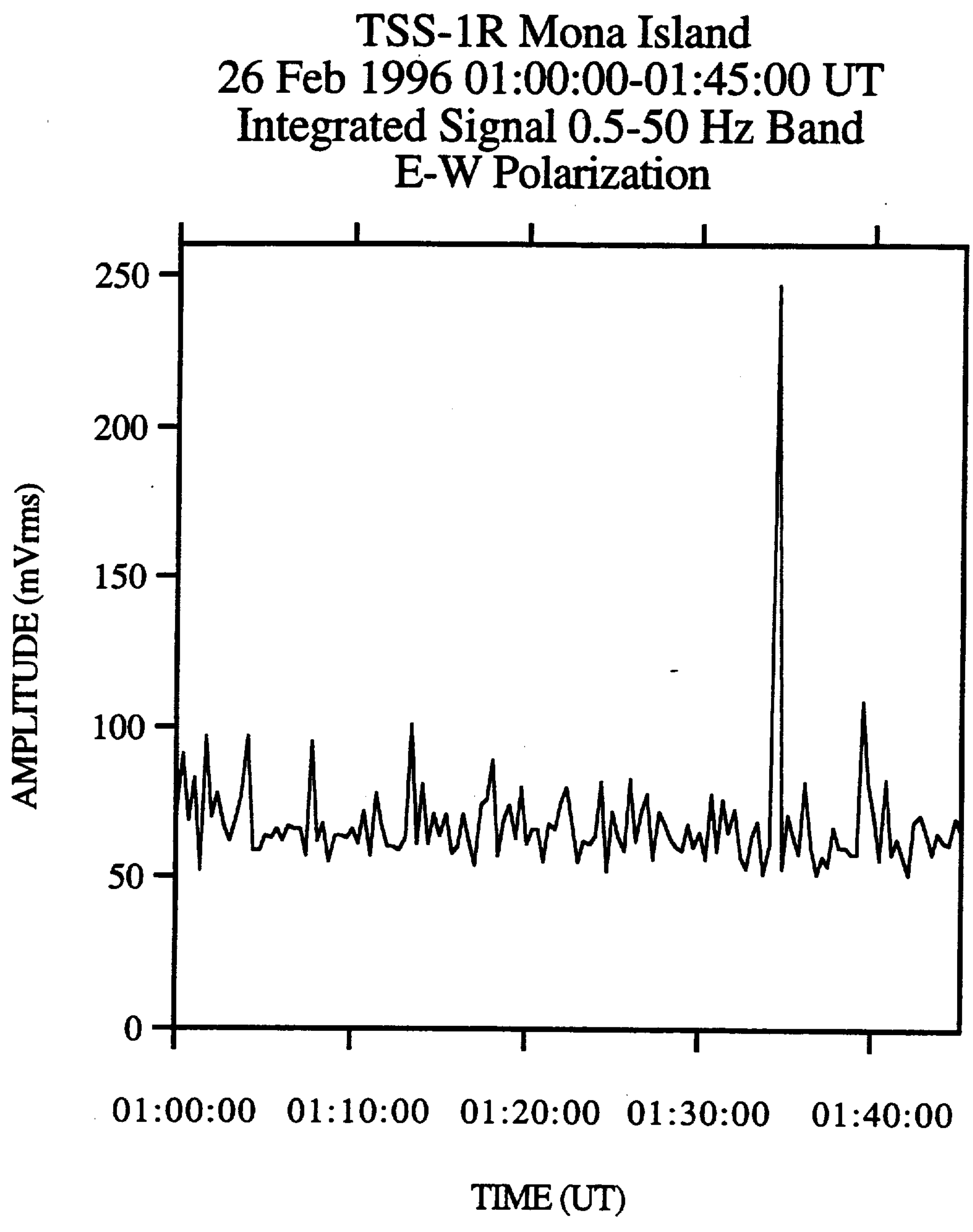
TSS-1R Mona Island
26 Feb 1996 01:00:00-01:45:00 UT
Integrated Signal 0.5-50 Hz Band
E-W Polarization
250
200
150
100
50
0
AMPLITUDE (mVrms)
01:00:00
01:10:00
01:20:00
01:30:00
01:40:00
TIME (UT)

Figure 22.

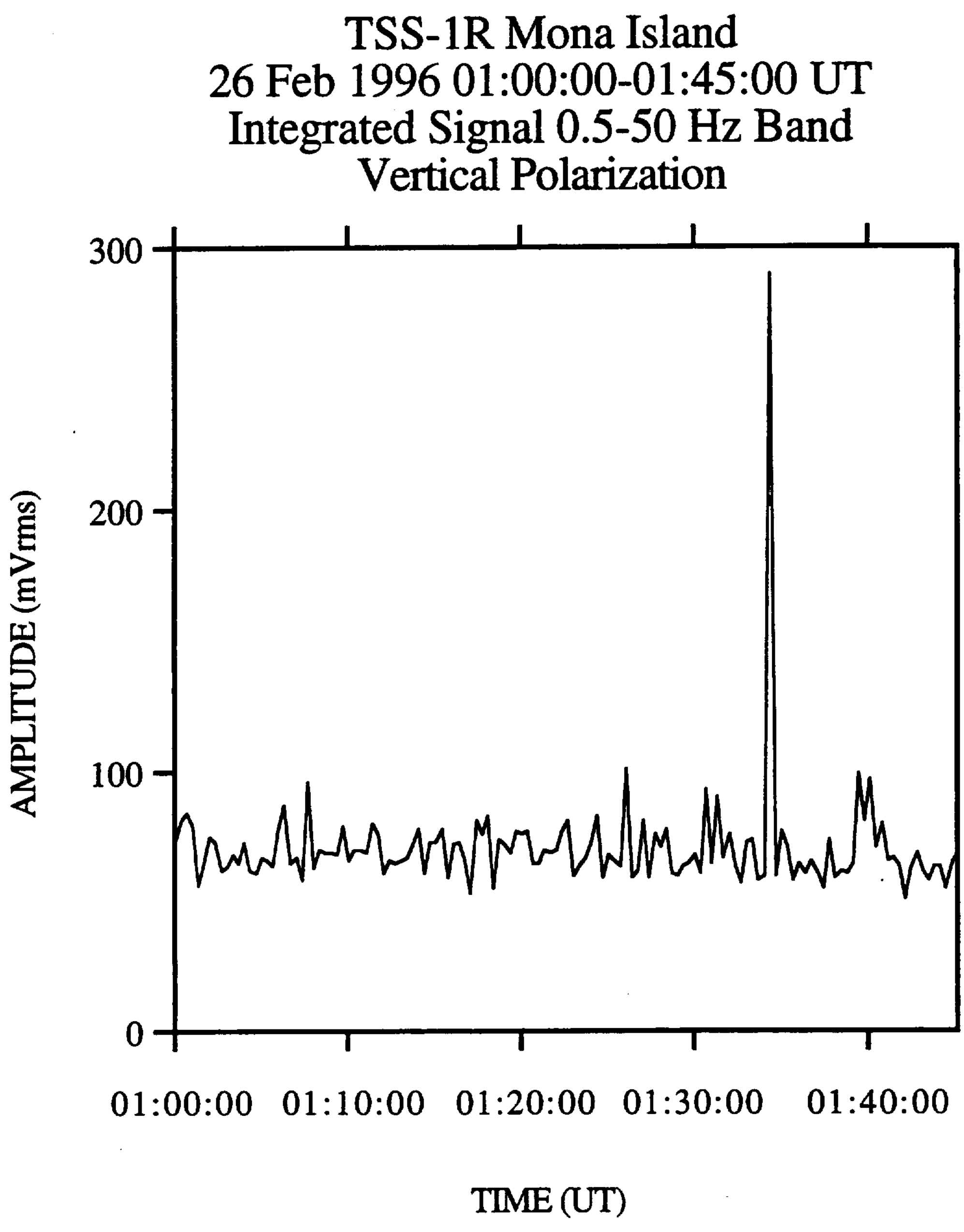
TSS-1R Mona Island
26 Feb 1996 01:00:00-01:45:00 UT
Integrated Signal 0.5-50 Hz Band
Vertical Polarization
AMPLITUDE (mVrms)
300
200
100
0
01:00:00
01:10:00
01:20:00
01:30:00
01:40:00
TIME (UT)

Figure 23.

Presumed Generator Shutdown Event: Mona Island

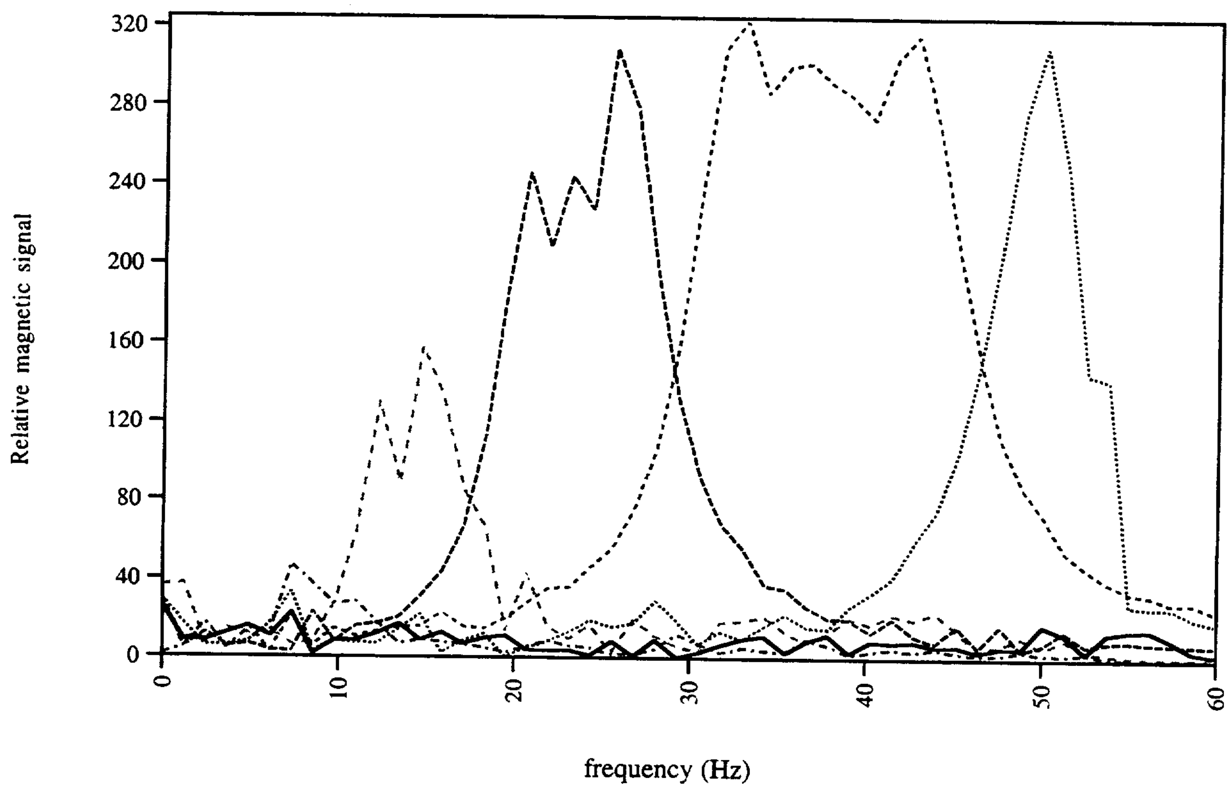

Solid line is NS spectrum for interval starting at 26-FEB-96, GMT 01:34:08.
Then spikes are for spectra at intervals of 0.8 seconds, moving to the left with increasing time.

Figure 24.

Based on the signature of the signal and the fact that a shutdown took place sometime in the general time frame of the observed event, we conclude that the event was almost certainly the generator shutdown. It is scarcely conceivable that the tether current could have caused such a strong perturbation to the magnetic field at Mona in any case.

THE SEARCH FOR POLARIZED SIGNALS

If Alfvén wings were excited in the ionosphere by the electrodynamic operation of the tether, as we should have expected, then our previous analysis[4] has shown that only the very longest wavelength components (lowest frequency components) would reach the Earth's surface with any likelihood of being detected. Furthermore, the magnetic signal should be polarized in the EW direction (or, more exactly, perpendicular to the geomagnetic field, but around Mona the difference is not significant). Not having seen anything of significance in the first look at data in the 0.5Hz-50Hz band, we decided to concentrate on the lowest frequency ULF data.

A striking feature of the Mona data presented us with a way to enhance our chances of seeing a polarized signal. Simply put, the data streams recorded from all three BF-4 (ELF-ULF) sensors on Mona Island were almost identical. The Bribie data, on the other hand, are not isotropic, which would seem to rule out a systematic data processing software error as the source of the observed isotropy in the Mona data.

Comparison of spectra from different channels shows that relative gain factors and data windows are exactly what they should be for the different channels with their respective signal conditioning. With the proper gain factors, the spectra for channels the NS channels 1 and 7, for example, are virtually identical (but not perfectly) within their common frequency range (overlap of windows), as they should be. But the same holds true for channels 1 and 8 (vertical), or any other combination of channels 1-9.

The only hypothesis consistent with the observations on the Mona spectra is that the signals going into the filter boxes for the BF-4 sensors are virtually identical. All other possible errors in wiring or software can be ruled out by the consistency of the data windows and gain factors of the different channels.

A review of photos taken of the setup on Mona conclusively found that the sensor wiring and alignments were correct in every respect. In addition, a spot check of TSS-1 mission data taken on Mona Island, years before TSS-1R, found the same isotropy in the detected signal. We have concluded that the Mona data is reliable, and that Mona is thus a very good location to look for polarized signals. This realization makes the failures of TSS-1 and TSS-1R to carry out the planned overflight experiments all the more disappointing.

The near-equality of the NS and EW signals observed in the Mona data gave us some hope of being able to pick out a polarized signal (e.g., one for which the EW component temporarily exceeded the NS component) in the difference of the NS and EW signals. Our first step was to look at the ULF spectra of the NS-EW signals. Integration times of 1.75 seconds enabled us to theoretically see frequencies down to 0.01 Hz. In the 0.01-0.1 Hz band, the output from the BF-4 sensors is no longer the B-field itself but the time derivative of the B-field, and we have taken this into account.

While the difference signal did show substantial time variation in its strength, we soon realized that this was not the most fruitful way to view the data. What we noticed was that peaks in the difference signal were matched by peaks in the NS and EW signals. This observation led us to make the hypothesis that there was a constant ratio (near unity) between the NS and EW signals. This would follow if the natural background were indeed isotropic and differences in NS and EW signals were due to differences in sensitivity (mV/nT) of the sensors and/or slight differences in the gain factors actually applied by the signal conditioners.

We obtained spectra of the NS signal and of the NS-EW signal for 217 intervals of 1.75 seconds each. Each sample contained 256 K data points. This included over an hour and a half of data taken on February 22, 1996 (three days before tether deployment) during a test with the receiving system running on battery power. This sample with DC power is significant because the tether-deployed data were taken with the generator running, and the comparison should allow us to see gross effects of the generator, if there were any. None were seen. We analyzed almost five hours of "real" TSS-1R data starting ten minutes after the beginning of tethered satellite deployment and ending some 25 minutes after the tether break.

Taking all of this data together, we then performed a least squares fit to obtain α in the expression $\alpha \bullet NS = (NS-EW)$, where NS and (NS-EW) represent the square roots of the sum of the squares of the amplitudes for the NS and (NS-EW) difference signals, respectively, summed over the interval 0.01 Hz to

0.1 Hz. The α thus obtained was 0.032. According to the manufacturer, the sensor that was aligned along the EW direction is about 2.6% more sensitive than the one aligned along the NS (for the band in which a sensitivity was quoted, which went down to 0.1Hz), so this is about what we should have expected.

Since the Mona difference signal tracks the signal of either sensor (NS or EW) very closely most of the time, with the strength of the difference signal roughly 3% of the NS signal, we are then most interested in deviations of the difference signal from (the best fit factor) 0.032 times the NS signal.

Figures 25 and 26 show the difference signal strength and 0.032 times the NS signal strength for the two periods mentioned above. Higher, sharper peaks are seen in the spectra for data collected during the deployed stage of the mission (Figure 25) than were seen in the Mona background data (Figure 26), but the two sets were taken at different local times of day. It is notable that the increase in average signal strength and the onset of spiking in the deployed data began around sundown (22:37 GMT). An optimist might point out that tether currents and lengths weren't all that significant before that time either. Since the spikes are not easily correlated with tether currents, we cannot ascribe them to TSS-1R activity.

The largest deviation (in the 6.3 hours of data examined) of the polarized signal from the best fit to the NS variation (0.0324 factor) is seen to occur in Figure 25 in the interval beginning at GMT 01:35:37. The start of this interval is about six minutes after the end of the largest (1A) and longest-sustained (1 minute) tether current, which began immediately before the tether break at GMT 01:29:17 (See Figure 15, p.20). The second largest deviation occurred in the interval beginning at GMT 01:31:57, i.e., 3.5 minutes earlier, and that much closer to the period of maximum tether current. These two points stand out clearly from the rest of the data. The generator shutdown event, considered in the preceding section, occurred completely within the interval between these two, and we have ruled out its having contributed to the spectral amplitudes of either, as it was of a few seconds duration and began around GMT 01:34:08.

The statistical significance of these two anomalous points may be estimated in the following way. We obtain the mean and the standard deviation for the distribution of the residuals (NS-EW)-0.032•NS for the different time intervals, as normalized in Figures 25-26. The mean is found to be 0.00033 $nT/\sqrt{Hz}$, and the

Mona Island 0.01-0.1 Hz Difference Signal (NS-EW) and NS Signal Scaled by Factor 0.032

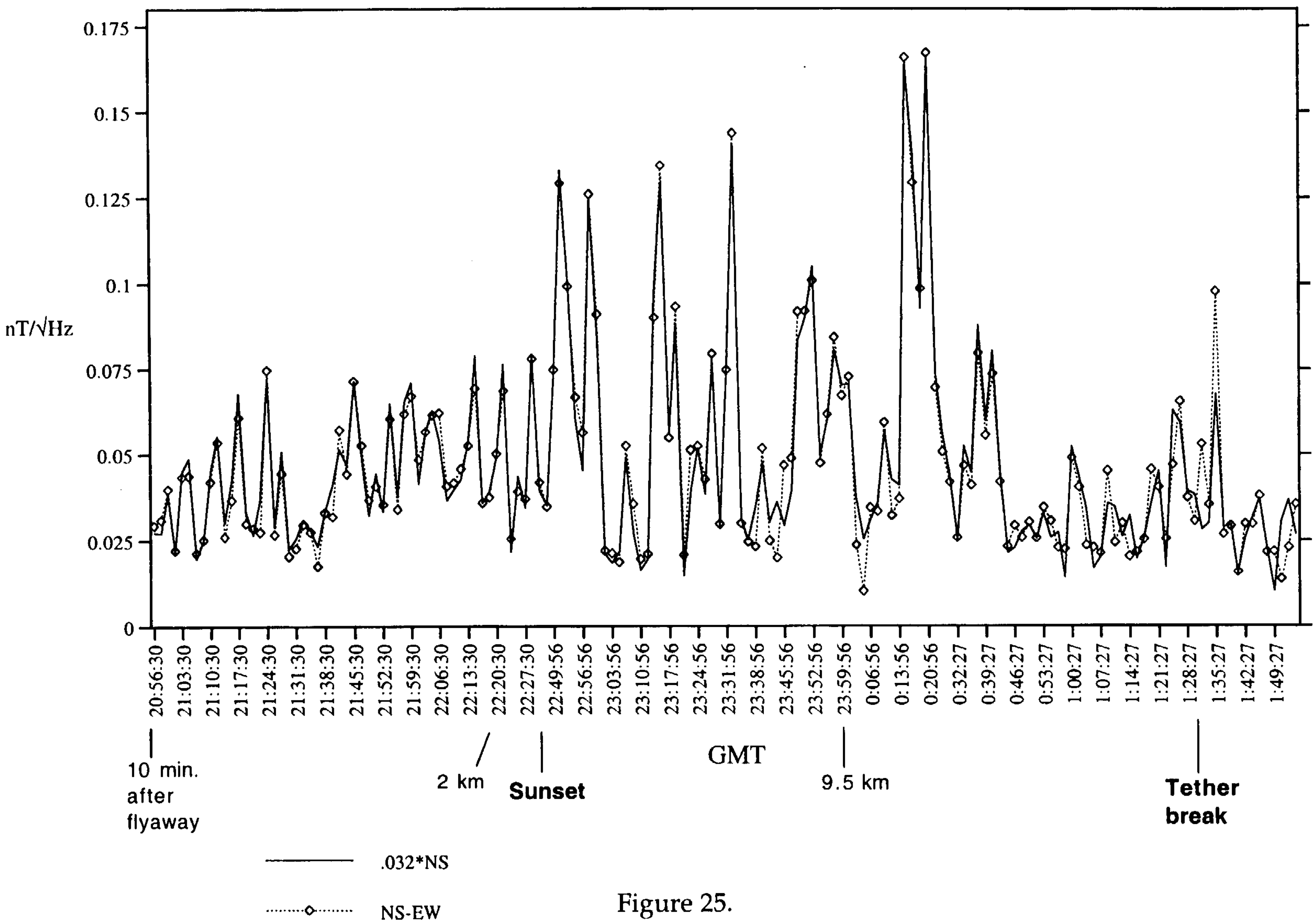

Figure 25.

Mona Island 0.01-0.1 Hz Difference Signal (NS-EW) and NS Signal Scaled by Factor 0.032

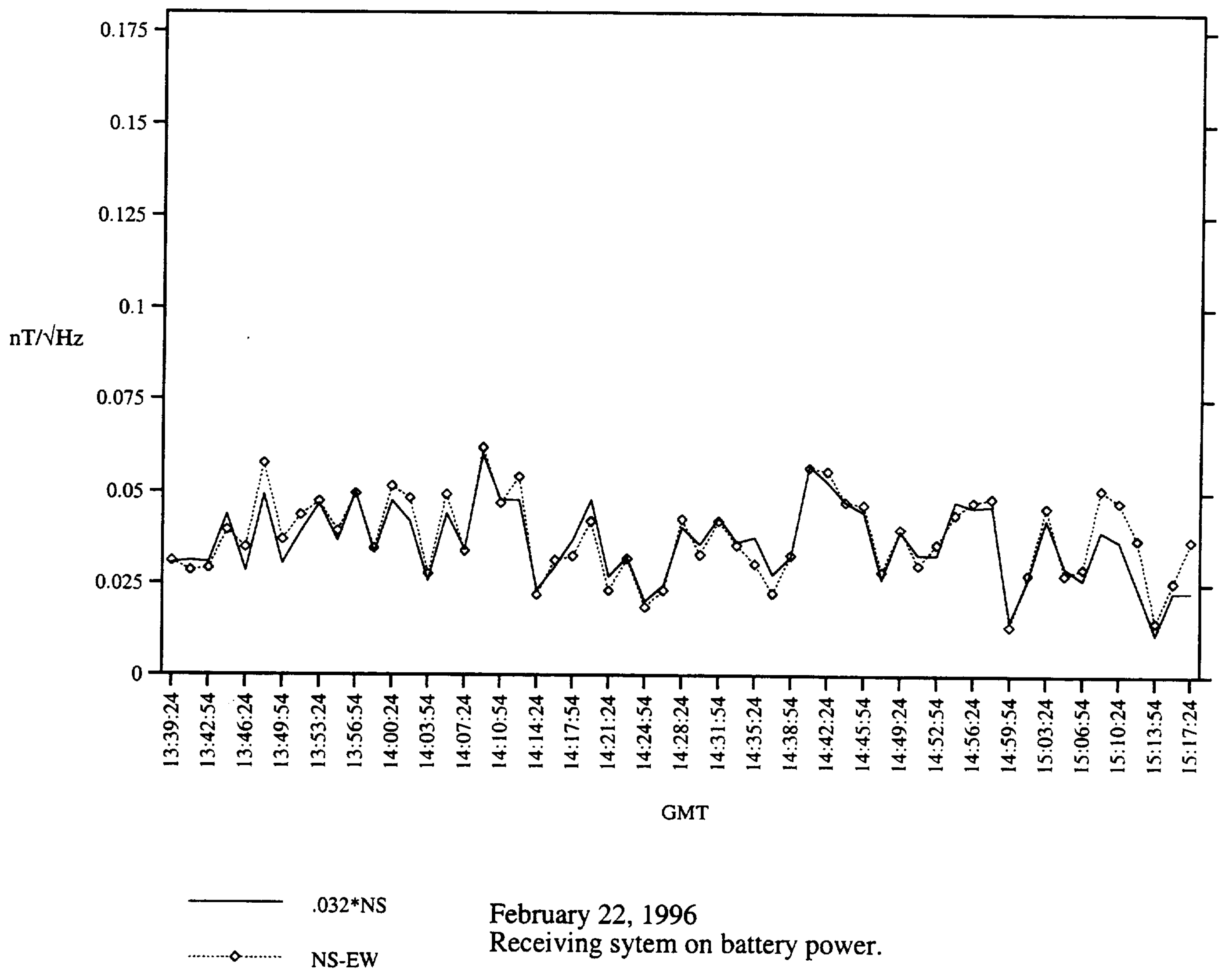

February 22, 1996
Receiving sytem on battery power.

Figure 26.

standard deviation σ to be 0.00615 nT/$\sqrt{}$Hz. When the fit is repeated with the two "anomalous" points excluded, we obtain the same factor 0.0324; the mean of the residuals is then 0.00023 nT/$\sqrt{}$Hz and the σ is 0.00595 nT/$\sqrt{}$Hz. Since the minimum of (NS-EW) is around 0.02 nT/$\sqrt{}$Hz, the mean of the residuals is insignificant. The residuals for the two standout points are seen to be 0.0246 nT/$\sqrt{}$Hz and 0.0299 nT/$\sqrt{}$Hz. These points lie 4.0 σ and 4.8 σ respectively from the mean, taking the larger standard deviation of the distribution using all points.

The distribution of the residuals (NS-EW)-0.0324•NS are shown in the histogram of Figure 27. We would describe this as a pretty good normal distribution for 215 points with two anomalous points far to the right hand side of the distribution. The same information is displayed in Figure 28, where the error bars are a standard deviation in length (and do not refer to independently estimated measurement uncertainties due to the instruments).

Despite the roundabout way we have taken to arrive at this point, it is hard to avoid the conclusion that something out of the ordinary happened to generate a polarized signal in the time periods in question. The question is, of course, what?; and we are not in a position to make a definitive answer.

The Mona log book records that a telephone call that lasted around three minutes was made using the Globe Sat satellite telephone around GMT 01:32. This battery-powered telephone set was turned on only when being used. Given the uncertainty in the actual timing of the call, we must allow that the call to Arecibo could have extended into the interval of greatest interest, while beginning somewhere in the earlier interval where the first polarized signal was observed. Two calls made to Huntsville earlier (at GMT 22:30 without success and at GMT 23:23, lasting around 2.5 minutes) in the same long stretch show no polarized signal of comparable strength for the time samples we have chosen. It is easy, however, to imagine a sequence of events in which a DC, partially polarized magnetic field was turned on and off at the right times to generate the ULF signal sequence we observe. Unfortunately, we recognized the telephone as a possible source of electromagnetic contamination too late to evaluate it before filing this report. A thorough analysis would include finding out what magnetic field the set would be likely to generate and calculating new spectra for different

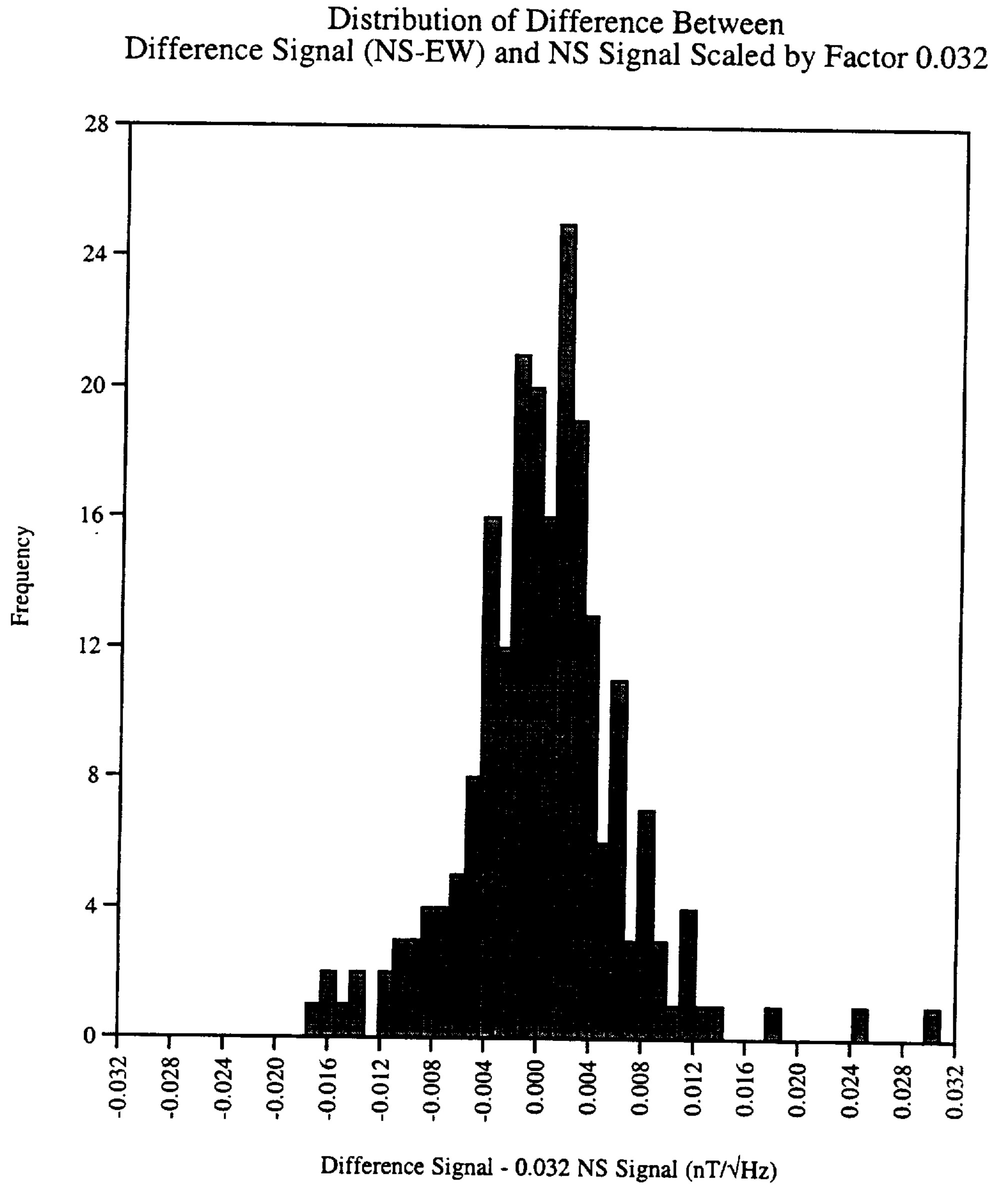
Distribution of Difference Between
Difference Signal (NS-EW) and NS Signal Scaled by Factor 0.032
Frequency
28
24
20
16
12
8
4
0
-0.032
-0.028
-0.024
-0.020
-0.016
-0.012
-0.008
-0.004
0.000
0.004
0.008
0.012
0.016
0.020
0.024
0.028
0.032
Difference Signal - 0.032 NS Signal (nT/√Hz)

Figure 27.

Mona Island 0.01-0.1 Hz Difference Signal (NS-EW) Minus NS Signal Scaled by Factor 0.032

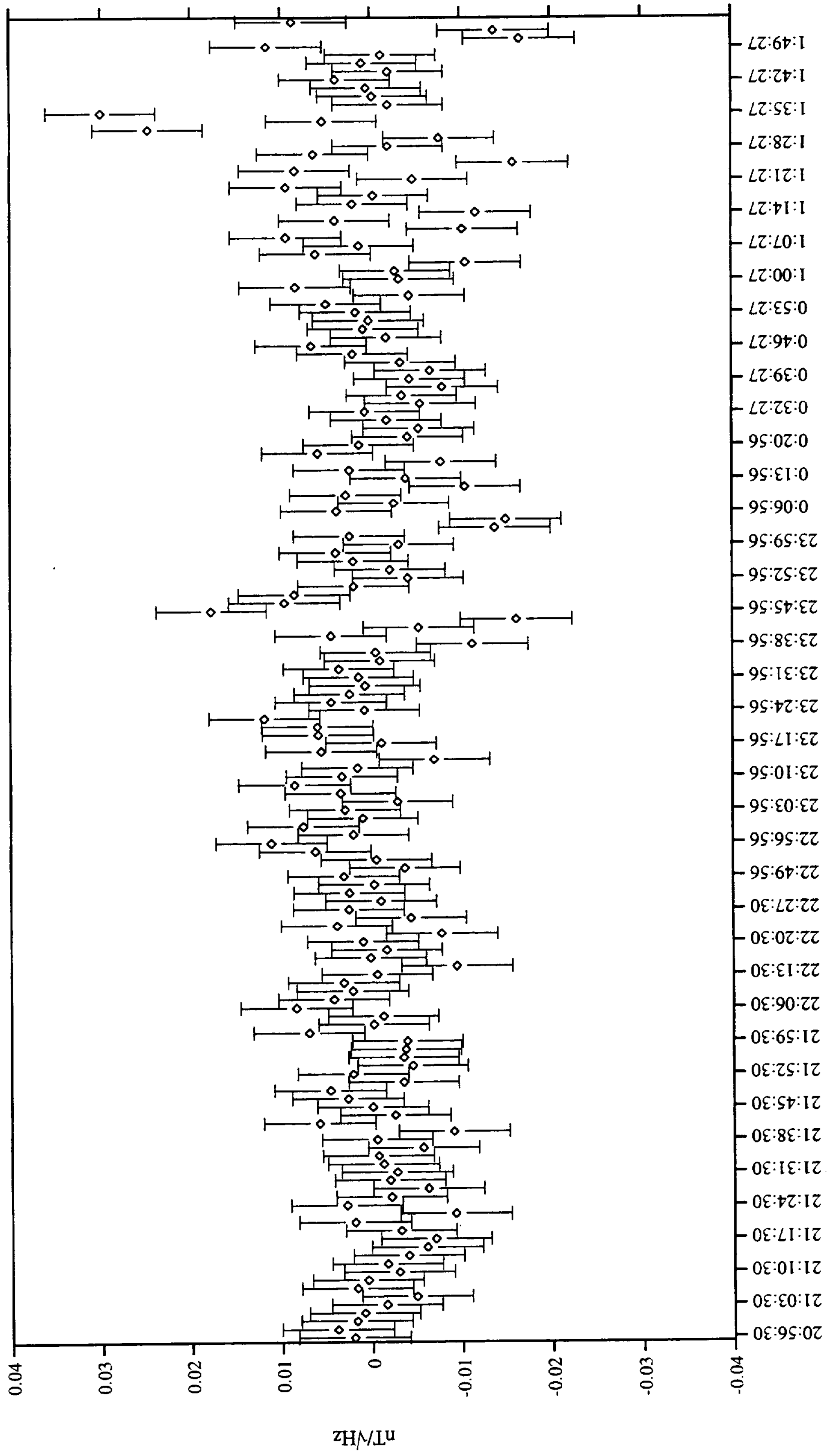

Figure 28.

time windowing in both the period of anomalously high polarized signals and during earlier times when the telephone was in operation.

Regarding the possibility of the tether current as a source, we have to say that we haven't (and so far as we know, neither has anyone else) tackled the complicated problem of what happens to the "Alfvén wings" (the Alfvén wave packets excited by the tethered satellite as it moves through the ionosphere exchanging charge with the plasma at each end of the system) when the tether current stops. These travelling disturbances would have been moving along with the Shuttle's EW velocity.

Let us engage in some speculative handwaving. Suppose the wave packet (spreading and dissipating as it went) continued on the same path with the same velocity through the ionosphere after the tether current stopped. Then we might expect the maximum chance for a signal to reach Mona to occur when the remnants of the wings passed through the Mona meridian. When would this occur? The Shuttle EW speed around the time of its equatorial crossing (current cessation) was $\cos(28.5°) \bullet 7.8$ km/sec = 6.9 km/sec. To cover the roughly 27° of longitude (95° W to 68° W), which corresponds to around 3,000 km, would then take 7.25 sec. Thus, the point at which we see our largest polarized signal is not that far off from what we get by this back of the envelope calculation. This says nothing about the smaller spike, seen in the interval beginning 3.5 minutes earlier, nor about when waves from different parts of the current interval would arrive. All we want to do is to raise the possibility that the the time interval between tether current flow and the observed signal may not be great enough to rule out a causal relationship between the two. The data are too insufficient by far to establish such a relationship.

We have verified that the spikes in the polarized signal are due to an enhancement of the EW signal, as we would expect if the signal were due to an Alfvén wave packet generated by tether current collection. On the other hand, we have difficulty in explaining Alfvén signals at frequencies so far below the ion collision frequency at the Shuttle altitude.

The spectral distribution in the 0.01-0.1 Hz band for three consecutive 1.75 minute intervals starting at GMT 1:31:57 are shown in Figures 29-31. Little new information is conveyed by these plots beyond the fact that the energy was concentrated in the 0.01-0.02 Hz band as one would have expected.

Data collected at the Bribie Island (Australia) site were seen not to have the same characteristics as the Mona Island (Puerto Rico) data. Specifically, the signals recorded by the different Bribie sensors oriented at right angles to each other differed significantly from each other, unlike the Mona data. Thus, the attempt to look for a polarized signal by taking the difference signal was not possible for the Bribie data. The Bribie data were also seen to be generally of a lower quality (noisewise) than the Mona data, though the Schumann resonances were clearly visible.

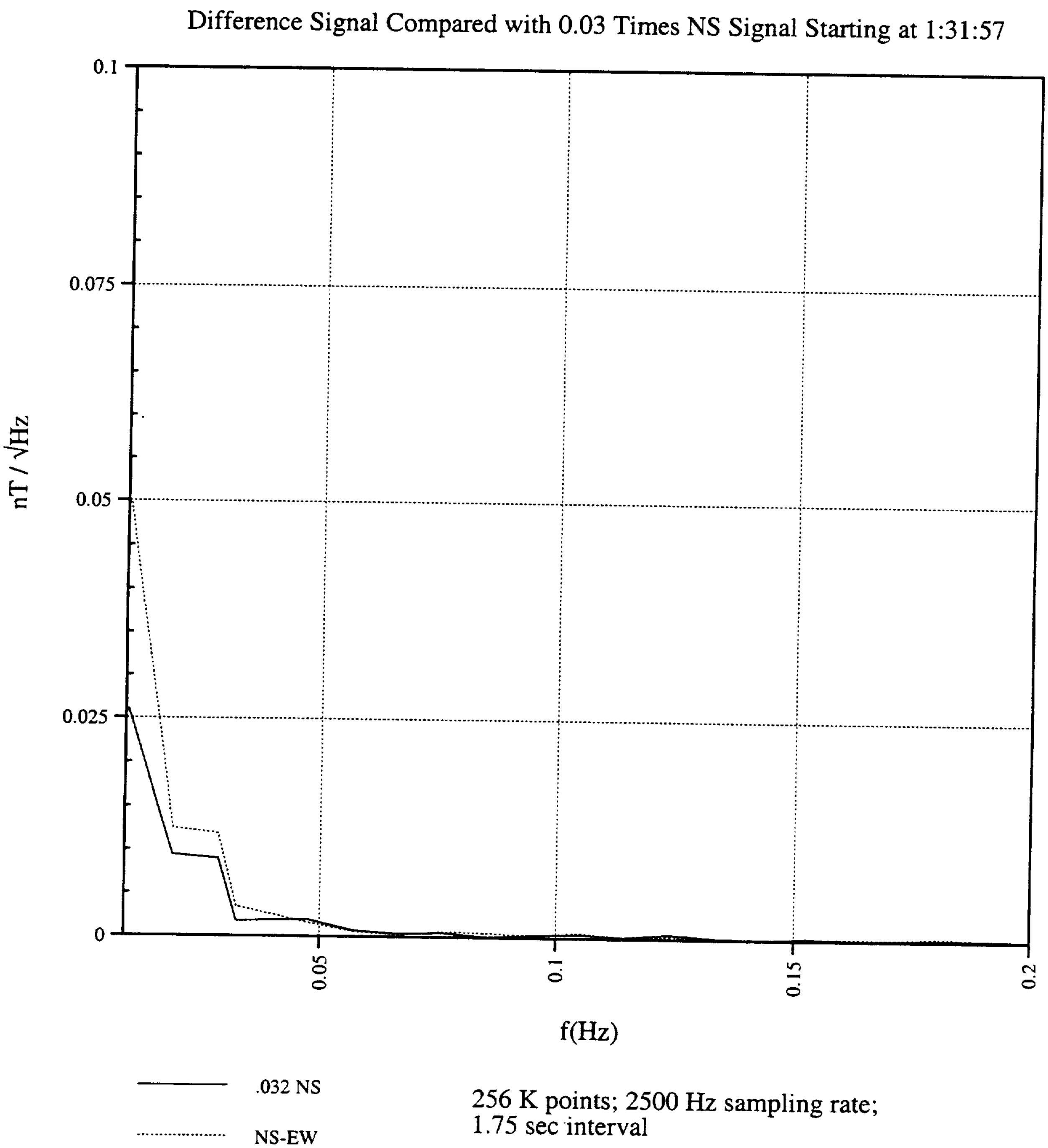
Difference Signal Compared with 0.03 Times NS Signal Starting at 1:31:57
0.1
0.075
0.05
0.025
0
nT / √Hz
0.05
0.1
0.15
0.2
f(Hz)
.032 NS
NS-EW
256 K points; 2500 Hz sampling rate;
1.75 sec interval

Figure 29.

Difference Signal Compared with 0.03 Times NS Signal Starting at 1:33:42

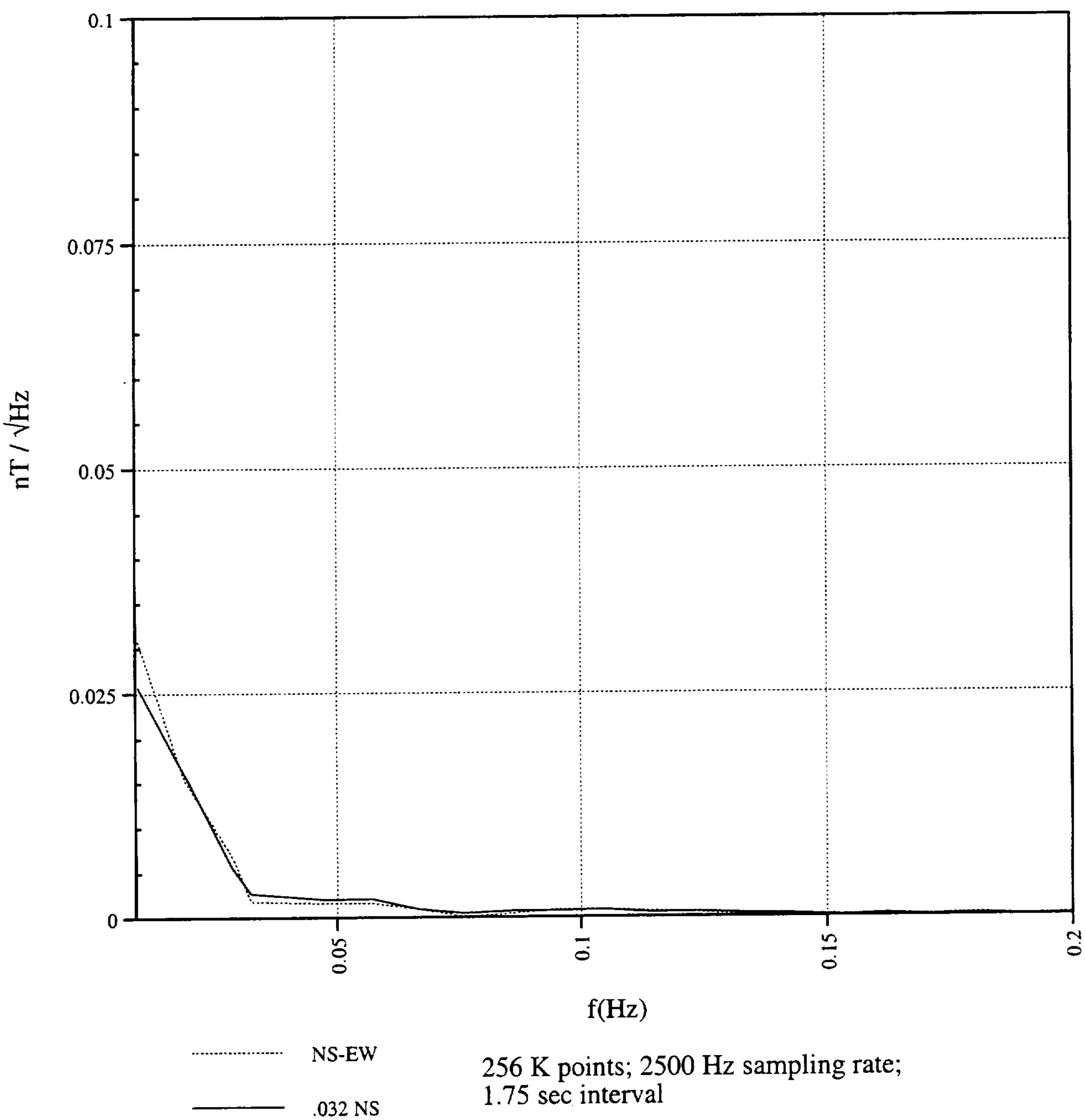

256 K points; 2500 Hz sampling rate;
1.75 sec interval

Figure 30.

Difference Signal Compared with 0.03 Times NS Signal Starting at 1:35:27

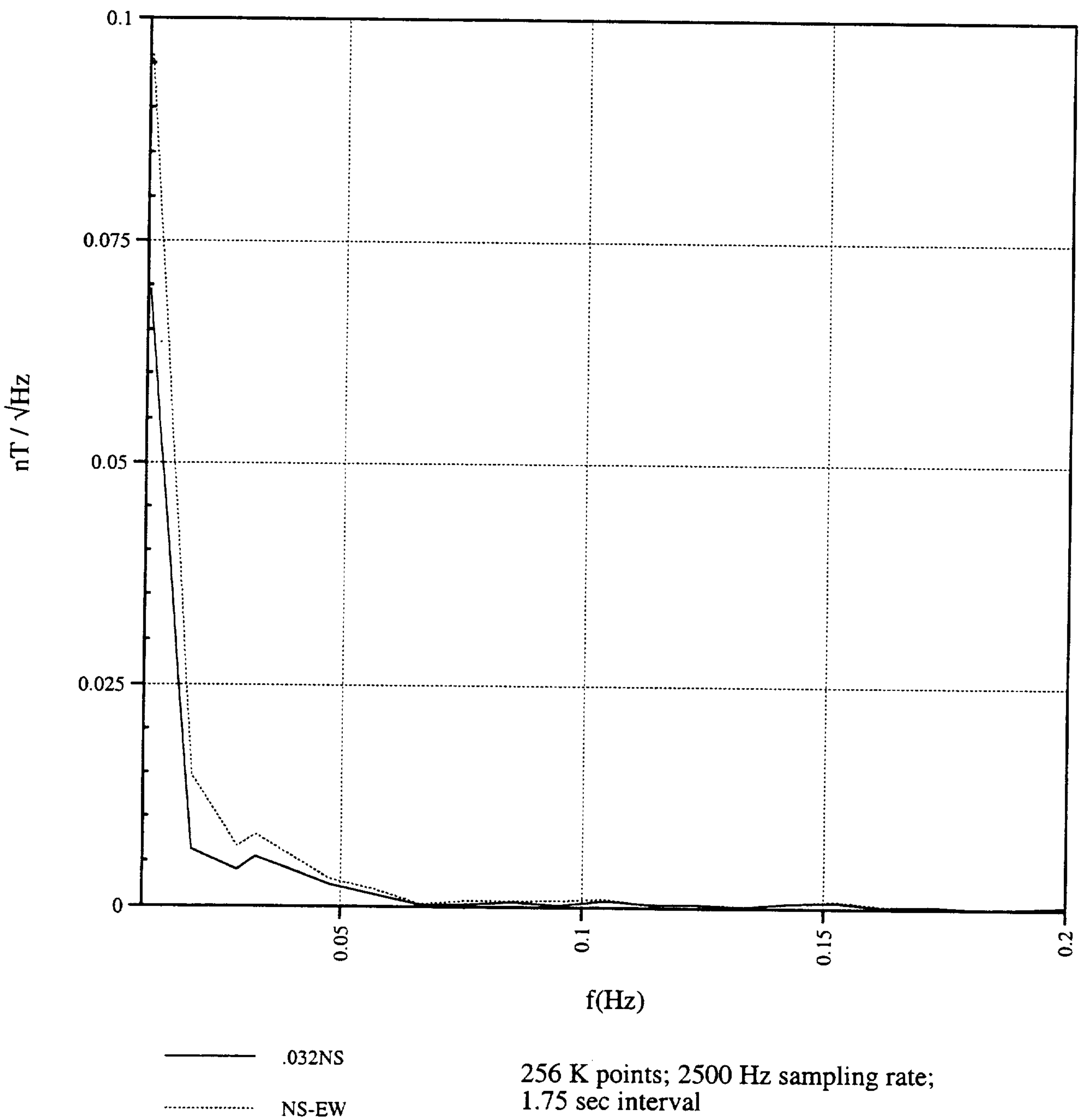

256 K points; 2500 Hz sampling rate;
1.75 sec interval

Figure 31.

SUMMARY

Given that the TSS-1R mission terminated several hours before our scheduled overflights and wave generation experiments were to have taken place, we had slight hope of observing tether generated signals in our data.

Nothing was seen in the magnetic sensor data that could be definitely ascribed to tether currents. A strong signal detected on Mona Island around GMT 57/01:34:08 proved to be due, almost certainly, to a generator shutdown on the island.

VLF data from the BF-6 sensors was not analyzed beyond a cursory examination of spectra with the digital analyzer at the times guessed to be most promising. Nothing of interest was noted.

Within our limited Mona data set, which does not include background data taken at the same local time as that of the tether deployment experiments, we see substantially higher ULF signals during the period of tether deployment, but not necessarily correlated with tether currents. Increased background noise due to the effect of sundown is perhaps a more likely cause.

Nothing striking seen was seen in the Bribie data. It was not possible to apply the method used in Mona polarized signal analysis due to the very noisy signal and the lack of a consistent signal in different channels.

We utilized the observed near equivalence of Mona EW and NS ULF signals as a way of looking for polarized signals in the NS-EW difference spectra. Examination of the data for signals with an EW polarization found that the largest deviation of over 4.8 σ from the best fit to a constant ratio between NS and EW signals to be in the 1.75 minute interval starting about 6 minutes after the tether break. A 4-σ deviation was seen in the interval starting 3.5 minutes earlier. The probability is thus small that the observed polarized signals are just statistical in nature.

However, in the absence of corroborative data or any theory about how a signal propagates after the cessation of tether current, we cannot ascribe the enhanced polarized signals to the tether's interaction with the ionosphere. Nor can we rule out the possibility of contamination of the recorded signal from local sources, notably the satellite telephone set.

The failure of TSS-1 and TSS-1R to fly close to our ground stations with the tether fully deployed and current flowing in the tether has left us more or less where we were before the missions in regard to tether wave emissions and ionospheric circuit closure. New opportunities for observations may be coming up with the proposed electrodynamic tether experiment ProSEDS, which should reach current levels of over 3 A, while orbiting the Earth for several days in August 2000. We hope that, if ProSEDS flies, the opportunity will not be missed.

REFERENCES

1. "The TSS-1R mission: Overview and scientific context," N. H. Stone and C. Bonifazi, *Geophys. Res. Lett.*, 25,4,409-412, 1998

2. "Alfvén waves from an electrodynamic tethered satellite system," R. D. Estes, *J. Geophys. Res.*, 93(A2), 945-953, 1988

3. "Alvén wave far field from steady-current tethers," J. R. Sanmartín and R. D. Estes, *J. Geophys. Res.*, 102(A7), 1,4,625-14,630, 1997

4. "Calculating the electromagnetic field on the Earth due to an electrodynamic tethered system in the ionosphere," R. D. Estes, *Proceedings of the Third International Conference on Tethers in Space*, ed. K. Anderson, Washington, DC: SRS Technologies, 1989

APPENDIX: THE RICE UNIVERSITY REPORT

Studies of ULF-ELF Emissions by the Electrodynamic Tether

Research Contract No: SV7-57005
from the Smithsonian Astrophysical Observatory
a subcontract under NASA contract No: NAS8-36809

Final Report

Principal Investigator
William E. Gordon

Prepared for
the Smithsonian Astrophysical Observatory
Cambridge, Massachusetts

Rice University
Department of Space Physics and Astronomy
Houston, Texas

June 1998

Contents

1. Background

In 1986, the Smithsonian Astrophysical Observatory (SAO) was selected by the National Aeronautics and Space Administration (NASA) to investigate analytically and observationally using ground-based systems the detectability of emissions by the electrodynamic tether. The investigation, dubbed EMET for Electromagnetic Emissions by the Electrodynamic Tether, was one of a number of investigations selected by NASA to examine science questions associated with tethers in space and, along with OESEE (Observations at the Earth's Surface of Electromagnetic Emissions by TSS), is responsible for ground-based measurements of tether emissions.

Rice University, with its experience in ground-based ionospheric observational systems, was subsequently chosen by SAO to handle the ground-based duties by developing a viable measurement program, assembling the necessary measurement system, recruiting field personnel, and coordinating and conducting the ground-based observations during the first TSS mission (TSS-1) in 1992 and its reflight (TSS-1R) in 1996. This Final Report provides details of the activity that Rice engaged in to accomplish these tasks. The focus here is centered primarily on the latter mission, TSS-1R, since both missions were carried out very similarly by the Rice effort and only the reflight yielded possibly meaningful data. This is in contrast to the first mission which was terminated well before any significant tether emission studies could be undertaken as a result of a malfunction with the tether deployment system on-board the shuttle.

2. Measurement Program

Many studies have been done which address the issue of waves excited by a conducting mass moving through a magnetized plasma. Some of these have specifically addressed the tether problem. Although it has been demonstrated that a tether of the kind employed for TSS will give rise to propagating electromagnetic waves in the ultralow (ULF) to very low (VLF) frequency bands, the production of waves which are intense enough to be observed by ground based receiving systems has not been well established. Information gathered by ground based measurement studies, such as this Rice study, can provide an important additional perspective and help determine the applicability of tethers as ULF-VLF communication devices. Within the ULF-VLF bands, tether emissions at Alfvén, lower hybrid, and whistler frequencies are predicted. Collectively, the theoretical work sets boundaries on the type and intensity of emitted waves that should be expected. An observational strategy was developed by Rice which is, to first order, rooted in the results of past theoretical endeavors.

Of primary interest to the global network is the study of signals received on the earth's surface from TSS induced Alfvén waves. Consequently, the receiving stations utilize sensors targeted for their detection. Likewise, higher frequency waves such as whistler and lower hybrid modes which are also theorized to be generated by the electrodynamic tether during its operation, are also to be part of the observational program. It is important, of course, that the sensors used in this study be situated with an understanding of the geometry associated with the propagation of the tether generated waves and operated in the appropriate environment to minimize unwanted signals. This places constraints on the sites which can be considered but improves the likelihood of detecting the desired signals.

In addition to the ground stations designed to detect tether emissions, simultaneous and supportive observations are conducted using the 430 MHz radar at Arecibo, Puerto Rico. The Arecibo facility is ideal for diagnosing the effects of the TSS on the ionosphere and providing meaningful results to the programs global data pool. Two goals of the Arecibo measurement program are to probe with the 430 MHz radar beam the region surrounding the tether during its operation as it passes over Arecibo and to use the 430 MHz radar to provide background information on the state of the ionosphere in close proximity to the medium as tether induced waves propagate to a nearby ULF-VLF ground station.

To maximize the science yield from the measurement program the following five conditions were considered in the ULF-VLF site selection process: 1) the first station selected should be situated in close proximity to the Arecibo radar to allow for complementary data collection; (2) the stations should be connected by a common shuttle ground track to permit same orbit studies; (3) the stations should be sufficiently separated to allow for day/night observations during the same orbit; (4) the stations should be sufficiently removed from population centers to reduce interference from artificial noise sources; and (5), the stations should be situated to permit maximum overflight opportunities while satisfying (1)-(4) above--the shuttle's nominal launch trajectory is due east from the Kennedy Space Center and thus overflies points on the ground up to a maximum latitudinal extent of 28.5° north and south. Thus, both field stations will fall within this latitudinal band. Overflight opportunities are greatest near the maximum latitudinal extent where orbital conditions result in a denser packing of the flight paths over those found more equatorially.

Using the above criteria, ground-based observational sites at Mona Island, Puerto Rico and Bribie Island, Australia were selected and operated by Rice in support of the TSS missions at ULF-VLF. A map showing these sites (USA) along with the OESEE sites (ITA) is displayed in Figure 1. The Mona Island site and its proximity to Arecibo is illustrated in Figure 2. Additional details about the selection of these sites is provided in Sections 2.1 and 2.2. Once the sites were identified, NASA teams and the science investigators created special operational sequences for the tether during the few minutes that the orbital system is over the ground stations. These sequences became part of the mission timeline. Since tether length influences the amplitude of the emissions, the overflights will occur in the nominal flight plan when the tether is fully deployed, i.e., at on-station one (OST-1).

2.1 Mona Island Station

Mona Island was selected as a receiving station because of its proximity to Arecibo and its remote location. The site was familiar to Rice scientist through previous and unrelated ULF wave studies. Since Arecibo is located away from the region where overflights are most concentrated, it is impossible for Mona to have a high concentration of overflights. This limitation, however, is offset by the fact that the shuttle's orbit is designed to overfly Arecibo with NASA selecting launch parameters to accomplish this goal.

For the ULF-VLF studies it is important that electromagnetic interference be minimized so that the potentially weak signals from the tether can be observed. Mona Island is about 80 km off the west coast of Puerto Rico and has no permanent population and can only be accessed by private plane or boat. The main compound is located at the southwest corner of the island and is home to a rotating crew of about eight persons from the Puerto Rican police force and the Department of Natural and Environmental Resources. The ground station is located at the extreme southern end of the compound about 300 m from the main collection of buildings. A generator is used to provide power to the compound and can be switched off during observations to minimize interference.

2.2 Bribie Island Station

The selection of the sister site at Bribie Island followed the selection of Mona Island with its general location fixed by the condition that it be situated in the opposite hemisphere to assure day/night observations and along the orbital ground track that connects it to Mona Islands within the same orbital revolution. Further, locating the site just equatorward of the southern extent of the orbit to maximize exposure to overflights narrowed the prospective region to Australia. An ionospheric research facility located about 50 km northeast of Brisbane, Australia just off the coast on Bribie Island (27.0° S, 153.2°E) was identified which satisfied the conditions. The facility was established by the University of Queensland, Brisbane, Australia.

3. ULF-VLF Measurement System

The receiving system developed by Rice University to support the ground-based observations consist of four general subsystems: (1) signal acquisition and conditioning; (2) data analysis; (3) data storage; and (4), power delivery. Together, the subsystems represent a self-contained transportable ULF-VLF receiving system with data recording and data analysis capabilities. A block diagram of the system is provided in Figure 3. Each of the two ULF-VLF stations was equipped with a fully integrated system. To keep cost low and within budget limits, however, only components to assemble one complete receiving system were purchased by Rice. The second system was comprised of a combination of purchased components and leased components.

Central to the signal acquisition and conditioning subsystem are EMI Model BF-4 and BF-6 magnetometer sensors. General specifications of the sensors are provided in Table 1. These low-noise and highly sensitive sensors utilize a magnetic feedback design to provide stable flat response over several decades of frequency. In their application to TSS the BF-4 sensors are used to detect the low-frequency signals up to 500 Hz while the BF-6 captures the high-frequency signals from 500-40,000 Hz. Since the TSS related signals that reach the earth's surface are expected to be weak, it was important to select sensors that do not introduce excessive noise into the system. A comparison of the BF-4 noise level to that of the more costly SQUID (superconducting quantum interference device) sensor and natural field is shown in Figure 4. For the band under consideration, the noise level of the selected sensors is equal to or less than that of SQUIDs and comparable to or less than the level for the natural field. The BF-6 sensors are also low-noise.

TABLE 1 SENSOR SPECIFICATIONS

	BF-4	BF-6
FREQUENCY RANGE	0.001 - 1000 Hz	10 - 100,000 Hz
FREQUENCY (3dB POINTS)	0.3 - 500 Hz	100 - 100,000 Hz
SENSITIVITY	0.1 - 0.5 V/nT	0.02 - 0.2 V/nT
POWER CONSUMPTION	12 mA at ± 12 V	5 mA at ± 12 V
LENGTH	133 cm	71 cm
DIAMETER	6 cm	4 cm
WEIGHT	8.2 kg	1.8 kg

In all, six sensors are required, three high frequency and three low frequency. Both sets are arranged along three mutually perpendicular axes and buried to minimize mechanically introduced interference. The sensors are situated a minimum of 50 m away from the remainder of the receiving system. The signals from the coils are passband filtered and gain adjusted prior to being passed on to the data recording and analysis subsystems.

Battery power is used during critical measurement periods to ensure low noise conditions. At other times, the system is operated on AC using a 1 kW generator. Approximately 22 hrs of DC power is available. This can, however, be increased to any capacity by including additional batteries. Standard TSS-1R operating procedures call for primary power to be DC during the time the tether is fully deployed (OST-1 operation). This includes the time of the planned overflights.

A portion of the data is examined in real-time. This process is undertaken primarily to monitor the state of the receiving system and to view the background field. The field operated analysis system utilizes a Hewlett Packard model 3561 instrument. Analysis can be made continuously when AC power is available. At times when DC-only operation is in effect, no real-time analysis takes place. The HP 3561 is a single channel Fast Fourier Transform (FFT) signal analyzer covering the frequency range to 100 kHz. The measurement capabilities include magnitude, time, and phase. The 80 dB dynamic range of the instrument allows measurement of signals where the signal of interest exists in the presence of large unwanted signals, as with 50 and 60 Hz power line emissions, or in cases where rapid changes in amplitude occur, i.e., the 1/f regime; see Figure 4. The signal processing capabilities include a variety of averaging techniques.

The large dynamic range associated with the low-frequency signal easily surpasses that attainable with conventional analog recording systems and presses 12 and 16 bit digital systems to their limit. In a compromise between capability and economy, a Metrum Model RSR 512 rotary storage data recorder was chosen. This recorder is a portable and versatile 16 channel instrumentation system that utilizes one-half inch video tape cassettes. The characteristics of FM recording are combined with the accuracy of digital recording in this unit. The recorder accepts data in analog form and converts it to digital form for recording on the tape cassette. In playback, the data is available in both digital and analog formats. The RSR 512 uses a 12 bit A/D converter providing >70 dB dynamic range. This is a considerable improvement over the dynamic range offered by conventional analog recorders and thus reduces the demand placed on signal conditioning in order to satisfy recorder limitations. Nonetheless, the signal must be windowed to fit the range of the recorder. To capture the entire low-frequency band in the TSS data and ensure that weak signals are recorded, the signal is split into three paths. Each path is passband filtered to isolate various portions of the spectrum, and each recorded separately at the appropriate level. Another feature of this recorder that is important to this application is AC/DC capability. During critical measurement periods, such as when the overflights occur, DC power must be used to minimize artificially generated electromagnetic noise. At other less critical times, the system can be operated off AC power.

Communication links between the various stations is critical. Land lines were available at Bribie and Arecibo. A satellite communications system which utilizes the standard telephone network was operated at Mona. Electronic mail between Arecibo, Bribie, and the space center, was also frequently utilized. EMET personnel at the Payload/Science Operations Control Center at the space center acted as point men for the field teams during the observations. Tether function and other mission decisions which could influence the ground observations during the mission were made by NASA teams and the science investigators: EMET (Dr. Estes, SAO), OESEE, and the TSS Investigators' Working Group. Any changes to the flight timeline that affected the observation schedule were relayed by telephone or electronic mail to the field by Dr. Estes or his designated representative. Appropriate adjustments to the observing timeline were then initiated by field personnel.

4. Arecibo Facility

At Arecibo, the 430-MHz incoherent backscatter radar uses a 300 m fixed dish antenna and a moveable line feed which allows the beam to be steered within 20° of the zenith. The orbit of the shuttle is selected to allow it to be viewed by Arecibo. Under nominal conditions, the shuttle is within viewing range of the Arecibo radar immediately following the overflight of Mona Island. The transmitters peak power output is 2.5 MW and its duty cycle is a maximum 6%.

Information about the ionosphere is derived by examining the power of the signal returned from the ionosphere by the electrons. The beamwidth at the shuttle altitude in the F-region is approximately 1 km. For electron density studies a vertical resolution of 600 m and a temporal resolution of a few seconds is typical. Temperature profiles are constructed by examining the spectrum of the returned signal and are coarser in both vertical and temporal resolutions than the density measurements. Both temperature and density measurements are taken in support of the overflight.

5. Field Personnel

Three teams of highly qualified individuals were required to operate the specialized equipment used in the measurement program. Through a recruiting effort, two teams were assembled to handle the operational duties of the ULF-VLF stations. The Mona team consisted of Drs. Czipott (Quantum Magnetics, Inc.), Freeman (Loral Aerospace), Hinds (Space Telescope Science Institute), and McCoy (NASA). The

Bribie team included Drs. Frahm (SwRI), Noble (Rice), and Whitehead (University of Queensland). A week long training exercise was held prior to the observations in October 1995 to (re)familiarize the attendees with the various systems and their operation. For the Arecibo radar studies, the team was comprised of Drs. Gordon (Rice) and Sulzer (Arecibo Observatory).

6. TSS-1R ULF-VLF Station Activity and Data Collection

The TSS-1R mission was terminated prior to the timelined overflights due to a break in the tether. The break occurred near the end of the deployment phase with approximately 19.7 km unreeled. As a consequence of the break, tether experiments including the ground-based measurements were terminated before OST-1 studies could commence. The Mona and Bribie field stations collected data for a period shorter than planned under the nominal mission profile and did not collect overflight data since the overflights were OST-1 timelined. A brief synopsis of the field activity for the ULF-VLF ground stations is provided below. Arecibo was operated as scheduled until shortly after the break when it went off the air. The Arecibo data is archived at Arecibo. No post mission data reduction was performed on the Arecibo data.

6.1 Mona Island Station

Equipment and supplies were shipped from the U.S. to Arecibo where they were tested prior to deployment to Mona. Mona preliminary field activity began February 12, 1996. A single engine airplane was used to shuttle team members, equipment, and supplies between Arecibo and Mona. The station was fully operational during TSS operation. A total of five data tapes recorded under AC conditions were collected over the period beginning with tether deployment and extending to approximately 4 hrs after the break. Background tapes were also made on the days prior to deployment. Each tape spans approximately 100 min.

6.2 Bribie Island Station

Equipment and supplies were shipped from the U.S. to the University of Queensland, Brisbane, Australia a few weeks before the observations. The equipment and supplies were subsequently taken by automobile to Bribie where preliminary field activity began February 15, 1996. The station was fully operational during TSS operation. A total of three data tapes recorded under AC conditions were collected over the period beginning with tether deployment and extending to shortly after the break. Background tapes were also made on the days prior to deployment. Each tape spans approximately 100 min.

After the mission the ULF-VLF data tapes were sent to SAO where copies were made. The original tapes and the copies are currently at SAO.

7. Data Reduction and Analysis

During the deployment phase of the tether and prior to the break, tether current sequences were being carried out by science teams other than EMET and OESEE. The ULF-VLF ground stations were taking data at this time and these data have been reduced and analyzed for signs of detectable tether emissions. The findings are presented in the SAO report.

8. Summary

In support of the TSS program, Rice University, under a subcontract from the Smithsonian Astrophysical Observatory (SAO), conducted ground based measurements in an effort to detect tether based emissions. Rice University handled all aspects of the measurement program and assisted SAO with the data reduction and analysis effort. In conjunction with the former point, Rice developed a viable measurement program; identified and acquired suitable measurement sites; assembled the necessary hardware for the measurement system and delivered it to/from the field; recruited qualified personnel and trained them to operate the specialized systems; and, coordinated, manned, and conducted the ground-based measurements.

With the successful completion of these tasks, the ground-based measurement program carried out by Rice University provided full and effective support to this part of the TSS program and accomplished all of its goals as set forth in the contract with SAO.

Acknowledgment. The Arecibo Observatory is part of the National Astronomy and Ionospheric Center and is operated by Cornell University under contract from the National Science Foundation.

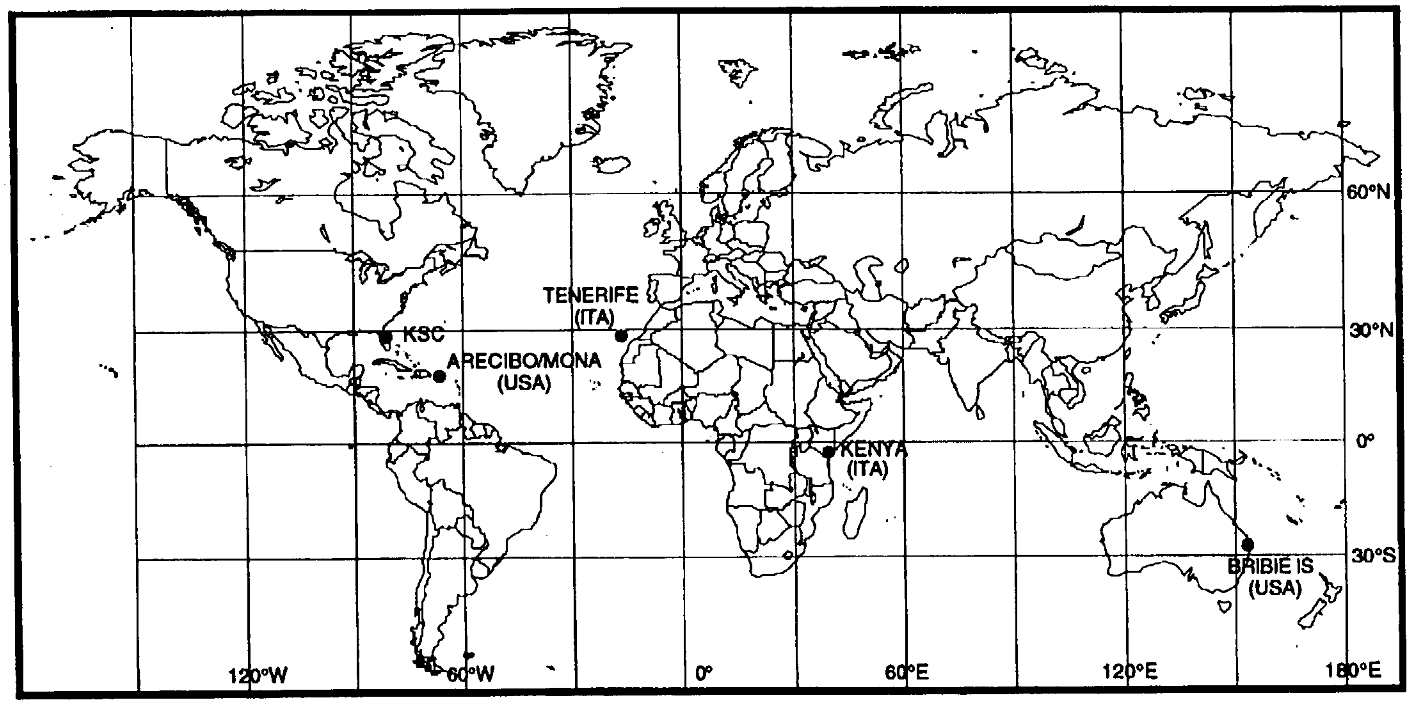

Figure 1. Map showing location of ground stations. Rice University operated stations indicated by "USA".

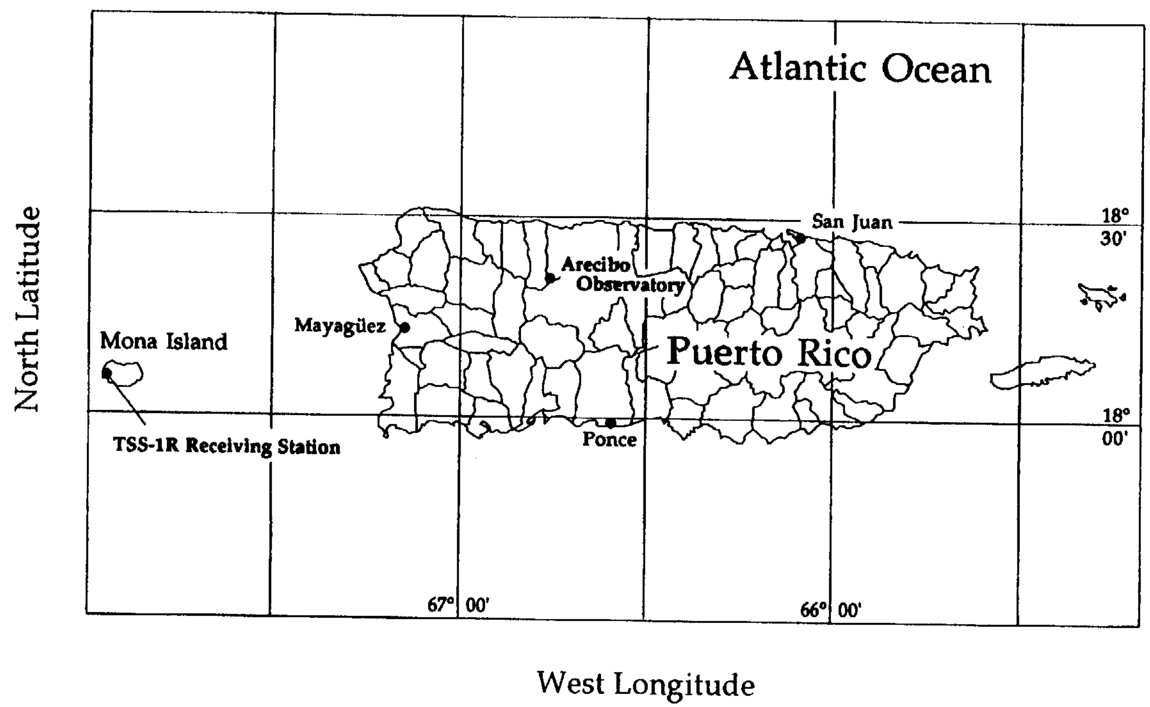

Figure 2. Map showing the Caribbean field stations at Mona Island and Arecibo.

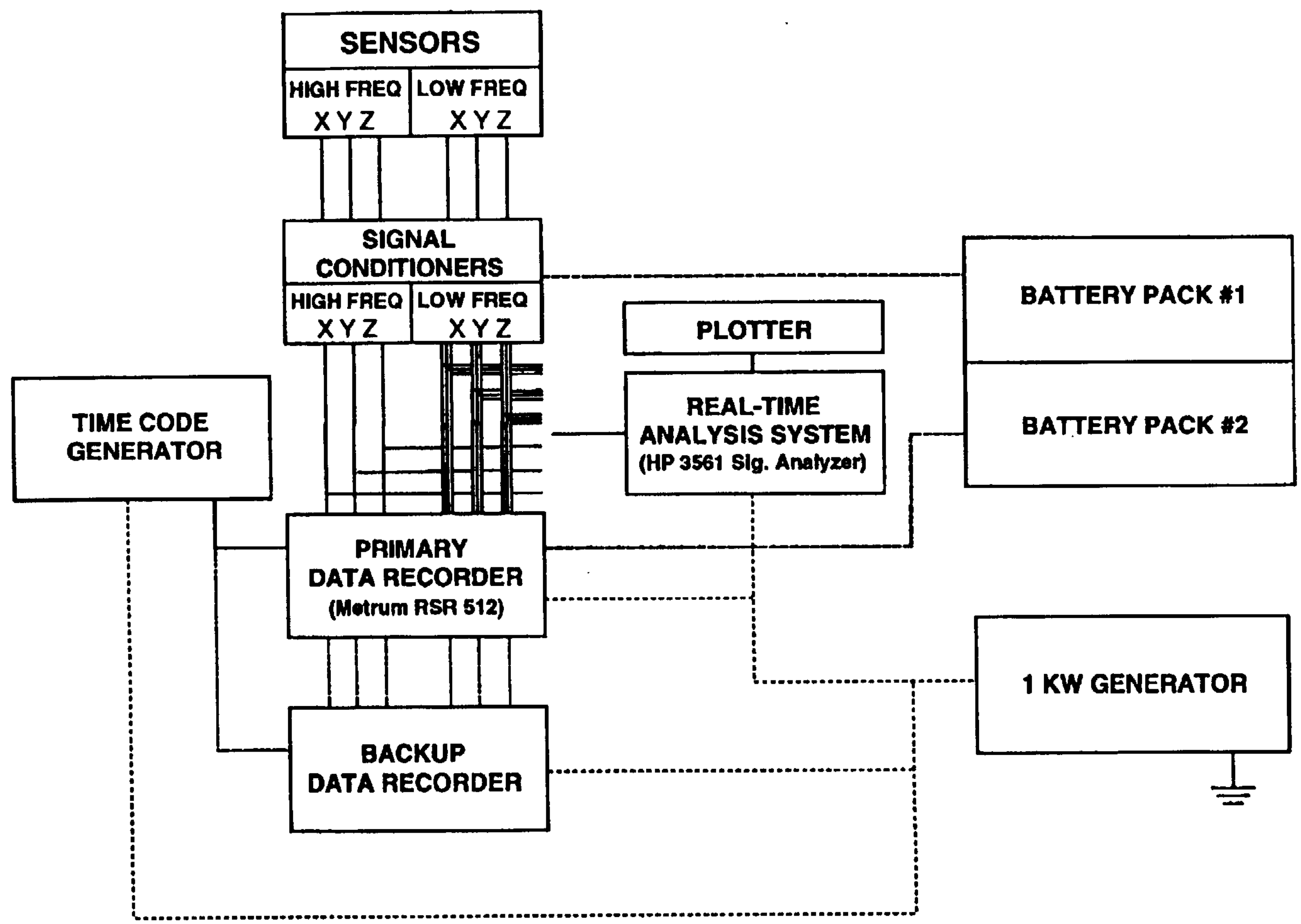

Figure 3. Block diagram of ULF-VLF receiving system.

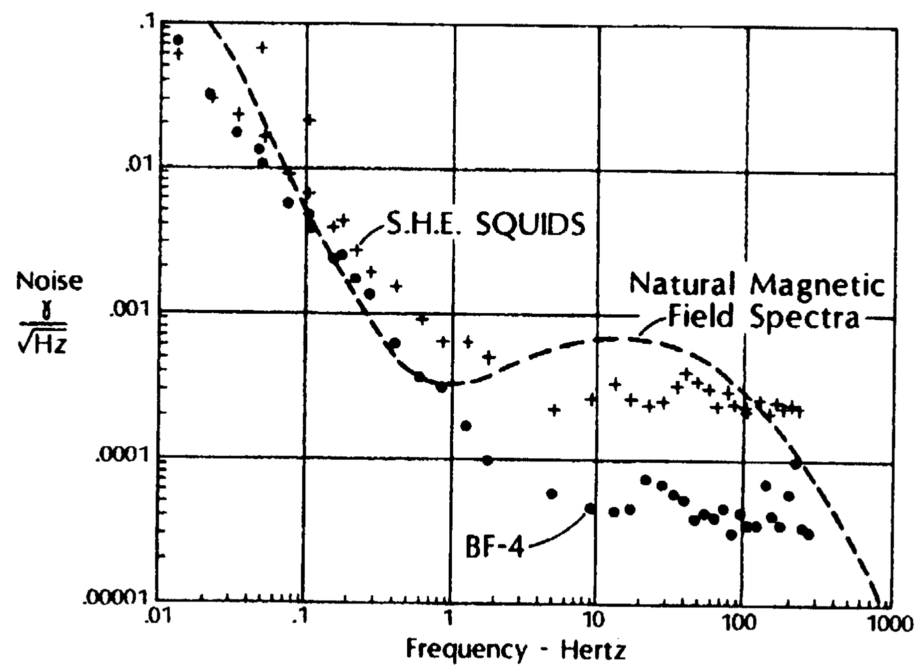

Figure 4. Noise level comparison between BF-4, SQUID, and natural magnetic field.

AT01S 0 2
TURNER J/PUBLICATION
MARSHALL SPACE FLIGHT CENTER
HUNTSVILLE AL.

DELETIONS OR CHANGES 544-4494
RETURN ADDRESS AT01D
Document Code: 2444